Review

Remote Sensing of Geomorphodiversity Linked to Biodiversity—Part III: Traits, Processes and Remote Sensing Characteristics

Angela Lausch [1,2,3,*], Michael E. Schaepman [4], Andrew K. Skidmore [5,6], Eusebiu Catana [7], Lutz Bannehr [8], Olaf Bastian [9], Erik Borg [10,11], Jan Bumberger [12,13,14], Peter Dietrich [13,14], Cornelia Glässer [3], Jorg M. Hacker [15,16], Rene Höfer [17], Thomas Jagdhuber [18,19], Sven Jany [20], András Jung [21], Arnon Karnieli [22], Reinhard Klenke [23], Toralf Kirsten [24,25], Uta Ködel [13], Wolfgang Kresse [26], Ulf Mallast [13], Carsten Montzka [27], Markus Möller [28], Hannes Mollenhauer [13], Marion Pause [8], Minhaz Rahman [29], Franziska Schrodt [30], Christiane Schmullius [31], Claudia Schütze [32], Peter Selsam [13], Ralf-Uwe Syrbe [33], Sina Truckenbrodt [31,34], Michael Vohland [35,36], Martin Volk [1,3], Thilo Wellmann [1,2], Steffen Zacharias [13] and Roland Baatz [37,38]

1 Department of Computational Landscape Ecology, Helmholtz Centre for Environmental Research–UFZ, Permoserstr. 15, D-04318 Leipzig, Germany; martin.volk@ufz.de (M.V.); thilo.wellmann@hu-berlin.de (T.W.)

2 Landscape Ecology Lab, Geography Department, Humboldt-Universität zu Berlin, Unter den Linden 6, D-10099 Berlin, Germany

3 Department of Physical Geography and Geoecology, Martin Luther University Halle-Wittenberg, Von-Seckendorff-Platz 4, D-06120 Halle, Germany; cornelia.glaesser@geo.uni-halle.de

4 Remote Sensing Laboratories, Department of Geography, University Research Priority Program on Global Change and Biodiversity, University of Zurich–Irchel, Winterthurerstrasse 190, CH-8057 Zurich, Switzerland; michael.schaepman@geo.uzh.ch

5 Faculty of Geo-Information Science and Earth Observation (ITC), University of Twente, AE 7500 Enschede, The Netherlands; a.k.skidmore@utwente.nl

6 Department of Earth and Environmental Science, Macquarie University, Sydney, NSW 2109, Australia

7 Eusebiu Catana, ERTICO, Avenue Louise 326, B-1050 Brussels, Belgium; e.catana@mail.ertico.com

8 Department of Architecture, Facility Management and Geoinformation, Institute for Geoinformation and Surveying, Bauhausstraße 8, D-06846 Dessau, Germany; l.bannehr@afg.hs-anhalt.de (L.B.); marion.pause@hs-anhalt.de (M.P.)

9 OT Boxdorf, Waldteichstr. 47, D-01468 Moritzburg, Germany; olaf.bastian@web.de

10 German Remote Sensing Data Center—DFD, German Aerospace Center—DLR, Kalkhorstweg 53, D-17235 Neustrelitz, Germany; erik.borg@dlr.de

11 Geodesy and Geoinformatics, University of Applied Sciences Neubrandenburg, Brodaer Strasse 2, D-17033 Neubrandenburg, Germany

12 Research Data Management—RDM, Helmholtz Centre for Environmental Research GmbH—UFZ, Permoserstraße 15, D-04318 Leipzig, Germany; jan.bumberger@ufz.de

13 Department of Monitoring and Exploration Technologies, Helmholtz Centre for Environmental Research—UFZ, Permoserstr. 15, D-04318 Leipzig, Germany; peter.dietrich@ufz.de (P.D.); uta.koedel@ufz.de (U.K.); ulf.mallast@ufz.de (U.M.); hannes.mollenhauer@ufz.de (H.M.); peter.selsam@ufz.de (P.S.); steffen.zacharias@ufz.de (S.Z.)

14 German Centre for Integrative Biodiversity Research (iDiv) Halle-Jena—Leipzig, Puschstraße 4, D-04103 Leipzig, Germany

15 College of Science and Engineering, Flinders University, Adelaide, SA 5000, Australia; jmh@flinders.edu.au

16 Airborne Research Australia (ARA), Parafield Airport, Adelaide, SA 5106, Australia

17 Department of Geoinformation, German Federal Agency for Nature Conservation, Alte Messe 6, D-04103 Leipzig, Germany; rene.hoefer@bfn.de

18 German Aerospace Center (DLR) Microwaves and Radar Institute, Oberpfaffenhofen, D-82234 Wessling, Germany; thomas.jagdhuber@dlr.de

19 Institute of Geography, Augsburg University, D-86159 Augsburg, Germany

20 MILAN Geoservice GmbH, Zum Tower 4, D-01917 Kamenz, Germany; s.jany@milan-geoservice.de

21 Institute of Cartography and Geoinformatics, Faculty of Informatics, Eötvös Loránd University, Pázmány Péter Sétány 1/A, H-1117 Budapest, Hungary; jung@inf.elte.hu

22 The Remote Sensing Laboratory, French Associates Institute for Agriculture and Biotechnology of Drylands, The Jacob Blaustein Institutes for Desert Research, Ben-Gurion University of the Negev, Be'er Sheva 8499000, Israel; karnieli@bgu.ac.il

23 Department of Community Ecology, Helmholtz Centre for Environmental Research—UFZ, Permoserstr. 15, D-04318 Leipzig, Germany; reinhard.klenke@ufz.de

24 Institute for Medical Informatics, Statistics and Epidemiology, Leipzig University, Härtelstr. 16–18, D-04107 Leipzig, Germany; toralf.kirsten@medizin.uni-leipzig.de

25 Department for Medical Data Science, Leipzig University Medical Center, Liebigstr. 20, D-04103 Leipzig, Germany

26 Faculty of Landscape Sciences and Geomatics, Neubrandenburg University of Applied Sciences, Brodaer Strasse 2, D-17033 Neubrandenburg, Germany; kresse@hs-nb.de

27 Institute of Bio- and Geosciences: Agrosphere (IBG-3), Forschungszentrum Jülich, D-52425 Jülich, Germany; c.montzka@fz-juelich.de

28 Julius Kühn Institute (JKI), Federal Research Centre for Cultivated Plants, Institute for Crop and Soil Science, Bundesallee 58, D-38116 Braunschweig, Germany; markus.moeller@julius-kuehn.de

29 Agrosphere, Institute of Bio and Geosciences, Forschungszentrum Jülich, D-52425 Jülich, Germany; minhaz.rahman@outlook.com

30 School of Geography, University of Nottingham, University Park, Nottingham NG7 2RD, UK; franziska.schrodt1@nottingham.ac.uk

31 Department of Remote Sensing, Institute of Geography, Friedrich Schiller University Jena, Leutragraben 1, D-07743 Jena, Germany; c.schmullius@uni-jena.de (C.S.); sina.truckenbrodt@uni-jena.de (S.T.)

32 Department of Computational Hydrosystems—UFZ, Permoserstr. 15, D-04318 Leipzig, Germany; claudia.schuetze@ufz.de

33 Leibniz Institute of Ecological Urban and Regional Development (IOER), Weberplatz 1, D-01217 Dresden, Germany; r.syrbe@ioer.de

34 German Aerospace Center (DLR), Institute of Data Science, Mälzerstraße 3–5, D-07743 Jena, Germany

35 Geoinformatics and Remote Sensing, Institute for Geography, Leipzig University, Johannisallee 19a, D-04103 Leipzig, Germany; michael.vohland@uni-leipzig.de

36 Remote Sensing Centre for Earth System Research, Leipzig University, Talstr. 35, D-04103 Leipzig, Germany

37 Leibniz Centre for Agricultural Landscape Research (ZALF), Eberswalder Str. 84, D-15374 Müncheberg, Germany; roland.baatz@zalf.de

38 Scientific Coordination Office International Soil Modelling Consortium ISMC, D-52428 Jülich, Germany

* Correspondence: angela.lausch@ufz.de; Tel.: +49-341-235-1961; Fax: +49-341-235-1939

Abstract: Remote sensing (RS) enables a cost-effective, extensive, continuous and standardized monitoring of traits and trait variations of geomorphology and its processes, from the local to the continental scale. To implement and better understand RS techniques and the spectral indicators derived from them in the monitoring of geomorphology, this paper presents a new perspective for the definition and recording of five characteristics of geomorphodiversity with RS, namely: geomorphic genesis diversity, geomorphic trait diversity, geomorphic structural diversity, geomorphic taxonomic diversity, and geomorphic functional diversity. In this respect, geomorphic trait diversity is the cornerstone and is essential for recording the other four characteristics using RS technologies. All five characteristics are discussed in detail in this paper and reinforced with numerous examples from various RS technologies. Methods for classifying the five characteristics of geomorphodiversity using RS, as well as the constraints of monitoring the diversity of geomorphology using RS, are discussed. RS-aided techniques that can be used for monitoring geomorphodiversity in regimes with changing land-use intensity are presented. Further, new approaches of geomorphic traits that enable the monitoring of geomorphodiversity through the valorisation of RS data from multiple missions are discussed as well as the ecosystem integrity approach. Likewise, the approach of monitoring the five characteristics of geomorphodiversity recording with RS is discussed, as are existing approaches for recording spectral geomorhic traits/ trait variation approach and indicators, along with approaches for assessing geomorphodiversity. It is shown that there is no comparable approach with which to define and record the five characteristics of geomorphodiversity using only RS data in the literature. Finally, the importance of the digitization process and the use of data science for research in the field of geomorphology in the 21st century is elucidated and discussed.
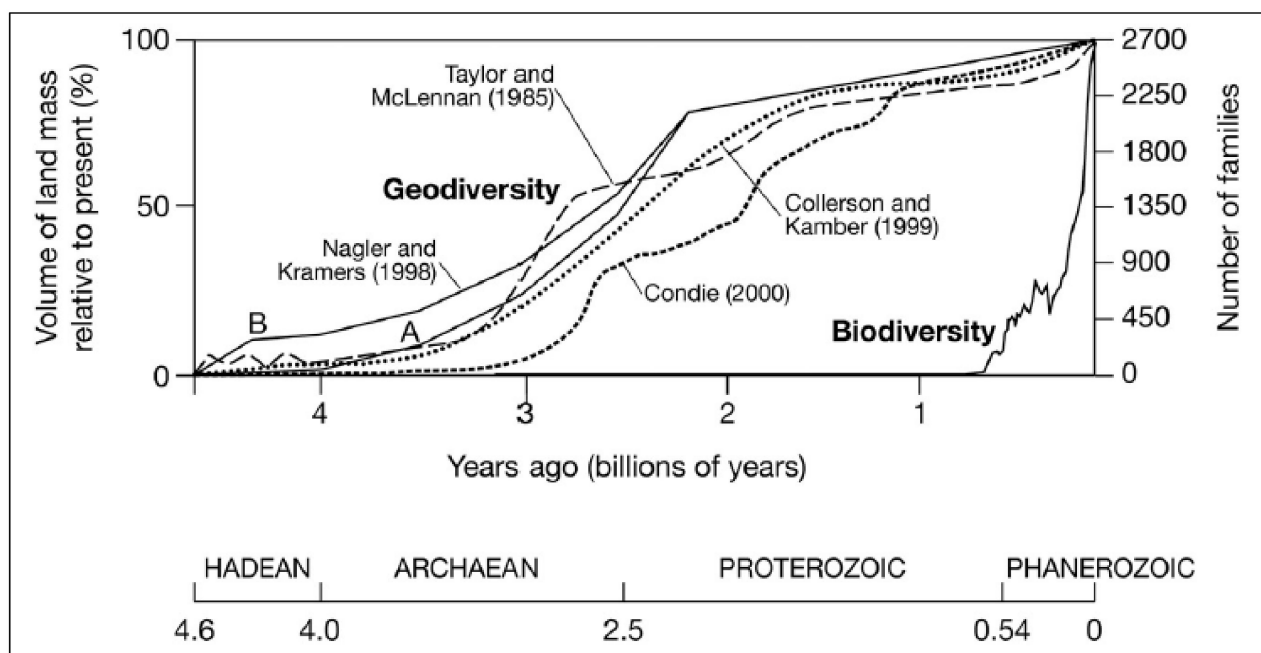
Keywords: geomorphology; geomorphodiversity; geodivesity; biodiversity; traits; spectral traits; geomorphic traits; genesis; taxonomy; structure; functions; terrain; landforms; land-use intensity; ecosystem integrity; remote sensing; earth observation; multi-mission; data science

1. Introduction

Geomorphology has shaped and structured the Earth's surface on all spatio-temporal scales, not only through long-term processes but also through medium- and short-term processes. Geomorphology is, therefore, a decisive control- and regulating variable in the entire development of landscapes as well as geo-and biodiversity.

There are various approaches to geomorphology, such as quantitative geomorphology [1,2], morphography and geomorphometry [3], functional geomorphology [4] or historic-genetic geomorphology and morphogenesis [5]. These can be applied to quantitatively and qualitatively measure and assess forms, form complexes, the structures and functions of the land surface and landforms, and to better understand and predict geomorphological process events, such as floods or flash floods, volcanic eruptions, mass erosion, the sedimentation of rivers and floodplains, or changes to the coastral landforms and permafrost, among others.

If we look at the evolution of the Earth's history, we see how geodiversity and geomorphology as a crucial part of it are the basis for the existence of life and the biodiversity of our planet, which originated some ~0.7 billion years ago [6] (see also Figure 1).

Figure 1. Curves of developing geodiversity and biodiversity, after Gray et al., [6], reprinted with permission from Gray et al., 2022, Elsevier. license no. 5225220111723.

Geomorphology can be therefore understood as "the promoting, controlling, regulating and limiting factor, as well as the most important control and regulating variable for landforms, landscape processes and thus a decisive factor for biodiversity" [7]. Biodiversity interacts with geodiversity, and "organisms live where they do; they respond to geodiversity and environmental change" (modified after Green [8]). It is, therefore, not surprising that the first research in the field of biogeomorphology was directed at either the study of interactions between vegetation dynamics and geomorphological processes [9] or the study of the influence of vegetation, animals, and microorganisms on geomorphological processes [10,11]. However, it was not until 1988 that Viles [12] defined biogeomorphology as a concept in its own right, dealing with the 'influence of landforms/geomorphology on the distributions and development of plants, animals, and micro-organisms; and the influence of plants, animals and micro-organisms on earth surface processes and the development of landforms' [12]. A comprehensive overview of the past, present, and future of the concepts of biogeomorphology and its related fields can be found in Viles [13].
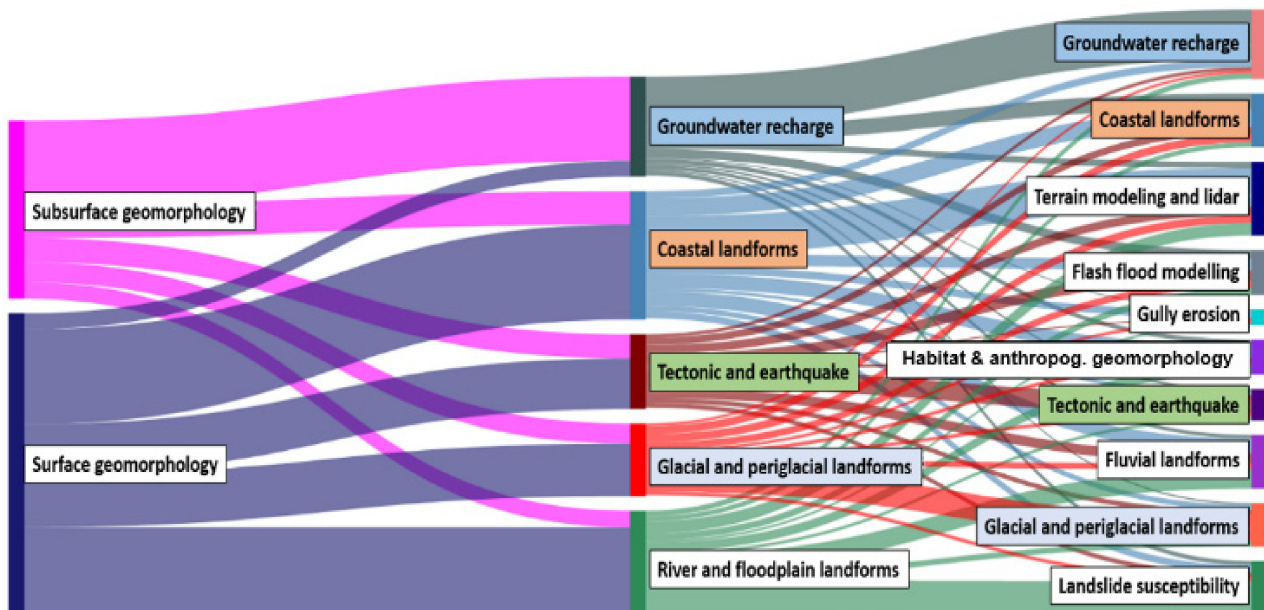
It goes without saying that anthropogenic activities have an even greater influence on geomorphological features than numerous other factors. For instance, a river is a geological zone that transports water and sediment from the mountains towards the oceans, depositing it on river and the riverbed. According to Grill et al. [14], dams and reservoirs lead to an interruption of the natural fluvial transport processes and, consequently, to an upstream and downstream fragmentation of flow regimes. Dams face the danger of overflowing, not only from water but also from debris, sand, silt, or stones, from microscopic grains to boulders, due to exogenous material being transported and numerous sedimentation processes, especially after heavy rainfall. Indeed, the approach of geomorphology in the Anthropocene was mentioned for the first time in 1979 by Rathjens [15]. Anthropogeomorphology is the study of human impacts and their effects on geomorphology and the ecosystem, which have led to changes and disturbances in the original geomorphology over shorter anthropogenic time scales [2,16–18]. Geomorphology is complex and its processes and interactions between geomorphology, biogeomorphology in the context of climate change, and increasing global intensification and urbanization by humans are only partially understood [15]. Therefore, a holistic or ecosystem integrity approach to monitoring and assessing geomorphological changes is required. Panizza [19] described the concept of geomorphodiversity for the first time back in 2009. The concept of geomorphodiversity fulfils the requirements of an approach encompassing ecosystem monitoring and assessment. Panizza [19] coupled different geomorphological indicators and compared them with each other (in an intrinsic way—morphoclimatic landforms on a global scale, landslides on a regional scale, and karst landforms on a local scale) and with those indicators from other areas (in an extrinsic way—dolomite landscapes on a global scale, morphostructural landforms on a regional scale) in order to assess their specificity and thus their geo(morpho)diversity [19]. Panizza [20] later developed his concept even further and integrated the intrinsic and extrinsic values of the geological heritage of the Dolomites, based on a subset of geomorphological indicators, such as stratigraphic, palaeontological, geomorphological and mineralogical indicators [20]. In numerous other case studies, geomorphodiversity indicators have been used to assess the relationship between geomorphodiversity and sediment connectivity in a small alpine catchment [21], to assess the geomorphodiversity and geomorphological heritage for Damavand Volcano Management [22], as well as in various geomorphodiversity indicators [23] and guidelines for generating landform geomorphodiversity maps [24].

RS and their traits and trait variation has emerged as a key method to quantitatively and qualitatively characterize, monitor or assess various natural and anthropogenic geomorphological properties, processes, features, structures and impending geohazards. This emergence is promoted by the growing human demand for the resources of the Earth's geosphere, the changes to and limitations of our geogenic resources and the resulting threat to limited, economically significant geo-resources, due to humans quest to perfect his lifestyle and an unsustainable approach to resource management. Numerous review papers have provided overviews of those traits and trait variations of landforms that can be detected with RS technologies [17,25–28].

To identify major research themes that prevail in the literature of "geomorphology and remote sensing", we analyzed the research published in the Web of Science using the respective terms in latent Dirichlet allocation (LDA) [29]. Considering a coarse two-topic structure, we identified the overarching topics of surface and subsurface geomorphology (Figure 2). These two overarching topics can be further subdivided into five smaller sub-topics, namely: groundwater recharge, coastal, landforms, tectonic and volcanic earthquakes, glacial and periglacial landforms, and river and floodplain landforms, which represent solid research topics that prevail with a finer topical structure. Other individual subtopics that were identified were terrain modeling and light detection and ranging (LiDAR), flash-flood modeling, gully erosion, habitat and anthropogenic geomorphology, fluvial landforms, glacial and periglacial landforms, and landslide susceptibility. These topics are highly inter-connected and are demonstrated by finer and broader joints. In

particular, habitat and anthropogenic geomorphology represent a direct link to ecosystems and biodiversity research.

Figure 2. The mapped sub-topics and the relationships among the sub-topics of the research articles found using the search terms "geomorphology" and "remote sensing". Two (left), five (center), and ten (right) topics were identified at the different levels, with shrinking proportion, respectively. The height of the topic bars corresponds to the topic proportion in the collection of articles. The bands' width is proportional to the number of documents affiliated with the inter-related topics. Colors are only meant to distinguish between topics.

With open access to RS data products, such as Landsat [30] and Copernicus [31–35], as well as the RS mission known as the environmental mapping and analysis program (EnMAP) (satellite launch on 01.04.2022) [36] and others, the potential of RS information for monitoring geomorphology has improved tremendously. New RS missions include the global ecosystem dynamics investigation (GEDI) high-resolution laser ranging of the Earth's forests and topography from the International Space Station (ISS) [37,38] or the radio detection and ranging (RADAR) missions Tandem-L [39,40], the NASA-ISRO synthetic aperture RADAR (NISAR) or the L-band synthetic aperture radar (Rose-L). There are also the new hyperspectral missions, such as EnMAP [36], the DLR Earth sensing imaging spectrometer for the ISS-MUSES platform (DESIS) [41], the Copernicus hyperspectral imaging mission (CHIME) [42], the hyperspectral infrared imager mission (HyspIRI) [43], or the use of small satellites, as well as the new multi-mission algorithm and analysis platform (MAAP, https://earthdata.nasa.gov/esds/maap, accessed on 5 January 2022), which also envisages direct links to in situ measurements. All these missions open up new pathways for monitoring and modeling geomorphology and ecosystem monitoring. It has long been recognised that long-term and interdisciplinary research and ecosystem intergrity monitoring approaches are needed to provide contious spatial-temporal data on geomorphodiversity in order to initiate conservation measures. Hyperspectral data with hundreds and in the future thousands of spectral bands in combination with TIR, RADAR and LiDAR technologies are the basis of new sensor technologies like the future HyspIRI-Mission. For example, the Surface Biology and Geology (SBG) mission of the National Aeronautics and Space Administration (NASA) will provide global spectroscopic images in the visible to short-wave infrared range (380–2500 nm) with high spatial resolution (~30 m), and traits and trait variations for monitoring gemomophodiversity in interaction with vegetation traits spatio-temporally (https://sbg.jpl.nasa.gov/satm, accessed on 5 January 2022) like the Science and Applications Traceability Matrix (SATM) for monitoring the suface biology and geology, https://sbg.jpl.nasa.gov/satm (accessed on 5 January 2022).

HyspIRI has to instruments: a hyperspectral visible (0.38–2.5 µm), to short wave infrared imaging spectrometer and a multispectral thermal infrared (TIR) imager. The TIR instrument will have eight spectral channels, seven of the channels are between 7 and 12 µm, with one additional channel at 4 µm [43].

The implementation of LiDAR technology for close-range RS, including terrestrial laser scanning (TLS) and airborne laser scanning (ALS), as well as the spaceborne GEDI-LiDAR technologies, all stand out as having been used with tremendous success for recording landform properties such as terrain, providing us with proof of the numerous fields of application for geomorphology using various RS technologies [7].

The large number of publications on the detection and assessment of geomorphic features and their changes, as well as geohazards, using different RS technologies indicates the rapidly growing importance of the use of close-range, air- and spaceborne RS sensors [7]. However, it has not yet been described how RS can achieve the geomorphodiversity approach first mentioned by Panizza [19]. In order to understand the detection of geomorphodiversity using RS, this paper introduces the five characteristics of geomorphodiversity that can be detected by RS. Since the spectral signal of RS is a result of or an integral of different domains, e.g., geomorphogenesis, structures, patterns, shapes and shape complexes, interactions between geomorphology and biogeomorphology, as well as changes in geomorphology, it makes sense to introduce the concept of spectral traits and trait variations to capture geomorphodiversity with RS techniques for a comprehensive understanding.

RS records the traits and trait variations of plant species [44], plant communities [45], animal species [46], pedology [47], or geomorphology [7]. Furthermore, traits are important for a better understanding of social-ecological patterns, dynamics, interactions, and tipping points in complex urban systems [48], as well as for monitoring urban intensification [49]. Traits are the central interface when it comes to linking different monitoring approaches and, thus, linking in situ and RS approaches [50]. The usage of traits and trait variations, as well as the importance of a new perspective and a new definition for monitoring geomorphodiversity with RS, has already been briefly introduced by Lausch et al. [7] in terms of geomorphology. However, in the study by Lausch et al. in 2020 [7], some of the questions and hypotheses remained open; these are now the subject of this paper. Therefore, the objectives of this paper are as follows:

- To describe the five characteristics of geomorphodiversity;
- To extensively discuss and explain the monitoring of the five geomorphodiversity features, based on RS approaches, which are geomorphic genesis diversity, geomorphic trait diversity, geomorphic structural diversity, geomorphic taxonomic diversity, and geomorphic functional diversity;
- To explain the approach when monitoring geomorphic traits and trait variations using RS technologies, and the advantages and constraints of RS technologies for monitoring the five characteristics of geomorphodiversity;
- To explore the need to consider the characteristics and the spatial-temporal distribution of geomorphic traits for successful RS-based monitoring;
- To discuss methods for distinguishing and classifying the five features of geomorphodiversity using RS;
- To discuss RS-based methods for monitoring geomorphodiversity in regimes with changing land-use intensity;
- To elucidate new approaches for monitoring geomorphodiversity, using multi-mission RS approaches and the ecosystem integrity approach;
- To highlight the importance of digitization processes and the use of data science approaches for geomorphological research in the 21st century.

2. Characteristics of Geomorphodiversity

Geomorphodiversity, as part of geodiversity, can be described by its five characteristics, namely: (a) geomorphic trait diversity, (b) geomorphic genesis diversity, (c) geomorphic structural diversity, (d) geomorphic taxonomic diversity, and (e) geomorphic functional

diversity [7]. These five characteristics of geomorphodiversity exist on all spatial, temporal, and directional scales of geomorphic organization (Figure 3) and interact and influence each other, as well as affecting biodiversity and further spheres of geodiversity such as the lithosphere, hydrosphere, or atmosphere, either directly or indirectly on all these scales. The five characteristics of geomorphodiversity are defined by Lausch et al. [7] as:

1. Geomorphic trait diversity, which represents the diversity of mineralogical, bio-/geochemical, bio-/geo-optical, chemical, physical, morphological, structural, textural, or functional characteristics of geomorphic components that affect, interact with, or are influenced by geomorphic genesis diversity, geomorphic taxonomic diversity, geomorphic structural diversity, and geomorphic functional diversity.
2. Geomorphic genesis diversity represents the diversity of the length of evolutionary pathways, linked to a given set of geomorphic traits, taxa, structures, and functions. Therefore, sets of geomorphic traits, taxa, structures, and functions are identified that maximize the accumulation of geomorphic-functional diversity.
3. Geomorphic structural diversity, which is the diversity of composition and configuration of 2D to 4D geomorphic structural traits.
4. Geomorphic taxonomic diversity, which stands for the diversity of geomorphic components that differ from a taxonomic perspective.
5. Geomorphic functional diversity, which is the diversity of geomorphic functions and processes, as well as their intra- and interspecific interactions.

Figure 3. The five characteristics of geomorphodiversity exist on all the spatial, temporal, and directional scales of geomorphic organization (modified after Lausch et al. [7]).

A clear separation and assignment of the five characteristics of geomorphodiversity is not always possible, but nevertheless helps to monitor, assign and assess the various indicators of in situ and RS approaches, as well as to understand the links between both approaches.

3. Monitoring Geomorphodiversity and Its Variability

Geomorphodiversity is investigated using two types of approaches: the in situ approach and the RS approach. In contrast to in situ approaches, RS approaches acquire

information about an object without physical contact. RS approaches are divided into close-range, airborne, and spaceborne approaches, depending on the distance (from millimeters to thousands of kilometers) of the monitored object from the RS sensor. To gain a clearer understanding of the common interfaces, advantages, and disadvantages, as well as the limitations and constraints of both approache types, these need to be considered in more depth.

3.1. In Situ Approaches—Field-Mapping Techniques

Historically, scientists such as Humboldt [51,52] used various in situ measurement techniques to detect, monitor, and classify features in geomorphology and geomorphodiversity and consequently to assess and predict natural and anthropogenic changes and/or disturbances. Early on, the in situ monitoring of geomorphodiversity adopted a holistic and interdisciplinary approach by observing, comparing, and investigating geo- and biodiversity; in particular, their interactions and feedback mechanisms. This approach also incorporates the basic idea of ecosystem integrity [53–55], which is reflected in the establishment of landscape and geoecological recording standards and mapping guidelines [56,57]. Special attention has always been paid to the monitoring of topography and relief, which is imperative for understanding processes, assessments, and ecosystem modeling.

Scientists acquire essential knowledge about geomorphology from practical work and the application of the latest technologies in various fields such as laboratory experiments [58], fieldwork [59], microstructural studies [60], analytical modeling [61], seismic studies or geoelectric studies—just to mention a few. Fieldwork is crucial for recording structures, patterns, tectonics, etc., and to understand the processes, functions, changes, and disturbances. It is helpful for understanding the genesis of different structures, formation types, and patterns (e.g., faults, fissures, folds, boudins or primary sedimentary and mineral structures). Understanding tectonic structures and their patterns is crucial for designing and interpreting geological maps [62], finding the genesis of different structures, locating and planning exploration programs, and acquiring geochemical and seismic data. Local measurements and wireless sensor networks are particularly important for the predicting and warning of geohazards such as volcanic activity, earthquakes, the detection of landslides, or, indirectly, the generation of tsunamis.

Furthermore, geophysical methods are often combined with other analytical, geotechnical, or RS methods to evaluate geomorphological processes. Among others, examples include the detection of weathering processes in rocks with time-lapse refraction seismic tomography [63], the evaluation of soil erosion processes by measuring magnetic susceptibility [64], the detection of landslides [65], e.g., moisture-induced landslides [66] or other kinds of landslides [67], rock glacier activity as mapped by ground-penetration radar (GPR) [68], permafrost monitoring using geophysical techniques [69], or electrical resistivity tomography (ERT) [69].

In addition to monitoring the direct methods for recording morphological traits and their changes, indirect methods, such as observing the interactions between geo- and biodiversity, are also used in assessment procedures. Plankton or terrestrial plant populations and communities have served as bio-indicators or proxies for geomorphological structures, patterns and processes and morphogens [70]. They provide important information on changes, disturbances, and shifts in resource availability [71]. For example, changes in water quality due to changes in stream morphology caused by river straightening or open cast mining activity, etc., can be monitored very well using direct methods that record changes in flow velocity, water bed changes, altered debris, and sedimentation characteristics, or via indirect methods as proxies for these effects by recording changes in water quality (turbidity, chlorine content, and mineral composition) using in situ as well as close-range, air- and spaceborne RS technologies (see also Section 4). Such measurements help us to better understand the interplay between geomorphology, environmental processes, and the effects of reshaping the geomorphology of landscapes through humans intervention. In situ methods for recording the various characteristics of geomorphoiversity not only have

certain advantages but also disadvantages, compared to RS approaches [72]. The following list points out some of these:

- In situ technologies are the most direct method for collecting the actual geological data required for calibrating and validating RS data, which are crucial for understanding, assessing and predicting geo-genesis and structural, taxonomic and functional geomorphodiversity;
- In situ methods enable high precision, timely measurements, are often weather-independent and offer continuous measurements with high temporal frequency;
- Time consumption, laboratory and technical expenditure is high;
- Intercalibrations have to be performed to achieve the comparability of different in situ sensor technologies;
- There are limitations to the spatial (grain or extent), directional and temporal resolution of in situ measuring devices; therefore, there are limited possibilities for investigating spatial-temporal as well as directional scale effects;
- There are limitations to investigating the interactions of geomorphological processes on a regional, continental and global scale.

3.2. RS Approaches

Due to the increased cost-free availability of different spaceborne RS information sources and access to RS-based data products, RS techniques have been widely used over recent decades for large-scale geological mapping, the identification of geomorphological features, the prediction and warning of geohazards, such as volcanic activity, earthquakes [73], and the detection of land-slides or of mass flow-induced tsunamis [74], as well as to support field measurements [75]. Research and monitoring have improved tremendously with the coupling of geographic information systems (GIS), RS data and field research [76]. However, for a successful coupling, it is imperative to understand how to capture the properties of geomorphodiversity deploying RS technologies and to identify the interfaces between in situ and RS technologies.

RS sensors for monitoring geomorphodiversity (stereo-optical, thermal, microwave or LiDAR sensors) can be mounted onto close-range RS platforms (terrestrial laser scanners (TLSs), wireless sensor networks (WSN), fixed and/or mobile towers, or balloons) airborne RS platforms (unmanned aerial vehicles (UAVs), microlights, gyrocopters, or aircraft) and spaceborne RS platforms (satellites, space shuttles, or space stations; see Figure 4). RS-based approaches are always non-destructive and are becoming increasingly cost-effective for end-users through the free access of analysis-ready data [35]. These allow the repetitive, comparable and, thus, standardized monitoring of a variety of characteristics of geomorphology [25], and are therefore crucial for modeling land surface processes, such as energy-related, geomorphological-hydrological [77] and biogeochemical processes [78] without being in direct contact with the object.

(a) (b) (c) (d) (e)

Figure 4. Different air- and spaceborne remote-sensing platforms for assessing geomorphodiversity, geomorphic traits, their changes and disturbances: (**a**) unmanned aerial vehicles (UAV or drone), (**b**) microlight—gravity-controlled; (**c**) gyrocopter or microlight helicopter; ((**d**)—top) ECO-Dimona; ((**d**)—bottom) Cessna and (**e**) satellite (from Lausch et al. [47]).

Geomorphic traits that can be monitored using RS techniques in various regions of the electromagnetic spectrum are called spectral traits (ST); the changes to these spectral

traits are referred as spectral trait variations (STV). Hence, the respective RS approaches are referred as RS spectral traits and RS spectral trait variations—concept (RS-ST/STV-C; see Figure 5) [47].

Figure 5. In situ and remote sensing (RS) approaches, common links, and the constraints of RS for monitoring the five characteristics of geomorphodiversity. Geomorphological traits are the crucial link between in situ and RS monitoring approaches (from Lausch et al. [7]).

Depending on its radiometric, geometric, spectral, angular, or temporal resolution and the available constraints (see Section 3.3), RS can only capture a part of the totality of geomorphic traits that can otherwise be captured by in situ monitoring approaches. This approach applies to all RS sensors on all RS platforms. However, the choice of an appropriate platform is crucial for an improved spatial and spectral differentiation of different geomorphic traits.

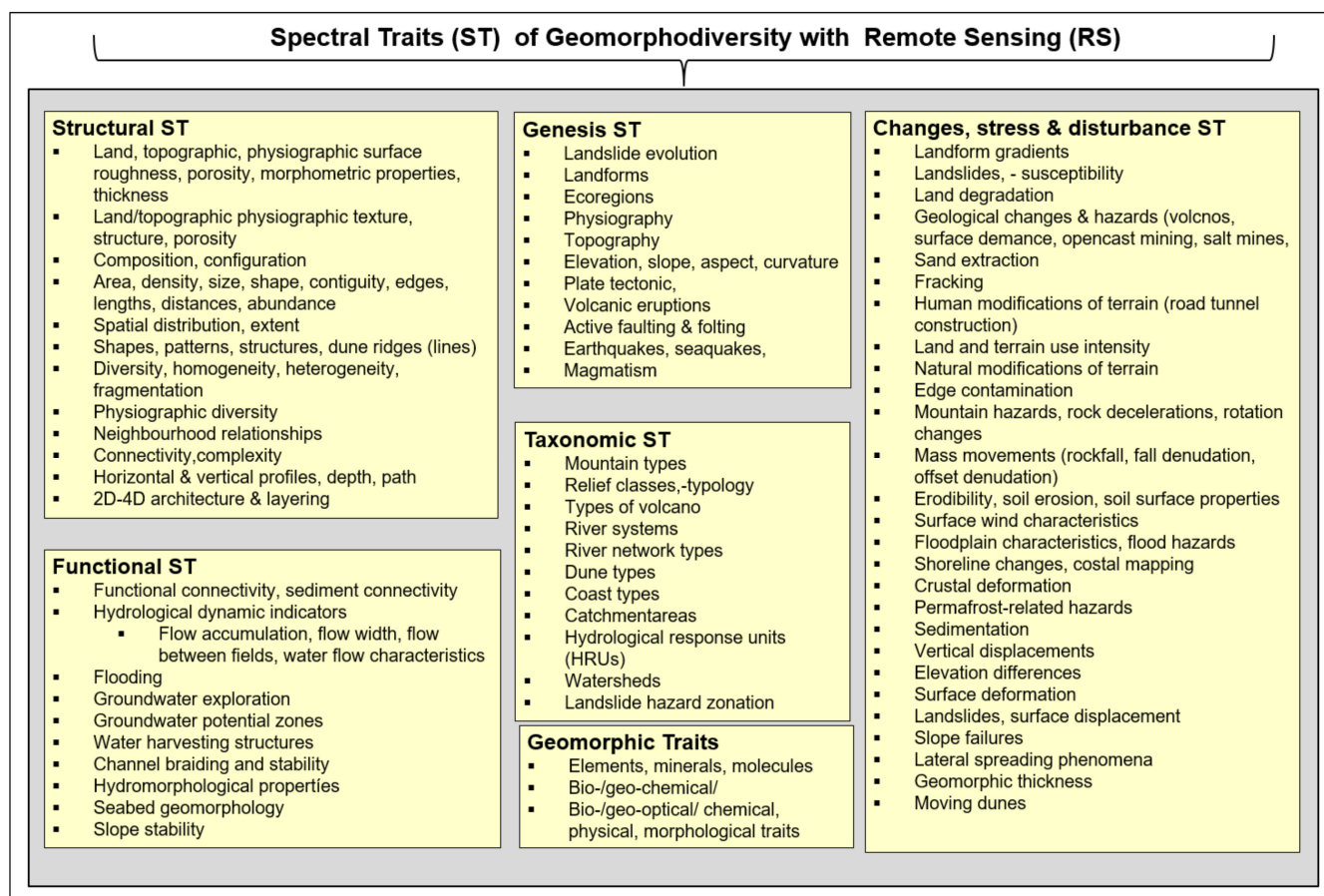Geomorphological traits are the crucial link between in situ and RS monitoring approaches and are imperative for the spatial-temporal normalization and standardization of derived geomorphologic RS products. Common links and the constraints of RS for monitoring the five characteristics of geomorphodiversity using in situ and RS approaches are shown in Figure 5 (from Lausch et al. [7]). The following sections explain this in detail, with focus on the presentation of air-and spaceborne RS technologies for monitoring geomorphodiversity. RS can capture all five characteristics of geomorphodiversity, namely: (i) geomorphic trait diversity, (ii) geomorphic genesis diversity, (iii) geomorphic structural diversity, (iv) geomorphic taxonomic diversity, and (v) geomorphic functional diversity.

A whole range of geomorphic traits can be recorded with different air- and spaceborne RS technologies (see Figure 4). Geomorphic traits are rarely recorded as 'pure geomorphic traits', but rather as trait combinations with RS. Since the constraints with RS play a decisive role, geomorphic traits can also be assigned to several groups at the same time. Figure 6 shows examples of spectral traits of geomorphodiversity, monitored by RS technologies

Spectral Traits (ST) of Geomorphodiversity with Remote Sensing (RS)

Structural ST
- Land, topographic, physiographic surface roughness, porosity, morphometric properties, thickness
- Land/topographic physiographic texture, structure, porosity
- Composition, configuration
- Area, density, size, shape, contiguity, edges, lengths, distances, abundance
- Spatial distribution, extent
- Shapes, patterns, structures, dune ridges (lines)
- Diversity, homogeneity, heterogeneity, fragmentation
- Physiographic diversity
- Neighbourhood relationships
- Connectivity, complexity
- Horizontal & vertical profiles, depth, path
- 2D-4D architecture & layering

Functional ST
- Functional connectivity, sediment connectivity
- Hydrological dynamic indicators
  - Flow accumulation, flow width, flow between fields, water flow characteristics
- Flooding
- Groundwater exploration
- Groundwater potential zones
- Water harvesting structures
- Channel braiding and stability
- Hydromorphological properties
- Seabed geomorphology
- Slope stability

Genesis ST
- Landslide evolution
- Landforms
- Ecoregions
- Physiography
- Topography
- Elevation, slope, aspect, curvature
- Plate tectonic,
- Volcanic eruptions
- Active faulting & folting
- Earthquakes, seaquakes,
- Magmatism

Taxonomic ST
- Mountain types
- Relief classes,-typology
- Types of volcano
- River systems
- River network types
- Dune types
- Coast types
- Catchmentareas
- Hydrological response units (HRUs)
- Watersheds
- Landslide hazard zonation

Geomorphic Traits
- Elements, minerals, molecules
- Bio-/geo-chemical/
- Bio-/geo-optical/ chemical, physical, morphological traits

Changes, stress & disturbance ST
- Landform gradients
- Landslides, - susceptibility
- Land degradation
- Geological changes & hazards (volcnos, surface demance, opencast mining, salt mines,
- Sand extraction
- Fracking
- Human modifications of terrain (road tunnel construction)
- Land and terrain use intensity
- Natural modifications of terrain
- Edge contamination
- Mountain hazards, rock decelerations, rotation changes
- Mass movements (rockfall, fall denudation, offset denudation)
- Erodibility, soil erosion, soil surface properties
- Surface wind characteristics
- Floodplain characteristics, flood hazards
- Shoreline changes, costal mapping
- Crustal deformation
- Permafrost-related hazards
- Sedimentation
- Vertical displacements
- Elevation differences
- Surface deformation
- Landslides, surface displacement
- Slope failures
- Lateral spreading phenomena
- Geomorphic thickness
- Moving dunes

Figure 6. Examples of spectral traits of geomorphodiversity, monitored by RS technologies.

RS technologies can record geomorphic traits, their diversity and variations, from which the other four geomorphodiversity characteristics are derived. However, compared to in situ measurements, RS approaches can only record certain parts of these geomorphic traits and their variations [7]. This is because capturing geomorphic traits and diversity using RS approaches is limited by various constraints, namely: (1) the characteristics and spatial-temporal distribution of geomorphic traits; (2) the characteristics of geomorphological processes; as well as (3) the RS sensor characteristics, the chosen RS platforms and the characteristics of RS data-processing and classification information. These constraints and limitations define the detectability, feasibility, accuracy, depth of information, repeatability, and, thus, standards disability in monitoring the five geomorphic characteristics using RS approaches.

3.3. Constraints for Monitoring Geomorphodiversity with RS

3.3.1. Characteristics and the Spatial-Temporal Distribution of Geomorphic Traits

Essential parameters for the detectability of geomorphic traits using RS are the geochemical, bio-/geo-optical, chemical, physical, or morphological characteristics of the traits. They could be manifested as color, density, condition, moisture, composition, and configuration of minerals, sediments, rocks, and morphological structures, as well as their spatial and temporal compositions and the configuration of geomorphic traits. Dune fields, for example, can be recorded with RS, since these are composed of relatively homogeneous and extensively distributed aeolian traits (i.e., sand, gravel, crushed stone, etc. (see Figure 7)). In contrast, small quantities of sand acting as a soil component cannot be recorded with RS or with high inaccuracy only [7]. The measurability of these traits based on RS is closely related to the spectral, spatial, directional, and temporal RS characteristics of the sensors used to monitor geomorphology (see Section 3.3.3). The focus for developing future RS

sensors and technologies is, thus, on detecting specific geomorphic traits that cannot yet be detected with current RS technologies.

Figure 7. (**a**) Dune sand, (**b**) sand and gravel, (**c**) gravel, (**d**) crushed stone, and (**e**) rubble; the characteristics and spatial-temporal distribution of geomorphic traits are important factors for monitoring geomorphodiversity.

3.3.2. Characteristics of Geomorphic Processes and Their Drivers

Another crucial constraint for monitoring geomorphodiversity with RS is the characteristic of geogenesis, as well as the whole geomorphic process sequence. Thus, the characteristics of geomorphic processes and process combinations, such as type, duration, intensity, consistency, intensity, extent, superposition, continuity, discontinuity and interaction define and record geomorphic structures, patterns, shapes, and form complexes that lead to a specific geomorphic trait with structural and taxonomic as well as functional diversity (see also Figure 3). The characteristics of geomorphic processes are the basis for the formation of specific geomorphic trait diversity. Plate tectonics or rock folds occur during a predominantly fracture-free crustal deformation. They are always as a consequence of compression. The five characteristics of geomorphodiversity are, thus, filters and crucial indicators of geogenesis processes and process combinations, and are the cause of changes, shifts, disturbances, and variabilities in geomorphology. Furthermore, they provide important indicators, are hotspots, and allow the prediction and differentiation between the natural and anthropogenic causes and drivers of disturbances and geohazards, such as sinkholes, landslides, subsidence phenomena, ground surface responses, mass changes, and mass transports or shifts in mass variability in the Earth's systems.
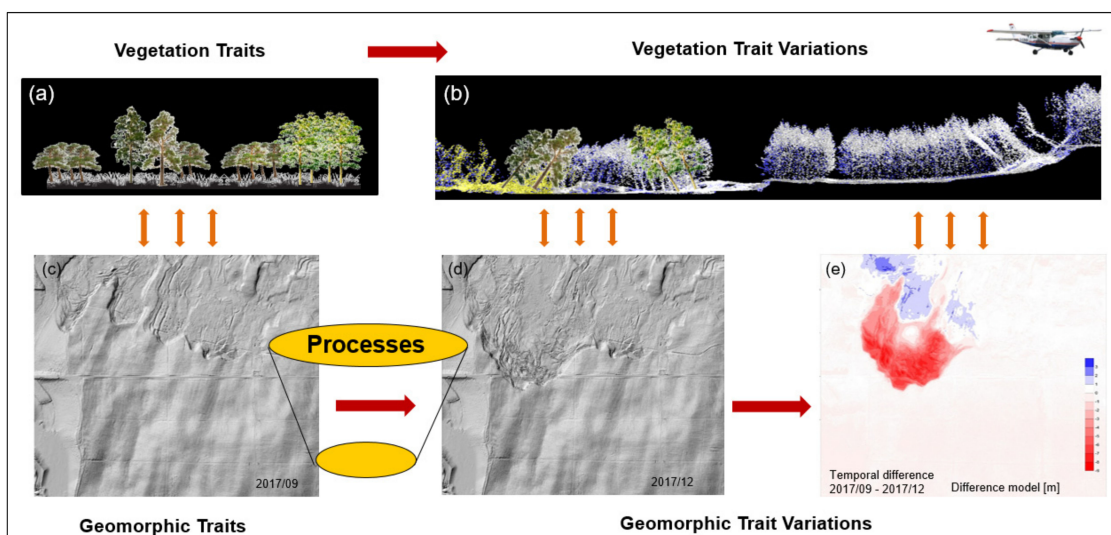
Airborne LiDAR sensors and numerous spaceborne RS technologies, such as long-term multi-sensor Interferometric Synthetic Aperture Radar (InSAR) analysis [79], GRACE [80], and GRACE follow-on (GRACE-FO) [81] can be used to record local to global properties and changes in the topography and geohazards of the Earth's surface. Measurements of mass variability can be carried out on the one hand by ALS, directly with multitemporal analyses and the difference modeling of digital elevation models (DEM) and, on the other hand, indirectly through the interactions of topography, soil and water (traits of geomorphodiversity) with traits of biodiversity, such as microorganisms [82] or plants [83]. Changes in bio-traits are crucial proxies of geomorphic processes and disturbances, which RS can measure. For example, the changes in woody plants due to an instability of the subsoil from sinkholes and mass changes could be recorded using ALS (Figure 8).

3.3.3. Sensor Properties and Platforms to Monitor Geomorphodiversity

Geomorphic processes and changes define the shapes of the traits, their combinations and trait variations on all scales of geomorphic organization (see also Figure 3). Therefore, geomorphological features should be captured by sensors on different RS platforms (from close-range to space-based platforms). An RS pixel can contain both pure and mixed spectral information about the geomorphological traits. Thus, on the one hand, the accuracy of the classification of geomorphic features that can be captured with RS depends on the properties and the spatio-temporal distribution of the geomorphic features (see Section 3.3.1). On the other hand, the properties of RS sensors, such as radiometric, spectral, geometric, directional, and temporal resolution, are crucial in the detectability and monitoring of geomorphic features. Thus, specific mines, mineral compositions, structures, and patterns, as well as distributions of geomorphic features, can only be detected by RS technologies if the
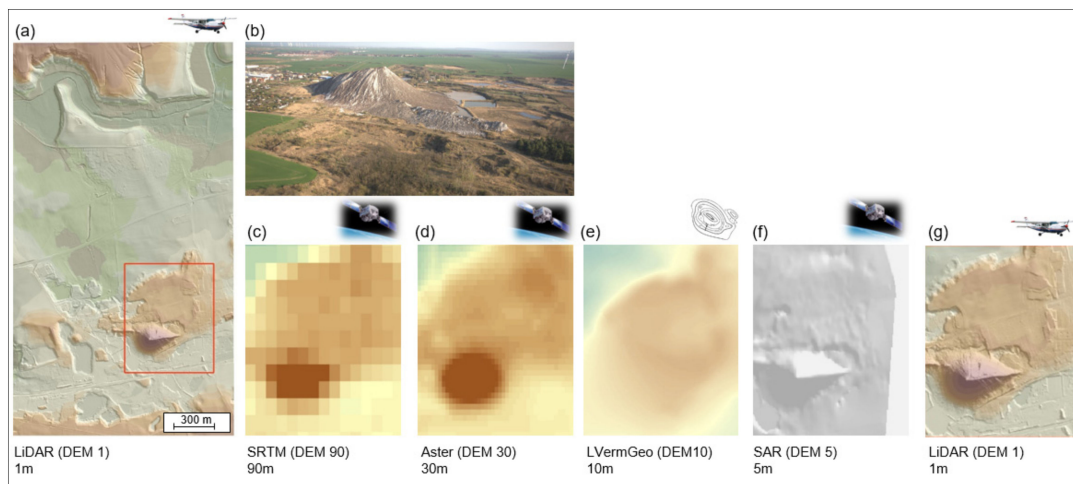
spectral characteristic or RS technology is suitable for detecting these features. For example, RS technologies with (about 20–400) spectral bands, such as hyperspectral technologies (e.g., airborne HySPEX, the airborne imaging spectrometer (AISA), the airborne PRISM experiment (APEX), space-borne DESIS, or EnMAP), are suitable for capturing the mineral composition of mountains with a high level of detail [84], or surface quartz content in sand dunes [85], boulders or bedrock. Meer et al. [86] provide an overview of multi- and hyperspectral geological RS. Multitemporal RS approaches (e.g., the Landsat 5–9 time series [30]) also allow continuity in the detection of changes and shifts in geomorphological features and, thus, the monitoring of changes and disturbances in bio- and geomorphodiversity caused, e.g., by river-straightening or the large-scale mining of construction sand in coastal regions. A wide range of other examples can be found in Table A1 in the Appendix A of this paper. Furthermore, the direction of solar radiation, as well as a change in the inclination of topographic features in the DEM or digital surface model (DSM) leads to a change in brightness depending on the direction of the solar radiation and is the basis for monitoring the direction of inclination [87].

Figure 8. Changes in geomorphic traits lead to geomorphic trait variations. These changes can also lead to a change in vegetation traits, as geo- and biodiversity interact with each other either directly or indirectly. This example shows changes in geomorphology caused by underground open-cast mining with subsequent landslides. (**a**) Woody plants at the edge of a watercourse, (**b**) Overthrow of woody plants as a result of the collapse of underground open-cast mining tunnels and subsequent landslides, (**c**) Digital elevation model (DEM) recorded by airborne laserscanning (ALS) three months before the event (2017/09), (**d**) DEM recorded by ALS after the event (2017/12), (**e**) Difference model shows the geomorphological changes caused by the event.

The temporal resolution of RS plays a particularly important role in monitoring dynamic morphological processes and changes. Examples are the automated spatio-temporal detection of landslides using Rapid-Eye RS data [88], the InSAR interferometry of surface deformations [89], dune spatial-temporal aeolic patterns (length, minimum spacing density, orientation, height, and sinuosity), aeolian dune composition configuration (complexity, diversity, shapes, patterns, and heterogeneity), dune ridges [90], coastal landforms, coastline and shoreline detection [91–93], the geomorphic delineation of floodplains and terraces, meander dynamics or channel characteristics.

The spatial RS characteristic defines the level of detail of geomorphological objects in a classification. It is crucial in the monitoring and use of DEM [7] (see Figure 9), whereas in taxonomic differentiation, the geometric as well as the spectral resolution (multispectral or hyperspectral) of the RS sensor is target-oriented.

Figure 9. For discrimination and successful monitoring, in addition to the characteristics and the distribution of geomorphic traits and their changes, the spatial characteristics of the deployed RS sensors are of major importance. Here the importance of the spatial resolution is illustrated through a comparison of DEMs of a post-mining potash tailings pile, Teutschenthal-Bahnhof, near Halle, Germany (see also Schwefel et al. [94]): (**a**) LiDAR (DEM 1)—1 m, (**b**) photo of the post-mining landscape with the 95 m high potash tailings pile, (**c**) SRTM (DEM 90)—90 m, (**d**) Aster (DEM 30)—30 m, (**e**) DEM generated from height information of the land surveying office—LVermGeo (DEM 10)—10 m, (**f**) SAR (DEM 5)—5 m, (**g**) LiDAR (DEM 1)—1 m (from Lausch et al. [7]).

3.3.4. Summary of Constraints

Summarized, the following factors are essential for a successful recording, discrimination and monitoring of geomorphodiversity and its changes with RS (from Lausch et al., 2020 [7]):

- The characteristics of the combinations of geomorphic processes (i.e., the scope, length, intensity, consistency, dominance, and overlay) that lead to the formation of characteristic geomorphic traits, geo-genesis, taxonomic, structural, and functional diversity.
- The characteristics, composition, and configuration, such as the shape, density or distribution of the geomorphic traits and trait variations in space and over time.
- The radiometric, spectral, spatial, and temporal resolution of the RS sensors are crucial for the successful detection and monitoring of the five features of geomorphodiversity.
- The choice of RS platform (close-range, air- or spaceborne) influences the spatial and temporal resolution and, ultimately, the recordability and precision of the RS sensor properties of the geomorphic traits.
- The choice of the classification method (spectral-based pixel classification or spectral-based geographic object-based image analysis (GEOBIA) [95]), and how well the applied classification algorithm and its assumptions fit the RS data and the spectral traits of geomorphology.
- Sensors with different sensing properties should be combined to detect different geomorphic traits and trait variations simultaneously.
- A multi-variate and multi-temporal implementation of RS sensors, such as multispectral, hyperspectral, LiDAR, RADAR, microwave radiometer, and thermal infrared (TIR) sensors, increase not only the number but also the characteristics and diversity of geomorphic traits and trait variations that can be recorded.
- Geomorphological features/traits should be captured with a combination of sensors to combine different RS advantages (a multi-sensor and multi-temporal RS approach) and to compensate for and/or complement the technological limitations of sensors. For example, synthetic aperture radar (SAR) data for 5 m^2 contains mixed information about geomorphic traits, with the advantages of other sensor technologies (e.g., 25 points/m^2 of LiDAR data to record DEM and its changes).

4. Monitoring Five Characteristics of Geomorphodiversity Using RS

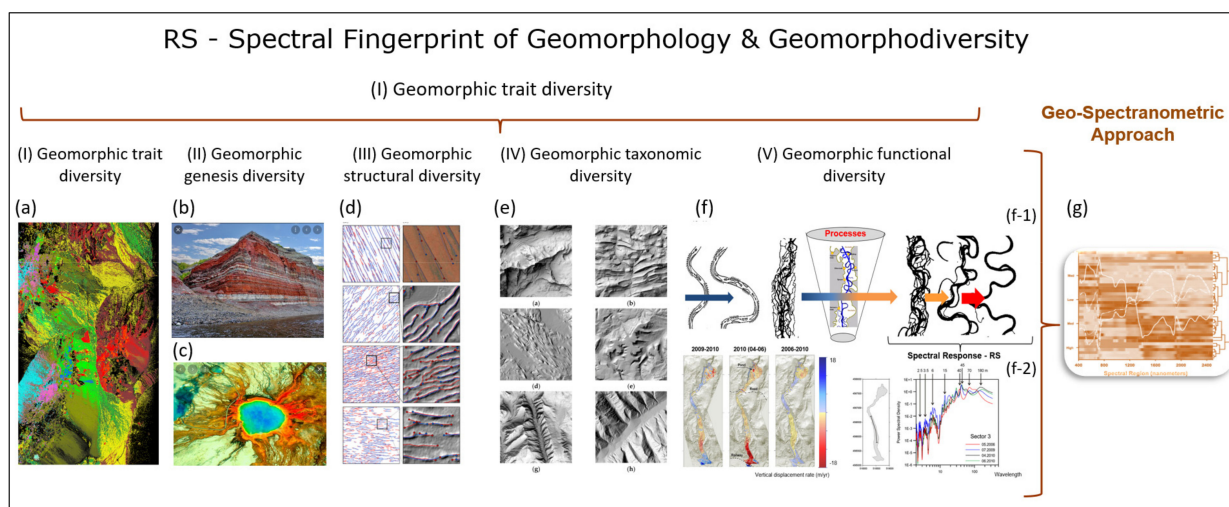*4.1. Geomorphic Trait Diversity and Its Changes Using RS*

"Geomorphic trait diversity represents the diversity of mineralogical, bio-/geochemical, bio-/geo-optical, chemical, physical, morphological, structural, textural or functional characteristics of geomorphic components that affect, interact with or are influenced by the geomorphic-genesis diversity, the geomorphic taxonomic diversity, the geomorphic structural diversity, and the geomorphic functional diversity" [7] (see Section 2).

Only when features, such as the radiometric, geometric, spectral, angular, or temporal resolution of RS sensors, are specific for the detection of geomorphological spectral features, these can be detected with RS. The requirements for the resolutions differ, for example, when different minerals (silicates, oxides, carbonates, sulfates, chlorides), material types (sand, rock, gravel, soils), material properties (texture, colors, shapes) or form features (river valleys, fracture steps, pits, slope inclinations, or curvatures of river loops) should be detected.

RS can record and monitor geomorphic trait diversity based on geomorphic spectral traits/trait variations. If the landforms to be recorded do not differ with respect to the mineralogical, bio-/geochemical, bio-/geo-optical, chemical, physical, morphological, structural, textural, or functional characteristics of their geomorphic components, then they cannot be differentiated from each other using RS technologies. The detectability of geomorphic trait diversity forms a crucial basis for the detection, differentiation, classification, and monitoring of the remaining four characteristics of geomorphodiversity.

In regions without vegetation cover compared to regions with vegetation cover, the recording of geomorphic trait diversity with RS technologies is possible using direct RS indicators. The spectral RS signal is the result or integral of the state and the changes, shifts and/or disturbances of geomorphic traits, geogenesis traits, structure traits, and taxonomy as well as functional traits. In regions covered by vegetation, water or ice, indirect indicators may be used in addition to the direct RS indicators that are integral to the response of traits in bacteria, algae, plants, populations, communities, and traits of landforms and their interactions. In Section 6, methods for the discrimination and classification of the five characteristics of geomorphodiversity are discussed in detail.

RS techniques are, therefore, the only and the most essential method and basis for monitoring geomorphic trait diversity, which is the basis of the geo-spectranometric approach and the "spectral fingerprint of geomorphology and geomorphodiversity" (see Figure 10).

Figure 10. All five characteristics of geomorphodiversity can be recorded using RS technologies. The individual characteristics of geomorphodiversity are illustrated by means of examples, which are: (I) geomorphic trait diversity, (**a**) AVIRIS hyperspectral RS data was used to classify the mineral distribution and the geomorphic traits in the Cuprite area, Nevada (from Clark et al. [96]); (II) geomorphic

genesis diversity, (**b**) photo of the characteristic relief forms created by the exogenous and endogenous genesis processes genesis, (**c**) TIR image of part of the Siberian Trap supervolcano; (III) geomorphic structural diversity, (**d**) derivation of dune pattern mapping with RS (from Shumack et al. [97]); (IV) geomorphic taxonomic diversity, (**e**) classification of different mountain types using RS (from Farmakis-Serebryakova et al. [98]); (V) geomorphic functional diversity, (**f-1**) processes of geogenesis and river degradation lead to changes in morphometric river features, (**f-2**) the morphometric changes can be recorded using RS data, reprinted with permission from Ventura et al. [99], 2021, Elsevier. license number: 4856041399548; (**g**) The integration and combination of all five features form the basis of the geo-spectranometric approach and lead to the 'spectral fingerprint of geomorphology and geomorphodiversity'. All features and individual figures are explained in detail in the following chapters.
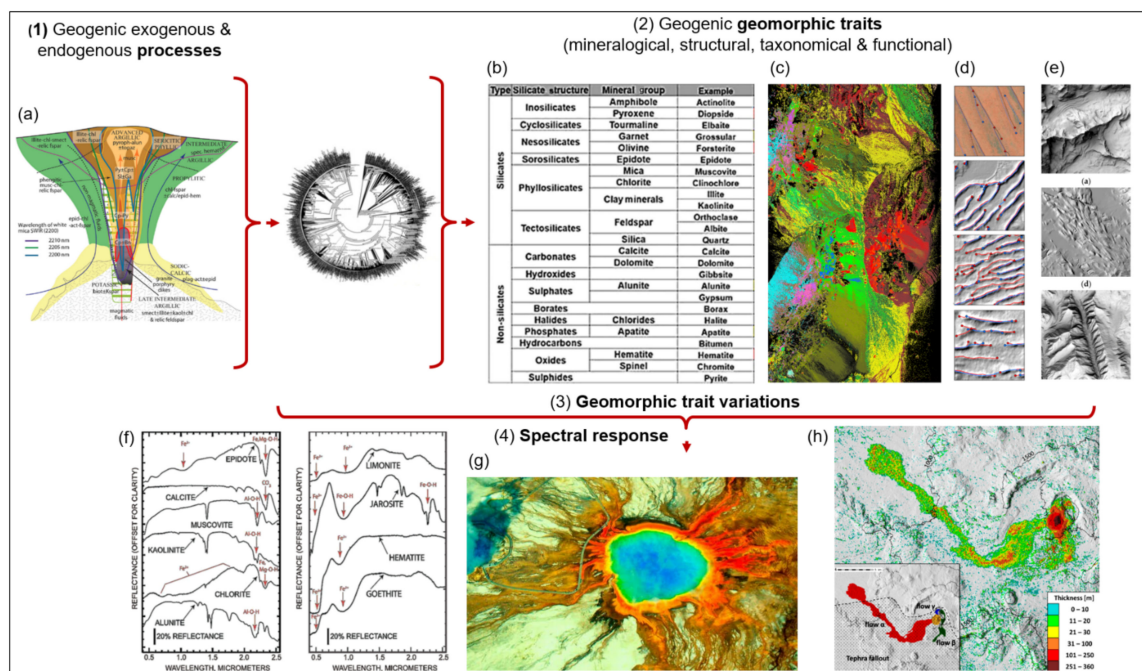
4.2. Geomorphic Genesis Diversity Using RS

"Geomorphic genesis diversity represents the diversity of the length of evolutionary pathways, linked to a given set of geomorphic traits, taxa, structures, and functions. Therefore, sets of geomorphic traits, taxa, structures and functions that maximize the accumulation of geomorphic functional diversity are identified" [7] (see Section 2).

The Siberian Trap and the Deccan Trap, also called the Deccan Large Igneous Province, are examples of geological volcanic eruptions that led to the formation of characteristic geomorphic genesis diversity [75]. As a result of the volcanic activity from 252 million years ago (the duration of the flood basalt event being ~900,000 years), extensive areas of flood basalt (with a total thickness of up to 6500 m) were formed in the Sibierian Traps. The Sibierian Traps extend from the West and North Siberian Lowlands and the Central Siberian Highlands as well as to part of the Central Yakutian Lowlands, including the western slope of the East Siberian Highlands. The impacts of the eruptions produced up to ~2000 km^3 of lava, leading to a large-scale distribution and volcanic deposit-covered area of ~7 million km^2. Enormous releases of sulfur dioxide, methane, carbon dioxide, and large amounts of hydrogen sulfide from volcanic as well as organic (bacterial) sources [100], resulting in the formation of mountain structures such as the Putorana Mountains. Present-day deposits of silicon-rich migmatites, large amounts of volcanic tuffs, and pyroclastic deposits such as rhyolite, and metal-bearing rocks such as nickel, copper, and palladium are mined from extensive deposits today. The eruptions and their impacts are thought to be causally related to the mass extinction at the end of the Permian era. Thus, the toxic effects and extreme temperature increase of terrestrial and marine areas by 8 to 10 °C led to the collapse of many ecosystems and the emergence of new forest habitats, which only repopulated larger areas after about 15 million years. In contrast to the ammonites, conodonts, and foraminifera (with a regeneration time of 1 to 3 million years), the damaged coral reefs needed some 8 to 10 million years for complete regeneration.

RS has added a new dimension to the monitoring of geomorphic genesis diversity, its characteristics, consequences, disturbances, and biodiversity. RS can describe genesis traits (minerals, rock types), taxa (mountain types) structures (genesis patterns, lineaments), and functions (run-off behavior), which represent geological tectonic architecture and its features [101]. Detailed structural and pattern analyses using RS technologies help to interpret, classify, discriminate and, thus, identify the genesis of various structures and patterns in the Siberian and Deccan Traps [75]. Thus, RS-based lineament analyses are crucial key elements for interpreting local, regional, and continental geogenetic structures [76]. Any naturally formed linear feature on the Earth's surface that is related by the processes of extension, compression, strike-slip, or as a result of the magmatic or metamorphic activity, is called a lineament [75]. There are various geotaxonomic forms of lineaments, including rock types, linear sinkholes, fault-related traps, fold hinges, faults, shear zones, dykes, mineralized veins, uplifted topography, or contacts between elongated fractures or fault-bound elongated valleys [76,102]. In addition to lineaments, terrain patterns or fluvial drainage patterns provide important clues about the causes, trends, and nature of subsurface structures that cannot be detected with RS [76]. Drainage patterns in flat terrain are usually

dendritic; however, in a dome or mountain structure, drainage patterns are radial and concentric [102]. Orthogonal, barbed, and double-drainage or compressed meanders are other examples of drainage patterns that control the course of water movement through their structure [75,76,103].

If lineaments, their patterns, or substructures are not directly visible and cannot be recorded using RS techniques, then, vegetation traits or plant functional types [50,104] or land-use anomalies and groundwater patterns [105], or the delineation of shallow Deccan basaltic aquifers using aerial photointerpretation [106], or channel widths, landslides, faults, or high-spatial-resolution Google Earth imagery in the study of Earth surface processes [107] can be used directly or as a proxy for geomorphic genesis diversity. Figure 11 shows the process of geogenesis that leads to the formation of geomorphic genesis diversity, which can be recorded with different RS technologies.

Figure 11. (1) Geogenic exogenous and endogenous processes, such as in such as a volcanic eruption (**a**) leads to characteristic geogenic geomorphic traits. (2) Geomorphic traits can be: mineralogical, structural, taxonomic and functional traits, such as: (**b,c**) different minerals, (**d**) different sturcural forms and form complexes, (**e**) different rock types. Consequently, the processes, e.g., volcanic eruptions lead to (3) geomorphic trait variations and the shaping of terrain and mountains. Geomorphic traits and trait variations produce a morphologogically specific (4) spectral response, which can be detected using different RS technologies. (**f**) Laboratory spectral features of different hydrothermal minerals and mapping results from RS analysis are crucial for mineral classification, (**c**) VNIR-AVIRIS hyperspectral data from the Cuprite area (Nevada) show results of lithography classification using hyperspectral RS data, (**g**) Representation of a volcanic eruption using RS of the Siberian Trap, (**h**) Distribution of volcanic deposits optained by differencing pre-eruptive and post-eruptive DEMs derived from ASTER and PlanetScope RS Data, location—Nabro volcano; Image sources: (**a,b**) from Peyghambari and Zhang [108], (**c,f**) from Clark et al. [96], (**d**) from Shumak et al., [97], (**e**) from Farmakis-Serebryakova et al. [98], (**h**) reprinted with permission from Calvari et al., [109], 2022, Elsevier. license number: 5303110916041.

4.3. Geomorphic Structural Diversity Using RS

"Geomorphic structural diversity is the diversity of composition and configuration of 2D to 4D geomorphic structural traits" [7] (see Section 2).

Exogenous and endogenous processes are responsible for generating relief and form, leading to the development, structuring, and shaping of our Earth's crust and entire ecosys-

tems. Geomorphometry, geomorphic structure, patterns, diversity, relief, and topography are all crucial for the functionality, feedback, and resilience of geomorphology and the biota controlling the Earth's surface processes and landforms [3,110,111]. Spatial-temporal heterogeneity and evolutionary geomorphological structures and patterns lead to plant and animal species diversity and gradients in ecosystems, increasing the niche dimensionality of species and consequently supporting species richness and biodiversity [112,113]. The 2–3D structures and sculpture forms, patterns, and communities enable essential conclusions to be drawn about the relief, structure, rock, and soil-formation processes during genesis. The diversity of geomorphic structures, patterns, and forms provides not only crucial information about the type and origin of the process but also its characteristics, such as the scope, length, intensity, consistency, dominance, and overlay of the process. Furthermore, spatial-temporal geomorphic patterns can equally be used to describe the degree of naturalness or anthropogenic influence or degree of human influence (hemeroby) [114,115] on geomorphology and landforms.

Through land use intensity (LUI) and urbanization, ponst-mining landscapes, forestry intensification or river regulation evolutionary geomorphic structures and shape patterns are altered and, in some cases, are so heavily overprinted that the original evolutionary structures are now challenging to monitor. Numerous examples of geomorphic imprinting define the terrain of our present-day cultural landscape, such as buildings, cities, streets, terraces, boundary walls, brownfields, ditches, canals, reservoirs, or restored wetlands. The characteristics of geomorphic structures are, therefore, crucial fingerprints of human influence [17]. For this reason, geomorphic structural diversity is an important indicator for measuring and assessing inferences regarding the state, changes, and the origin, type, and intensity of human influence. This allows essential conclusions to be drawn about the functionality and resilience of a particular ecosystem. In this way, for example, river straightening leads to measurable morphological changes in fluvial landforms, which influence their functionality [116], see also Section 4.5). Geomorphic structures and patterns are crucial for the discrimination of geomorphic taxa and, thus, the characterization of geomorphic taxonomic diversity using RS (see Section 4.4; see also Figure 12).

Figure 12. Geomorphic structural diversity, monitored with remote sensing technology. Examples of dune-field landscape patterns on remotely sensed data. (**a**) Barchan dunes, (**b**) linear dunes, (**c**) dome dunes, (**d**) reticulate dunes, and (**e**) longitudinal dunes (reprinted with permission from Zeng et al. [117], 2021, Elsevier. license no. 5176660806321).

Structural diversity exists on all levels of a geomorphic organization. Therefore, structural geomorphic traits can be recorded by different RS platforms and, thus, on all spatial-temporal and directional scales of geomorphology. To successfully record and monitor structural diversity and its traits, the spatial, spectral, radiometric, angular, and temporal characteristics of the RS sensors play a significant role. Moreover, the distribution, density, and composition, as well as the configuration of structural traits, also play a major role here (see also Section 3.3.1). Examples are the structures of fluvial landforms such as channel characteristics, floodplain morphology hydraulic channel morphology, geometries, topography, river width arc length, longitudinal transect or channel slope, or below waterline morphology. Morphometric patterns can be recorded with high-resolution
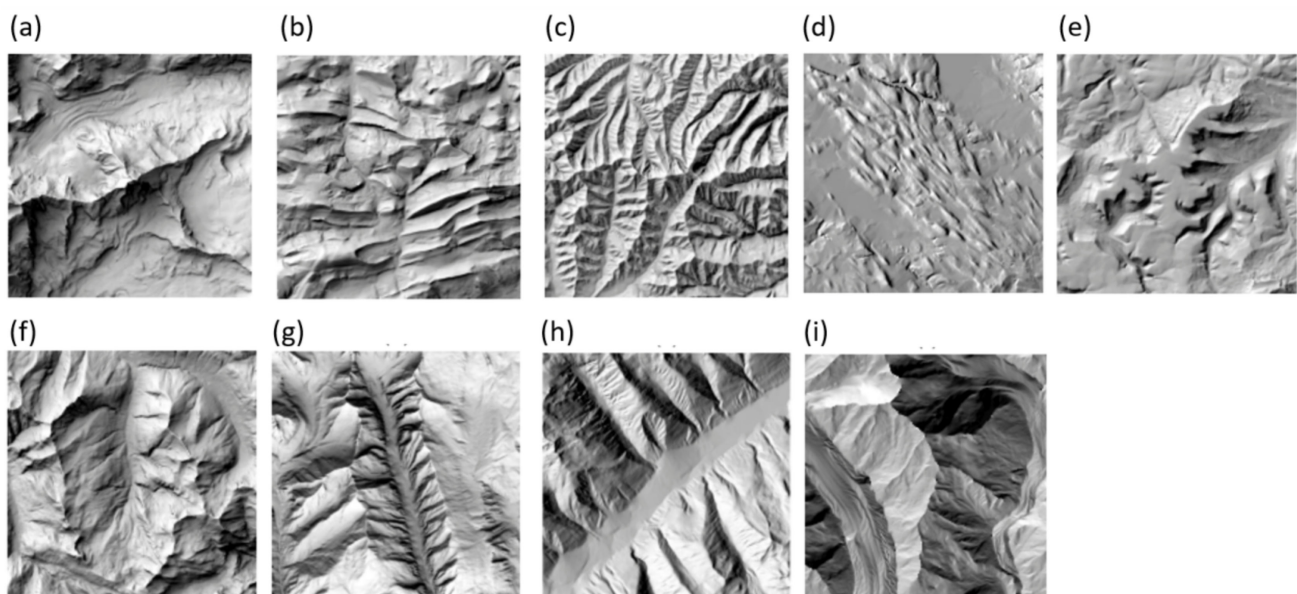
LiDAR technologies, whereas optical RS approaches are doomed to fail with a spatial resolution of only 20 cm.

The choice of sensor technologies and characteristics is crucial to capture the exact geomorphological structure, such as topography. This will determine the model quality and, consequently, the quality of the prediction of disturbance effects in landscapes. Thus, ecological and hydrological model predictions are only as good as the quality of the input data that are collected by RS [7]. For example, by capturing the detailed terrain structures of coastal regions through airborne LiDAR data, it has been demonstrated that more than three times as many people are at risk from climate change and rising sea levels than was previously calculated from less detailed shuttle radar topography (SRTM)-DEM-RS data [92].

4.4. Geomorphic Taxonomic Diversity Using RS

"Geomorphic taxonomic diversity is the diversity of geomorphic components that differ from a taxonomic perspective" [7] (see Section 2).

Different evolutionary processes (geogenesis), such as plate tectonics, mountain building, or volcanism are described by the numerous geomorphic taxa (also referred to as types, classes, or units) of mountains, reliefs, volcanoes, channels, rocks, and landforms, leading to the development of different geomorphic taxa with specific geochemical, mineralogical, and structural properties, forms, and shape classes. This taxonomic diversity, heterogeneity, and richness of different geomorphic types (mountains, dunes, coast, or dune types) define the state, stability, and resilience of the entire geosphere and biosphere, as they induce a high diversity of ecosystem processes, functions, forms, and types of structures, ultimately forming ecological niches (see also Figure 13).

Figure 13. Geomorphic taxonomic diversity using RS. The most suitable relief shading methods per landform based on the survey results: the clear sky model method for (**a**) block mountains; (**b**) folded mountains; (**c**) mountains formed by erosion processes; (**d**) cluster shading for drumlins; (**e**) plateaus; and (**f**) V-shaped valleys; (**g**) clear sky model with custom illumination (here, S) for U-shaped valleys; (**h**) standard hill-shading with custom illumination (here, W) for alluvial fans; and (**i**) aspect shading for glaciers (from Farmakis-Serebryakova et al. [98]).

Different geomorphic types (taxa) vary in terms of their different geomorphic traits, in their geogenesis, structure, and function. For example, the production of volcanic lavas, solids, and gases shapes various characteristic volcanic forms. In addition, there are differentiating properties of the resulting volcanic products, such as gaseous, viscous, or low viscosity to solid properties. Likewise, the character of the production of different

volcanoes differs, e.g., from explosive to effusive. Cinder volcanoes, for example, were formed from loose material and have a characteristic cone shape with a slope of 30–40°, leading to the formation of the distinctive concave slope shape. Furthermore, volcanic ash created the vast grass-covered savannah areas of the Serengeti, preventing the invasion and development of forest communities.

However, anthropogenic changes, such as land-use intensity, agricultural expansion, urbanization, climate change, or resource extraction have influenced, shaped, and defined a variety of landforms and geomorphic types for thousands of years [28]. This has led to changes in evolutionary types and the formation of distinctive anthropogenic-geomorphic types with strong anthropogenic features such as reservoirs, embankments, canals, mines, terraces or roads, buildings, and cities [17]. The expression of geomorphic characteristics and types present today, thus, range from "purely evolutionary types" to "strongly anthropogenic-geomorphic-dominated types", which demands special recording and assessment procedures. Anthropogenic geomorphic features, such as linear structures, river straightening, and the characteristic structures of terraces or mines can now be used to monitor the degree of human influence and to improve the discrimination and classification of geomorphic types.
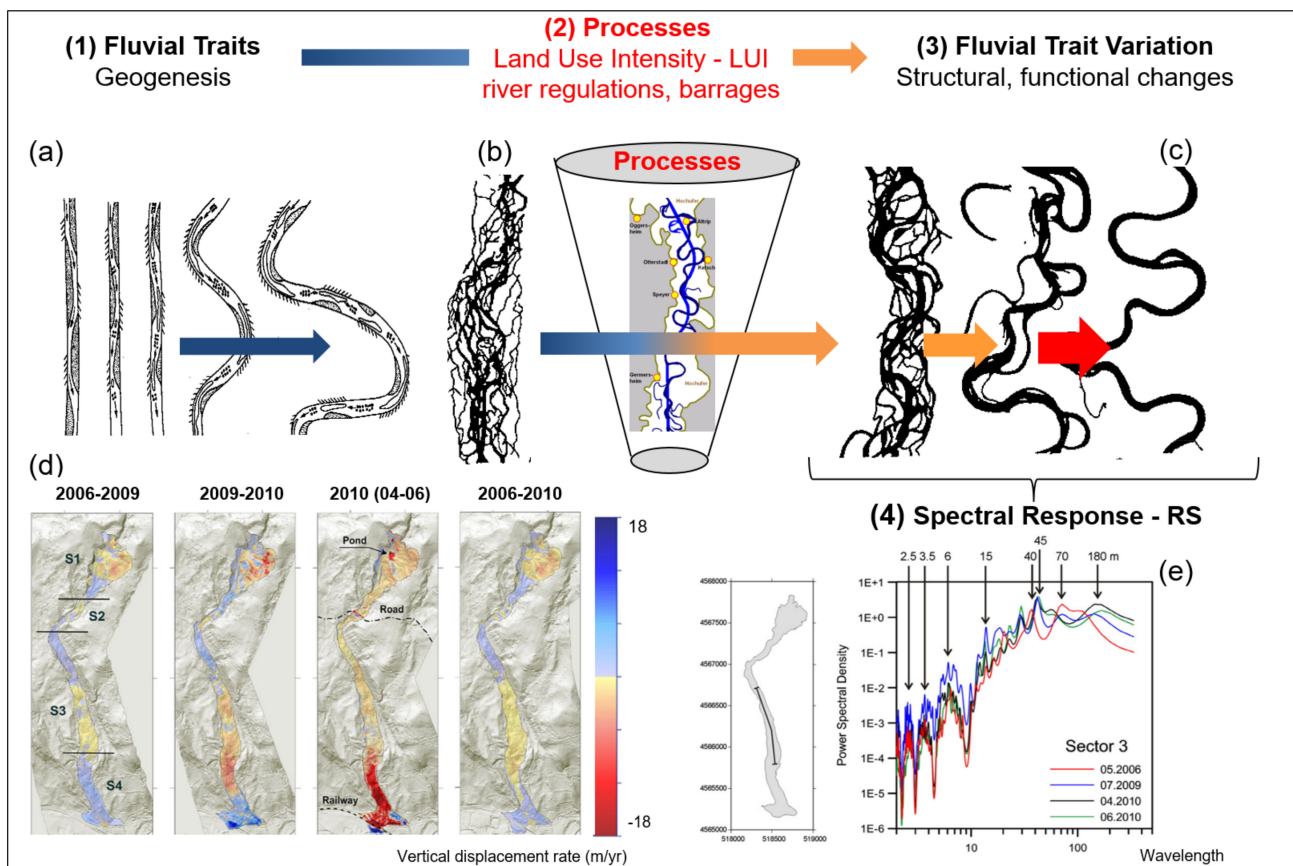
RS techniques can capture traits in geomorphology [7], soil characteristics [47], and the responses of above- and belowground diversity [118] as well as biodiversity [50,104], depending on their RS characteristics. Many RS technologies are being used to detect human impacts and changes in the geomorphic taxa through LUI, using spectral image analysis—such as the monitoring of river degradation, terrain creation [17], and coastal structure changes with LiDAR [92], or urbanization (cities and roads) using multispectral, LiDAR or RADAR technologies [17].

4.5. Geomorphic Functional Diversity Using RS

"Geomorphic functional diversity is the diversity of geomorphic functions and processes as well as their intra- and inter-specific interactions" [7] (see Section 2).

Through anthropogenic impacts, such as urbanization, land-use intensity, and river straightening, the 19th to the 21st centuries increasingly witnessed irreversible changes and disturbances to the natural geomorphology, leading to considerable disturbances in the functionality and resilience of geosystems. Using the example of river straightening, we briefly discuss the basic reasons why RS can record genesis and structural and functional changes.

Rivers adapt their path according to the temporal variations of their outflow. Hence, during geogenesis, meanders emerged due to convergent and divergent flow movements that were transverse to the general direction of flow (see Figure 14a). The number of factors influencing the formation of meanders can still not be fully explained today. However, it is understood that the meanders of a river are the expression of a stable, dynamic balance between the river and the riverbed, creating characteristic fluvial biodiversity with high self-purification potential. The geometry of meanders, both cut-off meanders and oxbows, can greatly differ since meanders are subject to a permanent positional change. In the 19th century, flood prevention measures were undertaken on the Upper Rhine (a reduction in areas prone to flooding), to regulate low-water levels (e.g., for year-round shipping) as well as regulations to produce hydropower.

Figure 14. Monitoring status and changes to geomorphic characteristics with RS. (**a**) Different processes during geogenesis lead to the formation of specific morphometric fluvial traits—the meanders, (**b**) the entire river system is characterized by these meanders. (2) Processes/drivers such as land-use-intensity, river regulations, or barrages lead to (**c**) changes in structural, functional fluvial traits (fluvial trait variations) (**d,e**). These fluvial trait variations lead to spectral responses in the remote sensing signal (**d**). Example of monitoring temporal changes of fluvial traits—vertical displacement rate of the river system from 2006–2010 with remote sensing technologies (LiDAR) (**d,e**). From Ventura et al. [99], Reprinted with permission from Ventura et al. [99], 2021, Elsevier. license no. 4856041399548.
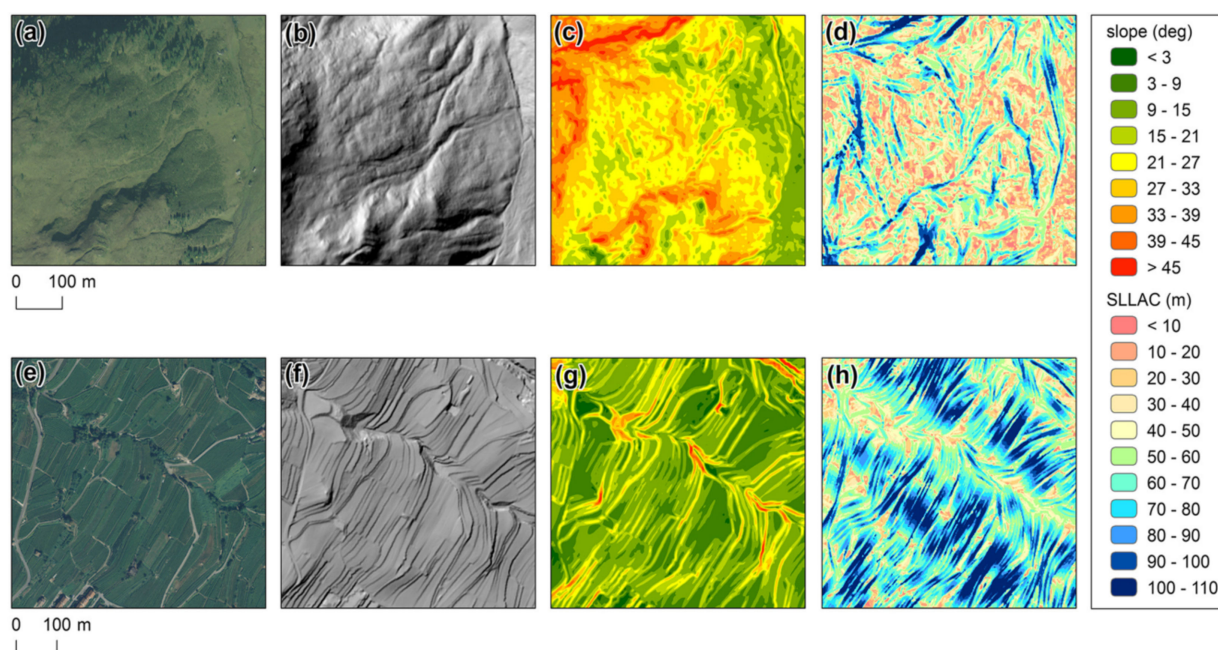
The morphological impacts of these "corrective measures" on the River Rhine in Germany altered the erosion and sediment behavior of the river. At the same time, the flow velocity increased, leading to strong vertical erosion of up to 7 m in the Rhine. As a result of this eroded material, sandbanks and gravel banks frequently formed, and these barrages acted as sediment traps, which meant that further measures were then required to regulate low-water levels [119]. Hence, river regulations or barrages (Figure 14b,c) lead to changes in the genesis, structural and functional fluvial traits, subsequently leading to fluvial trait variations (Figure 14c). The structural geomorphological changes in the original meandering or sediment displacement can now be recorded using RS approaches because these fluvial trait variations lead to spectral responses in the RS signal (Figure 14e). Figure 14d shows one example of monitoring the temporal changes of fluvial traits—the vertical displacement rate of the river system from 2006 to 2010—with RS technologies (LiDAR).

In addition to structural changes, hyperspectral technologies (HySPEX, AISA, CHIME, or EnMAP) can be used to make statements about changes to vegetation diversity and water quality (increasing eutrophication, chlorophyll content, and turbidity); in other words, impacts from river straightening. There are numerous examples of monitoring topography and relief (DEM, DSM) using RS technologies.

5. Monitoring Geomorphodiversity in Regimes with Changing Land-Use Intensity

The increasing global loss of river connectivity and consequently the loss of fully functioning ecosystems has had dramatic impacts on the world's coasts, e.g., in Brazil, Mexico, the USA, Greece, or Japan. Reservoirs alter the balance of sediment and coastal erosion, change the flora and fauna, and lead to a loss of functioning ecosystems ecosystems [14,120]. Deforestation and slash-and-burn practices also lead to severe erosion and the alteration of biodiversity and geomorphodiversity, as well as the entire hydrological regime in mountainous or rainforest areas [121], while mining or geothermal energy practices lead to subsidence or sinkholes. Although geomorphological genesis led to the formation of permafrost soils, which normally act as carbon sinks, the melting of permafrost due to climate change and the intensification of land use is now causing northern-hemisphere soils to release carbon back into the atmosphere [82]. The enormous complexity and interactions of natural endogenous and exogenous processes, as well as the increasing impact of intensification and urbanization on geomorphology, increasingly demand a multidisciplinary approach to monitoring and modeling geomorphic structures, functions, and hazards [122,123].
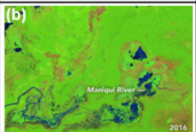
By comparing evolutionary and anthropogenically induced geomorphic structures and structural forms, conclusions can be drawn about the degree of anthropogenic overprinting. The anthropogenic fingerprint of geomorphology can be derived using RS technologies technologies [17,28] (see also Figure 15).
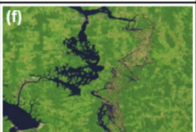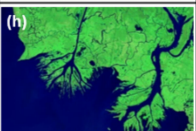

Figure 15. By comparing evolutionary and anthropogenically induced geomorphic structures and structural forms, conclusions can be drawn about the degree of anthropogenic overprinting. The anthropogenic fingerprint on geomorphology can be derived using RS technologies. "Images illustrating the detection of the anthropogenic topographic signature of terraced landforms in the Alpine context (Trento Province, central Italian Alps, Italy). Images of natural (**a**–**d**) and terraced landscapes (**e**–**h**) are derived from aerial photographs (**a**,**e**); shaded relief maps are derived from 2 m LiDAR digital terrain models (DTMs) (**b**,**f**); slope maps (**c**,**g**); and maps of the slope local length of auto-correlation (SLLAC) (**d**,**h**). The LiDAR dataset is offered as a free download by the Autonomous Province of Trento (Alps). Natural landscapes show maps of SLLAC with randomly distributed elements and highly noisy backgrounds, whereas the construction of terraces yields a clear topographic signature that results in more regular SLLAC maps, with ordered elongated elements that follow the terrace benches" (from Braun et al. [28]).

Increasing or decreasing intensity in human-induced process regimes is a significant force shaping geomorphodiversity [17]. Monitoring the associated spatio-temporal trait variations with active or passive RS techniques can be translated into taxonomic geomorphological changes and spatial-temporal trait variations (see Figure 16 for examples). Most of the time, increasing land-use intensity decreases the diversity in geomorphic forms and traits. River regulation and agricultural and urban expansion lead to a reduction in these features. The same applies to dam construction, where complicated stream patterns are replaced with a lake and a single large dam feature. Potentially, losses in geomorphodiversity can be restored in the case of declining land-use intensity. With increases in sediment loads, deltas can grow again, forming complex marshlands (Figure 16).

No	Land use intensity (LUI)	Process changes	Temp. scale	Trait changes observable with optical RS (or direct changes)	Trait changes observable with active RS (or indirect changes)	Taxonomic changes in landcover	Functional changes	Geo-morphic diversity	Time (t)	Time (Δ t)
1	low	natural meandering and flooding regimes	years to decades	continuous spatial-temporal trait variations	changing patterns in channel-systems	river to forest and forest to river	high geomorphic diversity leading to changes in the course of the Maniqui river in Bolivia	steady	(a)	(b)
2	increasing	river regulation	decades	landscape homogenization / texture changes	linear reservoirs	delta/marshland to agricultural	increase in agriculture along the Yellow River Delta, China	declining	(c)	(d)
3	increasing	dam construction	sudden	changes in spatial leaf area index distribution	large dam structure	forest to lake	a newly built dam along the Xingu river (Brazil) changes its flow characteristics	declining	(e)	(f)
4	declining	agricultural use changes leading to changes in sediment transport	decades	increased leaf area index	land formation	water to marshland	declining human pressure leading to regrowth of the the Wax Lake and Atchafalaya deltas, USA	increasing	(g)	(h)

Figure 16. A selection of fluvial geomorphic processes/changes, caused by natural processes or declining and increasing human land-use intensity, with images recorded by Landsat optical remote-sensing missions. The changes lead to different traits and taxonomical changes and act on different time scales. Image sources: Landsat satellite images, (https://earthobservatory.nasa.gov/, (accessed on 5 January 2022)); (**a**,**b**); land-use intensity—low https://earthobservatory.nasa.gov/images/89266/a-shape-shifting-river-in-bolivia, (accessed on 5 January 2022); (**c**,**d**) land-use intensity—increasing; https://earthobservatory.nasa.gov/world-of-change/YellowRiver/show-all, (accessed on 5 January 2022); (**e**,**f**) land-use intensity—increasing, https://earthobservatory.nasa.gov/images/91083/reshaping-the-xingu-river, (accessed on 5 January 2022); (**g**,**h**) land-use intensity—declining, https://earthobservatory.nasa.gov/world-of-change/WaxLake, (accessed on 5 January 2022).

6. Methods for Discriminating and Classifying the Five Characteristics of Geomorphodiversity

In regions without vegetation, water, or ice cover, detecting geomorphic trait diversity with RS technologies using direct RS indicators is easier than when detecting landforms with vegetation, water, or ice cover. The spectral RS signal is the result or integral of the state, changes, shifts, and/or disturbances of geomorphic traits, geogenesis traits, structure traits, taxonomy traits, and functional traits. In regions with vegetation, water, or ice cover, indirect indicators must be used in addition to the direct RS indicators, which are integral to the response of traits in bacteria, algae, plants, populations, communities, and the traits of landforms and their interactions.

Direct indicators for discrimination and classification with RS: RS indicators can be derived directly for the discrimination of geomorphodiversity characteristics without vegetation
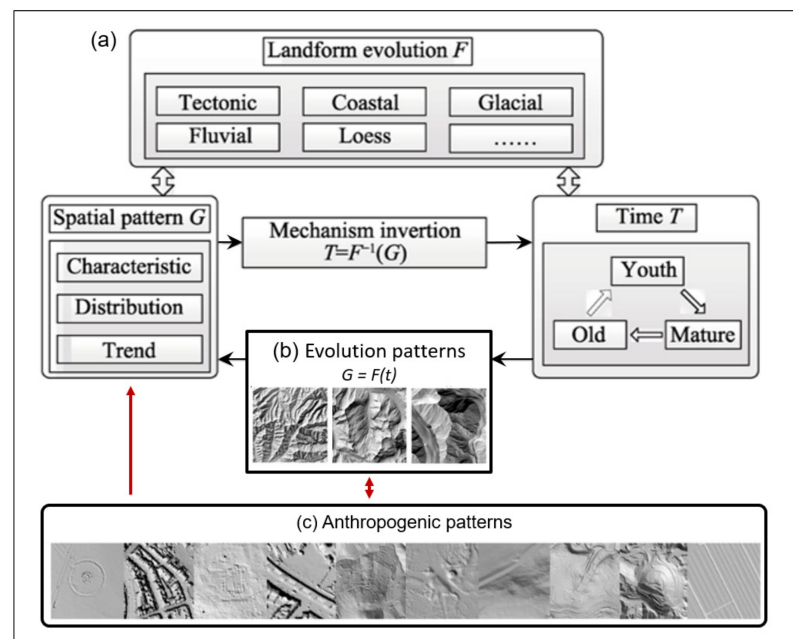
cover (e.g., volcanoes, mountains, dunes, mountain or rock types, fluvial and coastal structures, glades, periglacial formations, anthropogenically vs. geogenically formed structures). The spectral RS signal is a result of the geomorphic traits detected by RS sensors and their trait variations. Thus, geomorphic characteristics can be discriminated from each other using RS technologies if:

- The different geomorphic characteristics differ in their geomorphic traits, such as geochemical or mineralogical properties (color, grain size, aggregate state, geochemical characteristics, mineralogical composition, and configurations such as sand, clay, boulders, rock- and soil types) or water regimes.
- By their 2D–3D morphometric and structural properties, shapes such as horizontal and vertical structures, shape types, and shape groups differ from each other. Additional information, such as DEM-derived geomorphic variables including slope, aspect, indicators of roughness, relief shading, etc., can be used to improve discrimination performance [98].
- Likewise, the occurrence of specific lithological and soil characteristics resulting from evolutionary, climate, or anthropogenic drivers can be captured with RS data, which can improve discrimination performance.
- The geomorphometric delineation of landforms, such as fluvial landforms, i.e., flood-plains and terraces, using objectively defined topographic and morphometric thresholds [124].

If the different geomorphic characteristics cannot be distinguished from each other based on the criteria mentioned above, multitemporal RS data can be used to improve the discrimination:

- When the characteristic variations of geomorphic traits occur within short time periods (days, years, or decades), e.g., gravimetric mass movements, aeolian formations, glacial movements, coastal formations, climate-induced permafrost changes, specific processes during volcanic eruptions, or aeolian processes through wind erosion, leading to the formation of specific dune classes [125].
- Where evolutionary periods are required for the formation of shapes (tectonic, glacial, and fluvial formations), the use of the method "space-for-time substitution" in geomorphology is useful [126] (see Figure 17).
- In addition to 2D–3D spatial patterns of geomorphology, trait characteristics and their distributions are also determined. From this, the trend of possible changes from evolutionary and anthropogenic patterns over time can be determined.
- Changes in shapes and patterns can be used to draw important conclusions about the characteristics and causes of anthropogenic influences, as anthropogenic geomorphic features are characterized by specific shapes and geochemical compositions (like, buildings, cities, roads, middens, terraces, megaliths, boundary walls, reservoirs, and river regulations) [17].
- By comparing evolutionary with anthropogenically induced geomorphic structures and structural forms, conclusions can be drawn about the degree of anthropogenic overprinting. In this way, the anthropogenic fingerprint of geomorphology can be determined using RS technologies [17,28].

Figure 17. (**a**) Schematic diagram of space-for-time substitution from Huang et al. [126]; (**b**) evolution patterns of mountain types derived with RS, from Farmakis-Serebryakova and Hurni [98]; (**c**) examples of anthropogenic surface patterns derived with airborne LiDAR from Tarolli et al. [17].

Coupling of direct and indirect indicators for the discrimination of geomorphic characteristics with RS approaches: The expression of a specific micro-flora and fauna, vegetation structure, and biodiversity are directly related to geomorphology. Geomorphology is, thus, not only a crucial but also a resource-limiting factor for the development, condition, and resilience or health status of micro-organisms and biodiversity. For the discrimination of geomorphic characteristics covered by vegetation (geogenetic, aeolian, fluvial, coastal, glacial, and periglacial characteristics), direct and indirect RS methods must be used together. The spectral signal of RS data is the result of the traits detected by RS sensors and their variations from geomorphology, rocks, soil, water, plants, and vegetation. The geomorphic traits of rocks, soil, water, plants, and vegetation are proxies for different geomorphic taxa. Thus, geomorphic characteristics with vegetation can be discriminated from each other, utilizing RS, if:

- The above factors are used to derive direct indicators.
- Specific 2-3D structures such as DEM/DSM and their shifts or disturbances are derived by using specific RS techniques, such as In-SAR, RADAR, LiDAR, GEDI-LiDAR [7].
- The structure and functionality of various geomorphic characteristics differ [110,111,127].
- Different geomorphic characteristics lead to the development and distribution of characteristic bacteria, animal, and plant species (algae, weave, bacteria, symbiosis, animals, plants, and soil crusts), plant functional types (PFT, specific biological traits, growth characteristics, specific biochemical, structural and functional traits, or health status) of bacteria, plants or soil crusts as crucial bio-geomorphological indicators and proxies of different geomorphic characteristics, if specific geomorphic characteristics are present in the development of specific plant species, PFT, or in the context of geomorphodiversity as geo-plant fuctional types (G-PFT).
- Different geomorphic characteristics deviate in their geomorphic-specific ecological niches, and/or when various geomorphic characteristics lead to different geomorphic resource limitations for algae, weave, bacteria, specific symbiosis as well as specific animals, plants, and vegetation.
- The microclimate, outgassing, species composition changes, and chlorophyll or nitrogen increases (e.g., climate change or permafrost change) is supposed to change through anthropogenic influences.

The use of multi-temporal RS data is useful for the discrimination of geomorphic characteristics:

- If the different characteristics of geomorphodiversity are not distinguished from each other by the aforementioned traits, multi-sensor RS data are used to improve the discrimination of geomorphic features and the recording of geomorphodiversity.
- When variations in geomorphic traits occur within short geomorphic periods (days, years, or decades), e.g., gravimetric mass movements, aeolian formations, glacier movements, coastal formations, climate-induced permafrost changes, volcano or aeolian processes through wind erosion, which lead to the formation of specific dune classes [125,128–132].
- However, where evolutionary periods are required to form shapes (tectonic, glacial, or fluvial formations), the use of the method of space-for-time substitution in geomorphology is useful [126]. In addition to the 2D–3D spatial patterns of geomorphology, trait characteristics, and the distribution of geomorphic traits, the trend of possible changes from evolutionary, as well as anthropogenic patterns over time, are determined.
- Furthermore, crucial conclusions about the characteristics and the origins of anthropogenic influence can be drawn from the shape change and, thus, the anthropogenic geomorphic forms (buildings, cities, roads, middens, terraces, megaliths, boundary walls, or reservoirs) can be discriminated using RS [17].
- By comparing evolutionary with anthropogenically induced geomorphic structures and structural forms, conclusions can be drawn about the degree of anthropogenic overprinting. The anthropogenic fingerprint of geomorphology can be derived using RS technologies [17,28].

Since the geomorphodiversity is manifold, ranging from trait diversity to functional diversity (exact types are given in Table 1), the spectrum of observable phenomena calls for a multi-mission, necessitating a multi-sensor RS approach for the best possible characterization.

Table 1. Advantages and disadvantages of different RS imaging techniques regarding the five different geomorphic diversities: trait, genesis, structure, taxonomy, and function.

	Geomorphic—Trait Diversity	Geomorphic—Genesis Diversity	Geomorphic—Structural Diversity	Geomorphic—Taxonomic Diversity	Geomorphic—Functional Diversity
LiDAR/GEDI					
Advantage	Sensitive to height-/topography-related traits	Direct record of top of surface changes	Simple and straightforward detection of surface structures	Depending on point density, a diversity of geomorphic components detectable	Direct surface functions assessed
Disadvantage	Cloud affected	Only fast genesis detectable so far	Limited spatial extent	Limited penetration capabilities to access all geomorphic components	Many geomorphic functions are not measurable with LiDAR only due to function complexity
RADAR					
Advantage	Special sensitvity to geometry-/structure-related traits	Sub-surface gnesis also recorded	Detection of surface and sub-surface structures possible	Assessment of sub-surface components of taxonomy	Enlarging functional diversity to sub-surface phenomena
Disadvantage	No exact location of scattering center due to unknown penetration into natural media	Only fast genesis detectable so far	Speckle treatment necessary	Only a few taxonomy components can be assessed	Only some geomorphic functions can be assessed
InSAR					
Advantage	Sensitive to height-/topography-related traits	Detection of vertical genesis processes	Vertical structures detectable	Assessment of vertical components of taxonomy	Enlarging functional diversity to vertical phenomena
Disadvantage	Cloud-free, For long-term studies, persistent scatters are needed, but they do not occur everywhere.	Only fast genesis detectable so far	Only line-of-sight structural changes detectable	Only a few taxonomy components can be assessed	No sensitivity to surface (lateral) geomorphic functions

Table 1. *Cont.*

	Geomorphic—Trait Diversity	Geomorphic—Genesis Diversity	Geomorphic—Structural Diversity	Geomorphic—Taxonomic Diversity	Geomorphic—Functional Diversity
Multispectral					
Advantage	Sensitivity to surface-related geological-related traits	Longest time series (Landsat since 1978) for genesis tracking available	Multi-spectral traits indicate structural properties and dynamics at the surface	Multi-spectral traits are sensitive to several surface taxonomy components	Diversity in function reflects in several bands of the multi-spectrum
Disadvantage	Only surface features, no sub-surface features	Cloud cover hampers time series density	Structural diversity better mapped in 3D than in 2D	No sensitivity to non-surface taxonomy components	Water-related functional diversity easier to assess by microwaves
Hyperspectral					
Advantage	High sensitivity of single spectra to single traits	Genesis tracking with single spectral bands	Asessing diversity of composition by spectral bands	Covering of diversity in taxonomic components by single spectral bands	Spectral band diversity can detect functional diversity of the surface
Disadvantage	Only surface features, no sub-surface features	Longer time series missing	Complicate to assess 2D to 4D geomorphic structural traits	Only diversity of surface components can be assessed	No penetration into media—only to functional diversity of surfaces
Thermal—TIR					
Advantage	Sensitivity to energy-/temperature-related traits	Detection of thermal genesis possible	Composition diversity can only be assessed in the TIR range (e.g., hot lava)	Temperature-related taxonomy components detectable	Functional diversity expressed in thermal variation observable
Disadvantage	Cloud cover hampers time series density	Longer time series missing	Only structural diversity seen at TIR is detectable	Mass/water-related geomorphic components not detected	Only temperature-related functional diversity monitored
MAAP					
Advantage	Ready to use multi-source data portal and algorithm developer environment	-/-	Assessing diversity of biomass structure	-/-	-/-
Disadvantage	Above ground biomass (AGB) as main variable	-/-	Only focused on AGB	-/-	-/-
Multiple in situ/RS approaches					
Advantage	Highly adaptable due to in situ knowledge	Detection of complex genesis processes enabled	Complex structural diversity detectable	Complex taxonomy components can be assessed	Geomorphic functions and their intra- and inter-specific interactions can be assessed
Disadvantage	Only applicable on a small spatial scale where in situ data is available	Separation of different overlapping genesis processes	Dependence on in situ site conditions and their traits	In situ data-determined assessability of taxonomy components	Applicability reduced to sites with in situ measurements

- Across the acquisition modes and along the electromagnetic spectrum, several techniques, from active electro-optical imaging (LiDAR) to active microwave observation techniques (RADAR, InSAR), are applicable to assess the different geomorphic diversities.
- In Table 1, the advantages and disadvantages of the different RS techniques are summarized for a direct comparison.
- A major conclusion from Table 1 is that only a combination of RS techniques covering large parts of the electromagnetic spectrum from visible light to microwaves may have the capability to sufficiently monitor and map the five geomorphic diversities.
- The multi-mission algorithm and analysis platform (MAAP) is listed as one option for geomorphodiversity monitoring. This online portal serves as a multi-mission data and algorithm cloud environment for sharing and processing data from different ESA and NASA missions, with a special focus on aboveground biomass (https://earthdata.nasa.gov/esds/maap, (accessed on 5 March 2022)).

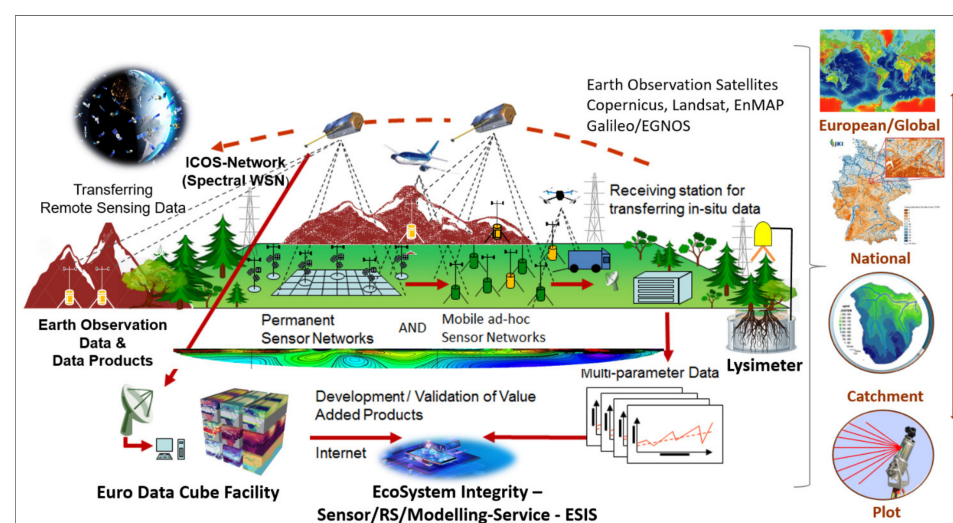## 7. Ecosystem Integrity—In Situ/RS/Modeling Approach for Monitoring Geomorphodiversity

A holistic and interdisciplinary approach to the in situ monitoring of geomorphology and different landforms, along with their processes and changes, has already been applied in the past by observing, comparing, and monitoring geomorphology in terms of its

interactions with geo-, hydro-, or biodiversity and their feedback mechanisms. Such a holistic monitoring approach is also the basic idea of ecosystem integrity [53–55]. For many years, this approach formed the main basis for establishing a harmonized and standardized geoecological monitoring system and monitoring standards for landscapes, as well as guidelines for field mapping and numerous geomorphological and topographic maps [56,57]. A complex multidimensional ecosystem integrity approach is required to assess and decide on the main drivers of conditions, disturbances, shifts, or the influence of LUI on structures and the functionalities of geomorphology, by linking in situ and RS data and data products with geomorphological and ecosystem modeling.

Such RS monitoring needs to integrate the spectral traits of different ecosystem domains, such as geomorphology [7], soil characteristics [47], water, the climate, plants, and vegetation [50,104] as well as variables and proxies that are indicators of the interaction between geo- and biodiversity [133]. Traits exist on all scales of geomorphodiversity, biogeomorphology, and vegetation diversity. Therefore, traits are scale-invariant and are ideally suited for coupling different monitoring approaches, such as in situ, close-range and air- and space-based RS technologies.

For this purpose, an ecosystem integrity–in situ/RS/modeling approach (ESIS) is currently being developed, based on developments from ILMS [134–136]. The following user requirements are placed on ESIS (see also Figure 18):

- An integration of in situ, close-range, air- and spaceborne RS monitoring technologies
- A link to the in situ monitoring approaches for the calibration and validation (cal/val) of RS data and the ability to support a data-driven modeling approach
- High-resolution remote sensing imagery [137]
- Modular coupling of spectral trait classification based on multi-sensor, multi-temporal RS data, and multi-mission algorithm and analysis platforms (like, MAAP)
- The identification and classification of geomorphic features, based on multi-algorithm and classification approaches, such as pixel-based classification, object-based image analysis (OBIA, [95]), the gray level co-occurrence matrix (GLCM [138]) modeling), geomorphic pattern recognition via artificial intelligence (AI), and machine learning [137]
- Direct links for recording spectral RS traits and data assimilation with process-modeling approaches (geomorphological models, morpho-hydrological models, biogeomorphological models, or vegetation models, such as the agent-based forest models).

Figure 18. Linking in situ/field-monitoring approaches with different RS platforms (high-frequency spectral wireless sensor networks, ICOS towers, drones, and air- and spaceborne sensors) for the comprehensive monitoring of the traits of geomorphology, geomorphodiversity, and biodiversity and their interactions, as well as improving the calibration and validation of remote sensing data (modified after Lausch et al. [139]).

8. Discussion of This Approach in the Context of the Existing Approaches of Geomorphodiversity

In order to compare the geomorphodiversity approach presented in this paper with the existing approaches, a Web of Science analysis was carried out using the keywords "geomorphodiversity" or "geomorphological diversity" or "landform diversity". Based on the frequency and co-occurrence of versions of the keywords from 653 papers, three thematic clusters were formed, vegetation diversity (shown in green), biodiversity (in blue) and geomorphodiversity and geodiversity (in red). Figure 19 provides a first impression of the enormous complexity, interconnectedness, and interdependencies of the indicators and assessment methods for characterizing and evaluating or monitoring geomorphodiversity.

Figure 19. Keywords and their co-occurrence in a bibliographic search in the Web of Science, with the topics: "geomorphodiversity" or "geomorphological diversity" or "landform diversity"; date of analysis, April 2022, finding 653 papers and around 100 keywords.

In the following section, references and approaches (i) to existing indicators of geomorphodiversity and (ii) the existing assessment methods of geomorphodiversity will be named and discussed. Since there are now a large number of indicators and assessment approaches for the characterization and detection of geomorphodiversity, only selected can be named and discussed here.

(I)   Approaches to the collection of indicators as a basis for the assessment of geomorphodiversity:

Berger [140] describes 27 geoindicators of mainly geomorphological changes, some of them are simple, single geomorphological indicators, such as the position of the shoreline or the stream channel morphology, whereas others are a complex of indicators, such as frozen soil activity or soil quality. Melelli et al. [23] developed different geomorphodiver-

sity indicators to assess geomorphological diversity. The indicators were derived from geological maps (geology), hydrological drainage networks (drainage density), and DEM indicators (roughness, slope position, and landform classification) and were created using high-resolution DTMs. By quantifying discrete and continuous indicators, this approach assigned an algebraic value to each cell that increases with the degree of diversity [23]. The indicators used and the assessment procedure are simple and quick to apply in the characterization of geomorphodiversity. The inclusion of discrete geological maps leads to uncertainties and erroneous assessments. Bollati and Cavalli [21] developed geomorphodiversity indicators to assess the relationship between geomorphodiversity and sediment connectivity in a small alpine catchment. Again, the indicators were generated based on points, lines and polygon data, with a GIS analysis.

Amatulli et al. [141] presented, for the first time, a globally comparable RS-based dataset of 26 indicators of geomorphometry. These were derived from a DEM—the multi-error-removed improved terrain (MERIT) DEM, at a spatial resolution of 90–250 m/pixel, which to date is considered the best effort in terms of global DEMs. This approach is based exclusively on the derivation of spectral geomorphological traits, using RADAR-RS data. The indicators resulting from this approach correspond to the geomorphic structural diversity indicators presented in the current paper. The 26 derived geomorphometric indicators that were derived are fully standardized, comparable, and continuously repeatable through the time series from RS data. The indicator set forms the basis for numerous subsequent ecosystem models and assessment procedures.

In order to develop a standardized monitoring of geodiversity indicators, which also includes numerous indicators of geomorphology, Schrodt et al. [142] evolved the first ideas about the "essential geovariables" (EGVs). This concept is based on the principle that is comparable to that one of "essential biodiversity variables" (EBVs), the "essential climate variables" (ECVs), as well as the "essential ocean variables" (EOVs). Essential variables are crucial for monitoring, measuring, and assessing changes taking place on our planet. ECVs are driving variables in the prediction of land surface will changes in response to climate change or human impacts, such as urbanization and intensification. Schrodt et al. [142] further show how geology, geomorphology, pedology, and hydrology can contribute to the achievement of the European Union's 17 sustainable development goals (SDGs). EGVs are comparable to the "geoindicators" (GEOIN) developed by the International Union of Geological Sciences (IUGS) in 1992 [140].

(II)   Approaches to geomorphodiversity and geodiversity assessment:

Panizza [19] described the concept of geomorphodiversity for the first time. He linked different geomorphological indicators with each other and described them on the one hand as: "intrinsic geodiversity", based on the geological complexity of the study area (morpho-climatic landforms and landslides on a regional scale as well as karst landforms on a local scale), and "extrinsic geodiversity" by comparing geological differences to other areas on a global scale. Further, Panizza [19] compared them to morphostructural landforms on a regional scale, in order to assess their regional geomorphological uniqueness. Different geomorphological indicators, such as "the geomorphological aspects and the morphostructural, morphoclimatic and fossil permafrost indicators" on different spatial scales, were integrated by Panizza [19], too. Zwoliński [24] developed routines to create landform geodiversity maps, based on RS- and GIS-based information, such as a map of the landform energy derived from an SRTM-3 digital elevation model, a map of landform fragmentation, created from a geomorphological map, and a map of contemporary landform preservation, derived from the CORINE land cover database. In this approach, the importance of integrating RS-based indicators derived from DEM/DSM becomes apparent. Moradi et al. [22] assessed geomorphodiversity and geomorphological heritage for Damavand Volcano Management. Therefore, he coupled in situ fieldwork informations, topography, geological maps, and RS-based indicators to quantify DEM/DSM and their derivatives. Probably the most comprehensive description and critical discussion of monitoring approaches to

geodiversity [143] and the indication of the need for an ecosystem approach [144], as well as a critical examination of existing assessment approaches are given by Gray et al. [6].

Relatively unknown, as they are mainly only published in German, are the monitoring approaches and assessment procedures for 'natural classification' [145,146] and 'natural order' [147–151] as well as 'landscape ecological structure and function models' [152–154]. These 'schools' of landscape- and geoecology form the fundamental and standardized methodologies of landscape ecology and geoecology [57] and, consequently, also the indicators and assessment procedures for landscapes. Among numerous references, the works of Haase and Mannsfeld [155], Mannsfeld et al., [156] or Haase et al. [157], which laid down the theoretical principles, guiding principles, indicators, methods and assessment procedures for recording natural space units, from the topical and choral to the regional, zonal and global dimension, should be highlighted here. According to [158], their methods and assessment procedures are based on an ecosystem integrity approach, whereby landscape or the landscape ecosystem [57] is described by the space-time structure, as well as the function and processes of the Earth's envelope, which is determined by the metabolism between humans and nature and must be considered and assessed in various dimensions. In doing so, a sameness (homogeneity) of functions and structures is assumed, which is adequate in each case to the dimension under consideration [156,158]. In their evaluation procedure, the determination of natural area units is based on defining criteria and structural features, these are: (1) the observation dimension—spatial dimension or dimensional level, (2) the landscape-genetic context, as determining criteria, and (3) an assessment through the structure, societies, and arrangement patterns of the natural area units of the next lower rank as structural features [158]. Table 2 shows the dimension-specific units of the natural area and their components.

Table 2. Dimension-specific units of the natural area and its components (modified after Sandner, 2015) [159].

Dimensions	Rock	Climate	Relief	Water	Soil	Vegetation	Animals	Natural Space
Global	Lithosphere	Atmosphere	Geomorpho-sphere	Hydrosphere	Pedosphere	Phytosphere	Zoosphere	Geosphere
Zonal	-	Climatezone	-		Pedozone	Phytozone	-	Landscape zone
Region	Rock region	Climate region	Geomorpho-region	Hydroregion	Pedoregion	Phytoregion	Zoo region	Landscape region
Megachoric	Substrate-megachore	Climate-megachore	Geomorpho-megachore	Hydro-megachore	Pedo-megachore	Phyto-megachore	Zoo-megachore	Geo-megachore
Macrochoric	Substrate macrochore	Climate-macrochore	Geomorpho-macrochore	Hydro-macrochore	Pedo-macrochore	Phyto-macrochore	Zoo-macrochore	Geomorpho-macrochore
Mesochoric	Substrate mesochore	Climate-mesochore	Geomorpho-mesochore	Hydro-mesochore	Pedo-mesochore	Phyto-mesochore	Zoo-mesochore	Geo-mesochore
Microchoric	Substrate-microchore	Climate microchore	Geomorpho-microchore	Hydro-microchore	Pedo-microchore	Phyto-microchore	Zoo microchore	Geo-microchore
Nanochoric	Substrate nanoochore	Climate nanoochore	Geomorpho-nanoochore	Hydro-nanoochore	Pedo-nanoochore	Phyto-nanoochore	Zoo-nanoochore	Geo-nanoochore
Topic	Substrate top	Climatetop	Geomorpho-top	Hydrotop	Pedotop	Phytotop	Zootop	Geotop

9. Conclusions of the Comparison

- So far, there is no comparable approach to capture the five characteristics of geomorphodiversity using only RS data and RS data products.
- Only the approach of Amatulli et al. [141], which derives 26 geomorphic indicators from RS, is partially comparable to the approach described here. Since spectral geomorphic traits exist on all spatial scales of geomorphology, indicators from the local and regional scales, up to the global scale, can be recorded by means of RS and used for assessment approaches.
- In the work of Melelli et al. [23] and Bollati and Cavalli [21], both discrete and continuous indicators are determined using GIS. RS data do not play a role in these

assessment methods, which means that inaccuracies and errors in the assessment of geomorphodiversity cannot be excluded.

- In terms of standardization and comparability across spatial scales, as described by Panizza [19] through the "extrinsic geodiversity" indicators, comparability across smaller spatial scales will be achieved, but this contradicts the approaches of [156–158] which state that each dimensional level is characterized by a specific geogenesis, structure, taxonomy, and functions and that the transition between spatial dimensions is defined by the criterion of homogeneity (geomorphic patch—a spatial unit that is homogeneous in its geomorphic traits).
- Geomorphic traits are defined by the thematic focus (genesis, structure, taxonomy, function, and process) and are subject to a spatial and temporal range of validity. Geomorphic traits exist on all spatio-temporal scales, but they are dimension-specific. In each spatial dimension, other geomorphic traits become more important. As the spatial dimension changes, the degree of generalization or abstraction level of the geomorphic traits changes. When applying the geomorphic trait/trait variation approach and the five characteristics of geomorphodiversity for the assessment and categorization of landscapes, the assessment approaches should be assessed according to the specific spatial dimension approaches (topic, choric, region, and zone).
- Standardized, comparable, repeatable indicators and monitoring and assessment procedures that are robustly applicable at all spatio-temporal scales of geomorphodiversity are needed [160].

10. Data Science to Monitor Geomorphodiversity

Geomorphological processes, changes, and disturbances determine the geomorphological traits at all scales of geomorphological organization (see Figure 3). Furthermore, geomorphological traits exist on all spatial scales of geomorphological organization, starting from rain dips, channels, gullies, or rock formations and ranging to talus slopes, valleys, and isolated hills, as far as continental plates, and should be recorded and monitored on all scales. The methodological approach to monitoring the state, changes, disturbances, and prediction of geomorphological diversity and geohazards is complex. Therefore, it is only possible when different platforms, sensor technologies, monitoring, and modeling approaches, as well as the latest technologies in data science, are combined to move from data, monitoring approaches, and information to knowledge and, thus, prediction, assessment and concentrated knowledge for decision-makers and politicians.

The following criteria are imperative for the successful implementation of the digitization process of geomorphological research, monitoring, assessment, and prediction in the 21st century:

- To connect to environmental research infrastructures, such as: the environmental research infrastructures, ENVRIplus and ENVRIFair (big networks of in situ research infrastructures, linked to most of the domains of Earth systems sciences—the biosphere, the atmosphere, marine systems, and solid Earth) [161]; the European Observatory for research infrastructures and in situ Earth observation networks (ENEON); the Committee on Earth Observation Satellites (CEOS); the European Association of Remote Sensing Companies (EARSC); Copernicus, and others.
- To use scalable indicators for monitoring the status, changes, and disturbances of geomorphology, geodiversity, and biodiversity, and their interactions, based on the spectral RS traits approach of geomorphology ([7], and this paper), geodiversity (soil [47]) and biodiversity [50,104,162].
- To unite the EVWs [163]; the EOVs [164], the ECVs [165]; as well as the EBVs [166–168]).
- To apply the EcoSystem Integrity RS/Modeling Service (ESIS) approach.
- To link in situ/field monitoring and IoT with close-range, air- and spaceborne RS platforms.
- To link different monitoring and modeling approaches with citizen science, etc.
- To use big data, open access, freely available data, open science clouds, distributed repositories, and the thematic exploitation platform (TEP).

- To integrate local, regional and global databases on geomorphology.
- To ensure the interoperability, standardization, and harmonization of data, monitoring, and decision-support systems. For example, with the help of metadata, using a standard open communication protocol, GoFAIR-Data (findable, accessible, interoperable, and re-usable) [169] and GoFAIR modeling approaches for scientific data management and stewardship related to metadata, data infrastructures (e.g., GAIA-X) and the International Data Spaces Association (IDSA), using the data cube approach with an n-D higher-dimensional array of values, including multi-petabyte data warehouses in clouds, the international data spaces (IDS) metadata broker, and the IDSA meta-model for geomorphology and RS time series.
- To integrate semantic data, semantic web/Web 4.0, ontology; linked open data (LOD) approaches based on the key enabling technologies (KETs) and knowledge organization systems (KOSs), and knowledge organization and management (KOMs), based on SNAP and SPAN ontologies [170], for the semantic interoperability of heterogeneous data [171].
- To implement complex data science modeling and analysis: AI, machine learning, deep learning, cloud computing, data mining, Hadoop, the Google Earth engine, hosting services, workflows, and others.
- To use data and RS data product cubes, the Euro Data Cube Facility, iCube, and open RS data cubes.
- To check the proof, trust, and uncertainties of in situ monitoring, RS, and data science uncertainties.
- To implement rapid warning systems for geohazards.
- To develop easy to handle software, tools for data managers, stakeholders, and politicians (visualization models, and dashboards).

11. Conclusions and Future Challenges for Monitoring Geomorphodiversity

Monitoring geomorphology, the changes and disturbances, as well as the interactions is complex, multidimensional, and multiscale in space, time, and its processes and drivers. Therefore, the concept of geomorphodiversity and landform diversity was developed by Panazza [19] and Zwoliñski [24] to provide a holistic and cross-scale monitoring approach to recording and assessing geomorphodiversity.

This paper is the first to describe in detail how geomorphodiversity can be recorded using RS-only technologies. For that, the paper presents a new perspective, definition, and recording of five characteristics of geomorphodiversity with RS technologies and discusses them intensively with examples. The five characteristics of geomorphodiversity are: (i) geomorphic trait diversity, (ii) geomorphic genesis diversity, (iii) geomorphic structural diversity, (iv) geomorphic taxonomic diversity, and (v) geomorphic functional diversity. Here, the recording of geomorphic trait diversity by means of RS plays a crucial role in deriving the final four characteristics of geomorphodiversity (ii–v).

RS can capture the spectral traits and trait variations of geomorphologic features. A variety of spectral geomorphic trait indicators are named in this paper (see Figure 6) and their detection by different RS technologies (LiDAR, RADAR, InSAR, multispectral, and hyperspectral) is documented by numerous references (see Table A1).

Furthermore, the paper extensively discusses the constraints and limitations of the recording of geomorphodiversity by RS, which are: (i) the influence of the characteristics and spatial-temporal distribution of geomorphic traits, (ii) the importance of characteristics of geomorphic processes, as well as (iii) the different RS sensor characteristics (spectral, geometrical, or temporal resolution), the deployed RS platforms, and the characteristics of RS data processing and classification approaches for the estimation of the five RS-aided geomorphodiversity characteristics.

In addition, the methods for the discrimination and classification of geomorphodiversity with RS technologies are presented in detail, whereby the combination of directly or indirectly derived indicators from geomorphology, as well as the influence of vegetation

traits and their interaction, are discussed. Likewise, the influence of LUI on the evolutionary patterns of geomorphology is discussed, and methods of monitoring anthropogenic geomorphology patterns and their changes via RS are shown.

Traits are a crucial interface between in situ, close-range, air- and spaceborne RS monitoring approaches. Therefore, RS technologies and monitoring approaches are a crucial interdisciplinary and linking method for monitoring the status, changes, and hazards of the geomorphology on all the spatio-temporal scales of geomophodiversity.

The monitoring of geomorphology is complex. For this monitoring of geomorphodiversity, a holistic and interdisciplinary approach, the ecosystem integrity in situ/RS/modeling approach (ESIS), is discussed. The discussion also includes the coupling of in situ field data with multisensorial and/or multitemporal RS data, and the direct link to ecosystem models within the assessment procedure. Using multi-sensor and-multi-temporal RS as well as MAAP missions, geomorphic traits, and vegetation traits, can be recorded at the same time and at the same angle, with different RS techniques. This simultaneous acquisition improves the classification quality as well as the model prediction, whereby the detection of status, changes, and geohazards can be improved by means of RS.

Likewise, the approach of monitoring the five characteristics of geomorphodiversity with RS, as presented in the paper, is discussed along with the already existing approaches of recording indicators, as well as approaches for assessing geomorphodiversity. It is shown that there is no comparable approach by which to define and record the five characteristics of geomorphodiversity using only RS data in the literature.

In the presented paper, numerous spectral traits indicators, as well as the five characteristics of geomorphology and their recording, are presented. However, it is not the purpose of this paper to subsequently carry out assessment procedures for the characterization of geomorphodiversity on the basis of these five characteristics. Instead, this paper offers important information and basics as a foundation for numerous subsequent case studies.

Finally, the paper presents the necessary methods of data science, which will significantly advance the successful digitization of geomorphology, and assess geomorphodiversity and the provision of state-of-the-art technologies for understanding the processes involved.

For future work with the approach presented in the paper, we emphasize that:

- The presented trait approach presented here and the resulting indicators—spectral traits of geomorphology/geomorphodiversity—should be included in the future indicator list for the EGVs.
- Comparable to the approach and paper published by Diaz [172] ("The global spectrum of plant form and function"), "The global spectrum of geomorphology/geomorphodiversity" should be determined using the spectral geomorphic trait approach and its indicators.
- Geomorphic traits exist on all spatio-temporal scales, but they are dimension-specific. In each spatial dimension, other geomorphic traits become important. As the spatial dimension changes, the degree of generalization or abstraction level of the geomorphic traits changes. When using the geomorphic trait and trait variation approach and the five characteristics of geomorphodiversity for the assessment and categorization of landscapes, the assessment approaches should be used according to the specific spatial dimension approaches (topic, choric, region, or zone) [157].

Conflicts of Interest: The authors declare no conflict of interest.

Appendix A

Table A1. Remote sensing (RS)-aided examples derived in monitoring the characteristics of geomorphodiversity (geomorphic traits, diversity, structural, taxonomic, and functional diversity characteristics), shifts, and disturbances (modified after Lausch et al. [7]).

Geomorphic Traits	Mission/Platform Sensor	References
Terrain and Surfaces/Traits		
Geomorpho90 m (90 m/100 m/250 m) (slope, aspect, aspect cosine, aspect sine, eastness, northness, convergence, compound topographic index, stream power index, east-west first-order partial derivative, north-south first-order partial derivative, profile curvature, tangential curvature, east-west second-order partial derivative, north-south second-order partial derivative, second-order partial derivative, elevation standard deviation, terrain ruggedness index, roughness, vector ruggedness measure, topographic position index, maximum multiscale deviation, scale of the maximum multiscale deviation, maximum multiscale roughness, scale of the maximum multiscale roughness, geomorphon)	(26 geomorphometric variables derived from MERIT-DEM [3/R]—corrected from the underlying Shuttle RADAR Topography Mission (SRTM3) and ALOS World 3D—30 m (AW3D30) DEMs)	[141]
Mountain types, relief types, relief classes	IKONOS OSA [3/M], DHM25 [3/R], GTOPO30—DEM [3/R], LiDAR [2/L]	[98,173,174]
Volcano types (volcanic full forms), volcanoes, lava flow fields, hydrothermal alteration, geothermal explorations, heat fluxes, volcanoes hazard monitoring, location, deformation	Doves-PlanetScop, Terra/Aqua MODIS [3/M], EO-1 ALI [3/M], Landsat-8 OLI [3/M/TIR], Terra ASTER [3/M/TIR], MSG SEVIRI [3/M/TIR], LiDAR [2/L]	[109,175–180]
Mountain hazards, mass movement (rockfall probability, boulders, denudation, mass erosion, rock decelerations, rotation changes, slope stability, rock shapes, mineral distribution, geological material discrimination, particle shapes, patterns, structures, faults and fractures, holes, and depressions) mountain monitoring system	InSAR [3/R], SAR [3/R], LiDAR [2/L], Digital Orthophoto [1/RGB], HySPEC [2/HSP], AVIRIS [2/HSP]	[96,181–192]
Landslide chances, landslide evolution	Digital Orthophoto [1/RGB]	[193]
Above ground—chances, disturbances Opencast mining, sand mining and extraction, tipping, dumps	TanDEM-X [3/R], SRTM DEM [3/R], ALOS PALSAR [3/R], ERS-1 [3/R], GeoEye GIS [3/M], WorldView-3 Imager [3/M], IKONOS OSA [3/M], Landsat-5 TM/-7 ETM ± 8 OLI [3/M/TIR], IRS-P6 LISS-III [3/M], High resolution satellite data of Google [3/M], LiDAR [2/L]	[194–200]
Vegetation traits as proxy of the geochemical parameters	HyMAP [2/H]	[201]
Below ground—chances, disturbances Salt mines, fracking	ERS-1/-2 [3/R], ASAR [3/R], ALOS PALSAR [3/R], Landsat-5 TM/-7 ETM ± 8 OLI [3/M/TIR]	[202,203]
Aeolian geomorphology/traits		
Desertification, soil and land-degradation, soil erosion	NOAA/MetOp AVHRR [3/R], ERS−1/−2 [3/R], SIR-C [3/R], ENVISAT [3/R], ASAR [3/R], RADARSAT−1 [3/R], ALOS PALSAR [3/R], Terra/Aqua MODIS [3/M], IRS1B LISS-I/LISS-II [3/M], Sentinel−2 MSI [3/M], Landsat-5 TM/−7 ETM ± 8 OLI [3/M], LiDAR [2/L]	[204–211]
Dune migration, migration rates, dune expansion, dune activity, moving dunes	ALOS PALSAR [3/R], Landsat-8 OLI [3/M], Sentinel-2 MSI [3/M], Context Camera [2/RGB], LiDAR [2/L]	[97,212–215]

Table A1. *Cont.*

Geomorphic Traits	Mission/Platform Sensor	References
Dune types, dune hierarchies, dune morphometry, dune hierarchies (free dunes—shifting sand dunes, bounded dunes, dune fields, dune shapes (crescent, cross, linear, stars, dome, parabolic, longitudinal dune)	SRTM [3/R], SIR-C/X-SAR [3/R], WorldView-2 WV110 [3/M], IRS-RS2 LISS-IV [3/M], Cartosat-1 PAN-F/-A [3/M], Landsat-7 ETM+ [3/M], Landsat MSS [3/M], LiDAR [2/L]	[125,128–132],
Dune spatial-temporal aeolic patterns (length, minimum spacing density, orientation, height, sinuosity), aeolian dune composition-configuration (complexity, diversity, shapes, patterns, heterogeneity), dune ridges (lines)	SRTM [3/R], SIR-C [3/R], Landsat-7 ETM+ [3/M], LiDAR [2/L], Digital Orthophoto [3/RGB]	[90,97,117,132,216–218]
Volume and their changes, intensity of dune	SRTM [3/R], SPOT-5 HRG [3/M], Terra ASTER [3/M], LiDAR [2/L]	[117,132,219,220]
Fluvial geomorphology/traits		
Flooding events, flood mapping, flash-flood susceptibility assessment, flood inundation modeling, floodplain-risk mapping, erosive impacts, sedimentation	SRTM [3/R], ALOS PALSAR [3/R], ALSAR-1 [3/R], SAR [3/R], ALOS-2 [3/R], TerraSAR-X [3/R], RADARSAT-2 [3/R], Sentinel-1 [3/R], Landsat-a5 TM/-7 ETM ± 8 OLI [3/M/TIR], Sentinel-2 MSI [3/M], IRS-1C/-1D LISS-III [3/M], IKONOS OSA [3/M], DEADALUS [2/H], LiDAR [2/L]	[92,221–233]
Flood mapping under vegetation, irrigation retrieval, groundwater flooding in a lowland karst catchment	SAR [3/R], Landsat-5 TM/-7 ETM ± 8 OLI [3/M]	[234–236]
Traits in plants and vegetation (flexibility, size, root form, clonal growth, perennation, Ellenberg F values, plant species) as proxy of the geochemical processes, heavy metal stress in plants	HyMAP [2/H], HySPEX [2/H]	[83,201,237]
River detection, small streams detection	SAR [3/R], Landsat-5 TM/-7 ETM ± 8 OLI [3/M], Aerial images [2/RGB], Aerial images [1/RGB], LiDAR [2/L]	[238–242]
Channel landforms, hydrogeomorphic units including coarse woody debris, hydraulic (fluvial) landform classification, taxonomy of fluvial landforms, hydro-morphological units, riverscape units, river geomorphic units, in-stream mesohabitats, tidal channel characteristics	SAR [3/R], Aerial images [2/RGB], LiDAR [2/L]	[239,243–245]
Channel characteristics, floodplain morphology hydraulic channel morphology, geometries, topography, river width arc length, longitudinal transect, (width, depth, and longitudinal channel slope, below water line morphology), Morphometric patterns of meanders (sinuosity, intrinsic wavelength, curvature, asymmetry), meander dynamics, channel geometry, Geomorphometric delineation of floodplains and terraces	SAR [3/R], ENVISAT [3/R], Terra/Aqua MODIS [3/M], Landsat-5 TM/-7 ETM ± 8 OLI [3/M], Sentinel-2 MSI [3/M], Aerial images [2/RGB], LiDAR [2/L]	[124,238,246–253]
Channel migration, channel migration rates, channel planform changes, tidal channel migration Channel changes, disturbances, temporal evolution of natural and artificial abandoned channels, canal position, systematic changes of the river banks and canal center lines	SAR [3/R], SRTM [3/R], Landsat-5 TM [3/M], Landsat-7 ETM ± 8 OLI [3/TIR], Aerial images [2/RGB]	[245,254–259]
Flow energy of stream power, channel sensitivity to erosion and deposition processes Channel stability assessment	Landsat-1 MSS/-5 TM/-8 OLI 3/M, LiDAR 2/L	[260,261]
River discharge estimation (river discharge, run-off characteristics)	ENVISAT [3/R], Jason-2/-3 [3/R], Sentinel-3A OLCI/SLSTR [3/R], CryoSat-2 [3/R], AltiKa [3/R], ENVISAT [3/R], Advanced RADAR Altimeter (RA-2) [3/R], Terra/Aqua MODIS [3/M]	[262,263]
Water and flow velocity	ENVISAT [3/R], Terra/Aqua MODIS [3/M], Aerial images [2/RGB], LiDAR [2/L]	[239,248,264]
Water height, water level, water depth	ENVISAT 3/R, AMSR-E 3/R, TRMM 3/R, Daedalus 2/H, Aerial images 2/RGB, LiDAR 2/L	[239,263,265–268]
Fluvial sediment transport, sediment budget, channel bank erosion, exposed channel substrates and sediments, suspended soil concentration and bed material, percentage clay, silt and sand in intertidal sediments, suspended sediments, flood bank overbank sedimentation, sediment wave, sand mining	LiDAR [2/L], Radio frequency identification [1/RFID]	[199,252,269,270]
Stream bank retreat	Aerial images [2/RGB], LiDAR [2/L]	[271–276]
Grain characteristics, grain size, gravel size, shape, bed and bank sediment size	Daedalus [2/H], Aerial images [2/RGB], Aerial images [2/RGB], LiDAR [2/L]	[277–282]
Pebble mobility	Radio frequency identification technologies [1/RFID]	[283]
River bathymetry	CASI [2/H], Daedalus [2/H], Aerial images [2/RGB], LiDAR [2/L]	[239,268,284–286]
Coastal geomorphology/traits		
Coast taxonomy, coast types (small delta, tidal system, lagoon, fjord and fjärd, large river, tidal estuary, ria, karst, arheic)	RADAR [3/R], optical RS Sensors [3/R]	[287]

Table A1. *Cont.*

Geomorphic Traits	Mission/Platform Sensor	References
Coastal dynamical and bio-geo-chemical patterns	NOAA/MetOp AVHRR [3/R], ERS-1 [3/R], TOPEX [3/R], Nimbus-7 CZCS [3/M/TIR]	[288]
Coastal landforms, coastline and shoreline detection	SRTM [3/R], ALOS [3/R], NOAA [3/R], Landsat-7 ETM+ [3/M], Terra ASTER[3/M], IKONOS OSA [3/M], LiDAR [2/L]	[91–93]
Spatio-temporal shoreline dynamic, shoreline erosion-accretion trends, coast changes, cliff retreat, erosion hotspots	SRTM [3/R], SAR [3/R], Landsat-4 MSS/-5 TM [3/M], Landsat-8 OLI [3/M/TIR], SPOT 5 [3/M], Sentinel-2 MSI [3/M], Aerial images [2/RGB], LiDAR [2/L]	[289–296]
Different morphometric shoreline indicators (morphological reference lines, vegetation limits, instant tidal levels and wetting limits, tidal datum indicators, virtual reference lines, beach contours, storm lines)	Different optical RS Sensors [3/M], LiDAR [2/L]	[215,297,298]
Cryography		
Permafrost changes methane emissions from discontinuous terrestrial permafrost		[82]
Geohazards		
Ground surface response to continuous compaction of aquifer systems	InSAR (Envisat ASAR [3/R], ALOS PALSAR [3/R], TerraSAR-X [3/R], Sentinel 1 [3/R])	[79]
Anthropogenic geomorphology		
Burial sites, geoglyphs, rock-shelter, Megaliths, buildings, cities, human settlement, including infrastructure, boundary walls, roads, middens, livestock trails, terraces, mines, ditches, canals, embankments, reservoirs, constructed wetlands, trenches	LiDAR [2/L]	[17]

The sensor is used on the RS platform: UAV [1]—unmanned aerial vehicles (UAV); airborne [2]—airborne RS platform; spaceborne [3]—spaceborne RS platform. RADAR [R], Multispectral (MSP) [M], Hyperspectral (HSP) [H], RGB [RGB], TIR [T], LiDAR [L], radio frequency identification [RFID].

References

1. Strahler, A.N. Quantitative analysis of watershed geomorphology. *Trans. Am. Geophys. Union* **1957**, *38*, 913. [CrossRef]
2. Piégay, H. Quantitative Geomorphology. In *International Encyclopedia of Geography*; John Wiley and Sons: Hoboken, NJ, USA, 2019; pp. 1–4. ISBN 9781118786352.
3. Sofia, G. Combining geomorphometry, feature extraction techniques and Earth-surface processes research: The way forward. *Geomorphology* **2020**, *355*, 107055. [CrossRef]
4. Dubois, J.-M.M. Functional geomorphology: Landform analysis and models. *Geomorphology* **1994**, *9*, 344–345. [CrossRef]
5. Hall, M.R.; Lindsay, R.; Krayenhoff, M. *Modern Earth Buildings*; Woodhead Publishing Limited: Sawston, UK, 2012; ISBN 978-0-85709-026-3.
6. Gray, M. Geodiversity: A significant, multi-faceted and evolving, geoscientific paradigm rather than a redundant term. *Proc. Geol. Assoc.* **2021**, *132*, 605–619. [CrossRef]
7. Lausch, A.; Schaepman, M.E.; Skidmore, A.K.; Truckenbrodt, S.C.; Hacker, J.M.; Baade, J.; Bannehr, L.; Borg, E.; Bumberger, J.; Dietrich, P.; et al. Linking the Remote Sensing of Geodiversity and Traits Relevant to Biodiversity—Part II: Geomorphology, Terrain and Surfaces. *Remote Sens.* **2020**, *12*, 3690. [CrossRef]
8. Green, J.L.; Bohannan, B.J.M.; Whitaker, R.J. Microbial Biogeography: From Taxonomy to Traits. *Science* **2008**, *320*, 1039–1043. [CrossRef]
9. Thome, C.R.; Zevenbergen, L.W. Estimating Mean Velocity in Mountain Rivers. *J. Hydraul. Eng.* **1985**, *111*, 612–624. [CrossRef]
10. Gilbert, G.K. *Monograph—Geology of the Henry Mountains*; Washington Government Printing Office: Washington, DC, USA, 1877.
11. Dikau, R.; Eibisch, K.; Eichel, J.; Meßenzehl, K.; Schlummer-Held, M. Biogeomorphologie. In *Geomorphologie*; Springer: Berlin/Heidelberg, Germany, 2019; ISBN 978-3-662-59401-8.
12. Viles, H. *Biogeomorphology*; Basil Blackwell: Oxford, UK, 1988.
13. Viles, H. Biogeomorphology: Past, present and future. *Geomorphology* **2020**, *366*, 106809. [CrossRef]
14. Grill, G.; Lehner, B.; Thieme, M.; Geenen, B.; Tickner, D.; Antonelli, F.; Babu, S.; Borrelli, P.; Cheng, L.; Crochetiere, H.; et al. Mapping the world's free-flowing rivers. *Nature* **2019**, *569*, 215–221. [CrossRef]
15. Rathjens, C. *Geomorphology and Global Environmental Change*; Slaymaker, O., Spencer, T., Embleton-Hamann, C., Eds.; Cambridge University Press: Cambridge, UK, 2009; ISBN 9780511627057.
16. Szabó, J.; Dávid, L.; Lóczy, D. (Eds.) *Anthropogenic Geomorphology*; Springer Netherlands: Dordrecht, The Netherlands, 2010; ISBN 978-90-481-3057-3.
17. Tarolli, P.; Cao, W.; Sofia, G.; Evans, D.; Ellis, E.C. From features to fingerprints: A general diagnostic framework for anthropogenic geomorphology. *Prog. Phys. Geogr. Earth Environ.* **2019**, *43*, 95–128. [CrossRef]
18. Goudie, A. The human impact in geomorphology—50 years of change. *Geomorphology* **2020**, *366*, 106601. [CrossRef]

19. Panizza, M. The geomorphodiversity of the Dolomites (Italy): A Key of geoheritage assessment. *Geoheritage* **2009**, *1*, 33–42. [CrossRef]

20. Panizza, M. Outstanding Intrinsic and Extrinsic Values of the Geological Heritage of the Dolomites (Italy). *Geoheritage* **2018**, *10*, 607–612. [CrossRef]

21. Bollati, I.M.; Cavalli, M. Unraveling the relationship between geomorphodiversity and sediment connectivity in a small alpine catchment. *Trans. GIS* **2021**, *25*, 2481–2500. [CrossRef]

22. Moradi, A.; Maghsoudi, M.; Moghimi, E.; Yamani, M.; Rezaei, N. A Comprehensive Assessment of Geomorphodiversity and Geomorphological Heritage for Damavand Volcano Management, Iran. *Geoheritage* **2021**, *13*, 39. [CrossRef]

23. Melelli, L.; Vergari, F.; Liucci, L.; Del Monte, M. Geomorphodiversity index: Quantifying the diversity of landforms and physical landscape. *Sci. Total Environ.* **2017**, *584–585*, 701–714. [CrossRef]

24. Zwoliński, Z. The routine of landform geodiversity map design for the Polish Carpathian Mts. *Landf. Anal.* **2009**, *11*, 77–85.

25. Tarolli, P.; Mudd, S.M. *Remote Sensing of Geomorphology*; Elsevier: Edinburgh, UK, 2020; ISBN 978-0-444-64177-9.

26. Smith, M.J.; Pain, C.F. Applications of remote sensing in geomorphology. *Prog. Phys. Geogr. Earth Environ.* **2009**, *33*, 568–582. [CrossRef]

27. Hjort, J.; Luoto, M. Can geodiversity be predicted from space? *Geomorphology* **2012**, *153–154*, 74–80. [CrossRef]

28. Brown, A.G.; Tooth, S.; Bullard, J.E.; Thomas, D.S.G.; Chiverrell, R.C.; Plater, A.J.; Murton, J.; Thorndycraft, V.R.; Tarolli, P.; Rose, J.; et al. The geomorphology of the Anthropocene: Emergence, status and implications. *Earth Surf. Process. Landf.* **2017**, *42*, 71–90. [CrossRef]

29. Blei, D.M.; Ng, A.Y.; Jordan, M.I. Latent Dirichlet Allocation. *J. Mach. Learn. Res.* **2003**, *3*, 993–1022.

30. Masek, J.G.; Wulder, M.A.; Markham, B.; McCorkel, J.; Crawford, C.J.; Storey, J.; Jenstrom, D.T. Landsat 9: Empowering open science and applications through continuity. *Remote Sens. Environ.* **2020**, *248*, 111968. [CrossRef]

31. Woodcock, C.E.; Allen, R.; Anderson, M.; Belward, A.; Bindschadler, R.; Cohen, W.; Gao, F.; Goward, S.N.; Helder, D.; Helmer, E.; et al. Free Access to Landsat Imagery. *Science* **2008**, *320*, 1011. [CrossRef]

32. Turner, W.; Rondinini, C.; Pettorelli, N.; Mora, B.; Leidner, A.K.; Szantoi, Z.; Buchanan, G.; Dech, S.; Dwyer, J.; Herold, M.; et al. Free and open-access satellite data are key to biodiversity conservation. *Biol. Conserv.* **2015**, *182*, 173–176. [CrossRef]

33. Wulder, M.A.; White, J.C.; Loveland, T.R.; Woodcock, C.E.; Belward, A.S.; Cohen, W.B.; Fosnight, E.A.; Shaw, J.; Masek, J.G.; Roy, D.P. The global Landsat archive: Status, consolidation, and direction. *Remote Sens. Environ.* **2016**, *185*, 271–283. [CrossRef]

34. Zhu, Z.; Wulder, M.A.; Roy, D.P.; Woodcock, C.E.; Hansen, M.C.; Radeloff, V.C.; Healey, S.P.; Schaaf, C.; Hostert, P.; Strobl, P.; et al. Benefits of the free and open Landsat data policy. *Remote Sens. Environ.* **2019**, *224*, 382–385. [CrossRef]

35. Wulder, M.A.; Loveland, T.R.; Roy, D.P.; Crawford, C.J.; Masek, J.G.; Woodcock, C.E.; Allen, R.G.; Anderson, M.C.; Belward, A.S.; Cohen, W.B.; et al. Current status of Landsat program, science, and applications. *Remote Sens. Environ.* **2019**, *225*, 127–147. [CrossRef]

36. Guanter, L.; Kaufmann, H.; Segl, K.; Foerster, S.; Rogass, C.; Chabrillat, S.; Kuester, T.; Hollstein, A.; Rossner, G.; Chlebek, C.; et al. The EnMAP Spaceborne Imaging Spectroscopy Mission for Earth Observation. *Remote Sens.* **2015**, *7*, 8830–8857. [CrossRef]

37. Eegholm, B.H.; Wake, S.; Denny, Z.; Dogoda, P.; Poulios, D.; Coyle, B.; Mule, P.; Hagopian, J.G.; Thompson, P.; Ramos-Izquierdo, L.; et al. Global Ecosystem Dynamics Investigation (GEDI) instrument alignment and test. *Opt. Modeling Syst. Alignment* **2019**, *11103*, 1110308.

38. Dubayah, R.; Blair, J.B.; Goetz, S.; Fatoyinbo, L.; Hansen, M.; Healey, S.; Hofton, M.; Hurtt, G.; Kellner, J.; Luthcke, S.; et al. The Global Ecosystem Dynamics Investigation: High-resolution laser ranging of the Earth's forests and topography. *Sci. Remote Sens.* **2020**, *1*, 100002. [CrossRef]

39. Krieger, G.; Pardini, M.; Schulze, D.; Bachmann, M.; Borla Tridon, D.; Reimann, J.; Brautigam, B.; Steinbrecher, U.; Tienda, C.; Sanjuan Ferrer, M.; et al. Tandem-L: Main results of the phase a feasibility study. In Proceedings of the 2016 IEEE International Geoscience and Remote Sensing Symposium (IGARSS), IEEE, Beijing, China, 10–15 July 2016; Volume 2016, pp. 2116–2119.

40. Moreira, A.; Krieger, G.; Gonzalez, C.; Nannini, M.; Zink, M. Tandem-L: A Highly Innovative Bistatic SAR Mission for Monitoring Earth's System Dynamics. *Geophys. Res. Abstr.* **2019**, *21*, 2019.

41. Alonso, K.; Bachmann, M.; Burch, K.; Carmona, E.; Cerra, D.; de los Reyes, R.; Dietrich, D.; Heiden, U.; Hölderlin, A.; Ickes, J.; et al. Data products, quality and validation of the DLR earth sensing imaging spectrometer (DESIS). *Sensors* **2019**, *19*, 4471. [CrossRef]

42. Nieke, J.; Rast, M. Towards the Copernicus Hyperspectral Imaging Mission For The Environment (CHIME). In Proceedings of the IGARSS 2018-2018 IEEE International Geoscience and Remote Sensing Symposium, IEEE, Valencia, Spain, 22–27 July 2018; pp. 157–159.

43. Abrams, M.J.; Hook, S.J. NASA's Hyperspectral Infrared Imager (HyspIRI). In *Thermal Infrared Remote Sensing*; Springer: Dordrecht, The Netherlands, 2013; pp. 117–130.

44. Jeliazkov, A.; Mijatovic, D.; Chantepie, S.; Andrew, N.; Arlettaz, R.; Barbaro, L.; Barsoum, N.; Bartonova, A.; Belskaya, E.; Bonada, N.; et al. A global database for metacommunity ecology, integrating species, traits, environment and space. *Sci. Data* **2020**, *7*, 6. [CrossRef]

45. Bruelheide, H.; Dengler, J.; Purschke, O.; Lenoir, J.; Jiménez-Alfaro, B.; Hennekens, S.M.; Botta-Dukát, Z.; Chytrý, M.; Field, R.; Jansen, F.; et al. Global trait–environment relationships of plant communities. *Nat. Ecol. Evol.* **2018**, *2*, 1906–1917. [CrossRef]

46. Morgan, L.R.; Marsh, K.J.; Tolleson, D.R.; Youngentob, K.N. The Application of NIRS to Determine Animal Physiological Traits for Wildlife Management and Conservation. *Remote Sens.* **2021**, *13*, 3699. [CrossRef]

47. Lausch, A.; Baade, J.; Bannehr, L.; Borg, E.; Bumberger, J.; Chabrilliat, S.; Dietrich, P.; Gerighausen, H.; Glässer, C.; Hacker, J.; et al. Linking Remote Sensing and Geodiversity and Their Traits Relevant to Biodiversity—Part I: Soil Characteristics. *Remote Sens.* **2019**, *11*, 2356. [CrossRef]

48. Andersson, E.; Haase, D.; Anderson, P.; Cortinovis, C.; Goodness, J.; Kendal, D.; Lausch, A.; McPhearson, T.; Sikorska, D.; Wellmann, T. What are the traits of a social-ecological system: Towards a framework in support of urban sustainability. *NPJ Urban Sustain.* **2021**, *1*, 14. [CrossRef]

49. Wellmann, T.; Haase, D.; Knapp, S.; Salbach, C.; Selsam, P.; Lausch, A. Urban land use intensity assessment: The potential of spatio-temporal spectral traits with remote sensing. *Ecol. Indic.* **2018**, *85*, 190–203. [CrossRef]

50. Lausch, A.; Bastian, O.; Klotz, S.; Leitão, P.J.; Jung, A.; Rocchini, D.; Schaepman, M.E.; Skidmore, A.K.; Tischendorf, L.; Knapp, S. Understanding and assessing vegetation health by in situ species and remote-sensing approaches. *Methods Ecol. Evol.* **2018**, *9*, 1799–1809. [CrossRef]

51. Rahbek, C.; Borregaard, M.K.; Colwell, R.K.; Dalsgaard, B.; Holt, B.G.; Morueta-Holme, N.; Nogues-Bravo, D.; Whittaker, R.J.; Fjeldså, J. Humboldt's enigma: What causes global patterns of mountain biodiversity? *Science* **2019**, *365*, 1108–1113. [CrossRef]

52. Schrodt, F.; Santos, M.J.; Bailey, J.J.; Field, R. Challenges and opportunities for biogeography—What can we still learn from von Humboldt? *J. Biogeogr.* **2019**, *46*, 1631–1642. [CrossRef]

53. Müller, F.; Hoffmann-Kroll, R.; Wiggering, H. Indicating ecosystem integrity—Theoretical concepts and environmental requirements. *Ecol. Modell.* **2000**, *130*, 13–23. [CrossRef]

54. Antonelli, A.; Kissling, W.D.; Flantua, S.G.A.; Bermúdez, M.A.; Mulch, A.; Muellner-Riehl, A.N.; Kreft, H.; Linder, H.P.; Badgley, C.; Fjeldså, J.; et al. Geological and climatic influences on mountain biodiversity. *Nat. Geosci.* **2018**, *11*, 718–725. [CrossRef]

55. Haase, P.; Tonkin, J.D.; Stoll, S.; Burkhard, B.; Frenzel, M.; Geijzendorffer, I.R.; Häuser, C.; Klotz, S.; Kühn, I.; McDowell, W.H.; et al. The next generation of site-based long-term ecological monitoring: Linking essential biodiversity variables and ecosystem integrity. *Sci. Total Environ.* **2018**, *613–614*, 1376–1384. [CrossRef]

56. Zepp, H.; Müller, M.J. *Landschaftsökologische Erfassungsstandards*; Forschung; Deutsche Akademie für Landeskunde, Selbstverlag: Flensburg, Germany, 1999; ISBN 3-88143-056-3.

57. Leser, H.; Löffler, J. *Landschaftsökologie*; Auflage: 5; Eugen Ulmer KG: Stuttgart, Germany, 2017; ISBN 3825287181.

58. Mukherjee, S.; Koyi, H.A.; Talbot, C.J. Implications of channel flow analogue models for extrusion of the Higher Himalayan Shear Zone with special reference to the out-of-sequence thrusting. *Int. J. Earth Sci.* **2012**, *101*, 253–272. [CrossRef]

59. Mukherjee, S. Higher Himalaya in the Bhagirathi section (NW Himalaya, India): Its structures, backthrusts and extrusion mechanism by both channel flow and critical taper mechanisms. *Int. J. Earth Sci.* **2013**, *102*, 1851–1870. [CrossRef]

60. Mukherjee, S. Tectonic Implications and Morphology of Trapezoidal Mica Grains from the Sutlej Section of the Higher Himalayan Shear Zone, Indian Himalaya. *J. Geol.* **2012**, *120*, 575–590. [CrossRef]

61. Mukherjee, S. Simple shear is not so simple! Kinematics and shear senses in Newtonian viscous simple shear zones. *Geol. Mag.* **2012**, *149*, 819–826. [CrossRef]

62. Bose, N.; Mukherjee, S. *Map Interpretation for Structural Geologists*, 1st ed.; Elsevier, Ed.; Elsevier: Amsterdam, The Netherlands, 2017; ISBN 978-0-12-809681-9.

63. Hilbich, C. Time-lapse refraction seismic tomography for the detection of ground ice degradation. *Cryosphere* **2010**, *4*, 243–259. [CrossRef]

64. Kruglov, O.; Menshov, O.; Miroshnychenko, M.; Shevchenko, M. Integration of geophysical, soil science and geospatial methods in the study of eroded soil. In Proceedings of the Geoinformatics: Theoretical and Applied Aspects 2020, Kyiv, Ukraine, 11–14 May 2020; pp. 1–5.

65. Jongmans, D.; Garambois, S. Geophysical investigation of landslides: A review. *Bull. Soc. Geol. Fr.* **2007**, *178*, 101–112. [CrossRef]

66. Whiteley, J.S.; Chambers, J.E.; Uhlemann, S.; Wilkinson, P.B.; Kendall, J.M. Geophysical Monitoring of Moisture-Induced Landslides: A Review. *Rev. Geophys.* **2019**, *57*, 106–145. [CrossRef]

67. Hussain, Y.; Cardenas-Soto, M.; Martino, S.; Moreira, C.; Borges, W.; Hamza, O.; Prado, R.; Uagoda, R.; Rodríguez-Rebolledo, J.; Silva, R.; et al. Multiple Geophysical Techniques for Investigation and Monitoring of Sobradinho Landslide, Brazil. *Sustainability* **2019**, *11*, 6672. [CrossRef]

68. Florentine, C.; Skidmore, M.; Speece, M.; Link, C.; Shaw, C.A. Geophysical analysis of transverse ridges and internal structure at Lone Peak Rock Glacier, Big Sky, Montana, USA. *J. Glaciol.* **2014**, *60*, 453–462. [CrossRef]

69. Kneisel, C.; Hauck, C.; Fortier, R.; Moorman, B. Advances in geophysical methods for permafrost investigations. *Permafr. Periglac. Process.* **2008**, *19*, 157–178. [CrossRef]

70. Tukiainen, H.; Kiuttu, M.; Kalliola, R.; Alahuhta, J.; Hjort, J. Landforms contribute to plant biodiversity at alpha, beta and gamma levels. *J. Biogeogr.* **2019**, *46*, 1699–1710. [CrossRef]

71. Eviner, V.T.; Chapin, F.S., III. Functional Matrix: A Conceptual Framework for Predicting Multiple Plant Effects on Ecosystem Processes. *Annu. Rev. Ecol. Evol. Syst.* **2003**, *34*, 455–485. [CrossRef]

72. Pazzi, V.; Morelli, S.; Fanti, R. A Review of the Advantages and Limitations of Geophysical Investigations in Landslide Studies. *Int. J. Geophys.* **2019**, *2019*, 2983087. [CrossRef]

73. Natsuaki, R.; Nagai, H.; Motohka, T.; Ohki, M.; Watanabe, M.; Thapa, R.B.; Tadono, T.; Shimada, M.; Suzuki, S. SAR interferometry using ALOS-2 PALSAR-2 data for the Mw 7.8 Gorkha, Nepal earthquake. *Earth Planets Sp.* **2016**, *68*, 15. [CrossRef]

74. Bovolo, F.; Bruzzone, L. A Split-Based Approach to Unsupervised Change Detection in Large-Size Multitemporal Images: Application to Tsunami-Damage Assessment. *IEEE Trans. Geosci. Remote Sens.* **2007**, *45*, 1658–1670. [CrossRef]

75. Dasgupta, S.; Mukherjee, S. Remote Sensing in Lineament Identification: Examples from Western India. In *Problems and Solutions in Structural Geology and Tectonics*; Elsevier Inc.: Amsterdam, The Netherlands, 2019; Volume 5, pp. 205–221. ISBN 9780128140482.

76. Prost, G.L. *Remote Sensing for Geoscientists*; T & F Group, Ed.; CRC Press: Boca Raton, FL, USA; London, UK; New York, NY, USA, 2013; ISBN 9781466561755.

77. Baatz, R.; Franssen, H.J.H.; Euskirchen, E.; Sihi, D.; Dietze, M.; Ciavatta, S.; Fennel, K.; Beck, H.; De Lannoy, G.; Pauwels, V.R.N.; et al. Reanalysis in Earth System Science: Towards Terrestrial Ecosystem Reanalysis. *Rev. Geophys.* **2021**, *59*, e2020RG000715. [CrossRef]

78. Jensen, J.R. *Remote Sensing of the Environment: An Earth Resource Perspective*, 2nd ed.; Prentice-Hall, Inc.: Upper Saddle River, NJ, USA, 2014; ISBN 9780131889507.

79. Haghshenas Haghighi, M.; Motagh, M. Ground surface response to continuous compaction of aquifer system in Tehran, Iran: Results from a long-term multi-sensor InSAR analysis. *Remote Sens. Environ.* **2019**, *221*, 534–550. [CrossRef]

80. Tapley, B.D. GRACE Measurements of Mass Variability in the Earth System. *Science* **2004**, *305*, 503–505. [CrossRef]

81. Flechtner, F.; Neumayer, K.-H.; Dahle, C.; Dobslaw, H.; Fagiolini, E.; Raimondo, J.-C.; Güntner, A. What Can be Expected from the GRACE-FO Laser Ranging Interferometer for Earth Science Applications? *Surv. Geophys.* **2016**, *37*, 453–470. [CrossRef]

82. Kohnert, K.; Serafimovich, A.; Metzger, S.; Hartmann, J.; Sachs, T. Strong geologic methane emissions from discontinuous terrestrial permafrost in the Mackenzie Delta, Canada. *Sci. Rep.* **2017**, *7*, 5828. [CrossRef]

83. O'Hare, M.T.; Mountford, J.O.; Maroto, J.; Gunn, I.D.M. Plant Traits Relevant to fluvial geomorphology and hydrological interactions. *River Res. Appl.* **2014**, *30*, 132–133. [CrossRef]

84. Notesco, G.; Ogen, Y.; Ben-Dor, E. Mineral classification of makhtesh ramon in israel using hyperspectral longwave infrared (LWIR) remote-sensing data. *Remote Sens.* **2015**, *7*, 12282–12296. [CrossRef]

85. Weksler, S.; Rozenstein, O.; Ben-dor, E. Mapping Surface Quartz Content in Sand Dunes Covered by Biological Soil Crusts Using Airborne Hyperspectral Images in the Longwave. *Minerals* **2018**, *8*, 318. [CrossRef]

86. Van der Meer, F.D.; van der Werff, H.M.A.; van Ruitenbeek, F.J.A.; Hecker, C.A.; Bakker, W.H.; Noomen, M.F.; van der Meijde, M.; Carranza, E.J.M.; de Smeth, J.B.; Woldai, T. Multi- and hyperspectral geologic remote sensing: A review. *Int. J. Appl. Earth Obs. Geoinf.* **2012**, *14*, 112–128. [CrossRef]

87. Tewksbury, B.J.; Dokmak, A.A.K.; Tarabees, E.A.; Mansour, A.S. Google Earth and geologic research in remote regions of the developing world: An example from the Western Desert of Egypt. In *Google Earth and Virtual Visualizations in Geoscience Education and Research*; Geological Society of America: Boulder, CO, USA, 2012.

88. Behling, R.; Roessner, S.; Golovko, D.; Kleinschmit, B. Derivation of long-term spatiotemporal landslide activity—A multi-sensor time series approach. *Remote Sens. Environ.* **2016**, *186*, 88–104. [CrossRef]

89. Haghighi, M.H.; Motagh, M. Sentinel-1 InSAR over Germany: Large-scale interferometry, atmospheric effects, and ground deformation mapping. *ZFV-Z. Geodasie Geoinf. Landmanag.* **2017**, *142*, 245–256.

90. Al-Masrahy, M.A.; Mountney, N.P. Remote sensing of spatial variability in aeolian dune and interdune morphology in the Rub' Al-Khali, Saudi Arabia. *Aeolian Res.* **2013**, *11*, 155–170. [CrossRef]

91. Kaliraj, S.; Chandrasekar, N.; Ramachandran, K.K. Mapping of coastal landforms and volumetric change analysis in the south west coast of Kanyakumari, South India using remote sensing and GIS techniques. *Egypt. J. Remote Sens. Sp. Sci.* **2017**, *20*, 265–282. [CrossRef]

92. Kulp, S.A.; Strauss, B.H. New elevation data triple estimates of global vulnerability to sea-level rise and coastal flooding. *Nat. Commun.* **2019**, *10*, 4844. [CrossRef] [PubMed]

93. Dang, K.B.; Dang, V.B.; Bui, Q.T.; Nguyen, V.V.; Pham, T.P.N.; Ngo, V.L. A Convolutional Neural Network for Coastal Classification Based on ALOS and NOAA Satellite Data. *IEEE Access* **2020**, *8*, 11824–11839. [CrossRef]

94. Schwefel, D.; Glässer, C.; Glässer, W. Dynamik anthropogen induzierter Landschaftsveränderungen im Bergbaufolgegebiet Teutschenthal-Bahnhof (Sachsen-Anhalt). *Hercynia* **2012**, *45*, 9–31.

95. Blaschke, T. Object based image analysis for remote sensing. *ISPRS J. Photogramm. Remote Sens.* **2010**, *65*, 2–16. [CrossRef]

96. Clark, R.N.; Swayze, G.A.; Livo, K.E.; Kokaly, R.F.; Sutley, S.J.; Dalton, J.B.; McDougal, R.R.; Gent, C.A. Imaging spectroscopy: Earth and planetary remote sensing with the USGS Tetracorder and expert systems. *J. Geophys. Res. Planets* **2003**, *108*, 5. [CrossRef]

97. Shumack, S.; Hesse, P.; Farebrother, W. Deep learning for dune pattern mapping with the AW3D30 global surface model. *Earth Surf. Process. Landf.* **2020**, *45*, 2417–2431. [CrossRef]

98. Farmakis-Serebryakova, M.; Hurni, L. Comparison of Relief Shading Techniques Applied to Landforms. *ISPRS Int. J. Geo.-Inf.* **2020**, *9*, 253. [CrossRef]

99. Ventura, G.; Vilardo, G.; Terranova, C.; Sessa, E.B. Tracking and evolution of complex active landslides by multi-temporal airborne LiDAR data: The Montaguto landslide (Southern Italy). *Remote Sens. Environ.* **2011**, *115*, 3237–3248. [CrossRef]

100. Mather, T.A.; Schmidt, A. *Environmental Effects of Volcanic Volatile Fluxes from Subaerial Large Igneous Provinces*, 1st ed.; Geophysical Monograph 255; Ernst, R.E., Dickson, A.J., Bekker, A., Eds.; Wiley Online Library: Hoboken, NJ, USA, 2021; ISBN 9781119507444.

101. Dasgupta, S.; Mukherjee, S. Remote Sensing in Lineament Identification: Examples from Western India. *J. Dev. Struct. Geol. Tecton.* **2019**, *15*, 205–221.

102. Gupta, R.P. *Remote Sensing Geology*; Springer: Berlin/Heidelberg, Germany, 2018; ISBN 978-3-662-55874-4.

103. Doeringsfeld, W.W., Jr.; Ivey, J.B. Use of photogeology and geomorphic criteria to locate subsurface structure. *Mt. Geol.* **1964**, *1*, 183–195.

104. Lausch, A.; Bannehr, L.; Beckmann, M.; Boehm, C.; Feilhauer, H.; Hacker, J.M.; Heurich, M.; Jung, A.; Klenke, R.; Neumann, C.; et al. Linking Earth Observation and taxonomic, structural and functional biodiversity: Local to ecosystem perspectives. *Ecol. Indic.* **2016**, *70*, 317–339. [CrossRef]

105. Nair, S.C.; Mirajkar, A. Land use-land cover anomalies and groundwater pattern with climate change for Western Vidarbha: A case study. *Arab. J. Geosci.* **2021**, *14*, 452. [CrossRef]

106. Kulkarni, H. Delineation of shallow Deccan basaltic aquifers from Maharashtra using aerial photointerpretation. *J. Indian Soc. Remote Sens.* **1992**, *20*, 129–138. [CrossRef]

107. Fisher, G.B.; Amos, C.B.; Bookhagen, B.; Burbank, D.W.; Godard, V. Channel widths, landslides, faults, and beyond: The new world order of high-spatial resolution Google Earth imagery in the study of earth surface processes. In *Google Earth and Virtual Visualizations in Geoscience Education and Research*; Geological Society of America: Boulder, CO, USA, 2012.

108. Peyghambari, S.; Zhang, Y. Hyperspectral remote sensing in lithological mapping, mineral exploration, and environmental geology: An updated review. *J. Appl. Remote Sens.* **2021**, *15*, 031501. [CrossRef]

109. Calvari, S.; Ganci, G.; Victória, S.; Hernandez, P.; Perez, N.; Barrancos, J.; Alfama, V.; Dionis, S.; Cabral, J.; Cardoso, N.; et al. Satellite and Ground Remote Sensing Techniques to Trace the Hidden Growth of a Lava Flow Field: The 2014–2015 Effusive Eruption at Fogo Volcano (Cape Verde). *Remote Sens.* **2018**, *10*, 1115. [CrossRef]

110. Elosegi, A.; Díez, J.; Mutz, M. Effects of hydromorphological integrity on biodiversity and functioning of river ecosystems. *Hydrobiologia* **2010**, *657*, 199–215. [CrossRef]

111. Corenblit, D.; Baas, A.C.W.; Bornette, G.; Darrozes, J.; Delmotte, S.; Francis, R.A.; Gurnell, A.M.; Julien, F.; Naiman, R.J.; Steiger, J. Feedbacks between geomorphology and biota controlling Earth surface processes and landforms: A review of foundation concepts and current understandings. *Earth-Sci. Rev.* **2011**, *106*, 307–331. [CrossRef]

112. Huryn, A.D.; Wallace, J.B. Local Geomorphology as a Determinant of Macrofaunal Production in a Mountain Stream. *Ecology* **1987**, *68*, 1932–1942. [CrossRef]

113. Stein, A.; Gerstner, K.; Kreft, H. Environmental heterogeneity as a universal driver of species richness across taxa, biomes and spatial scales. *Ecol. Lett.* **2014**, *17*, 866–880. [CrossRef]

114. Sukopp, H. Der Einfluss des Menschen auf die Vegetation. *Veg. Acta Geobot.* **1969**, *17*, 360–371. [CrossRef]

115. Lausch, A.; Blaschke, T.; Haase, D.; Herzog, F.; Syrbe, R.-U.; Tischendorf, L.; Walz, U. Understanding and quantifying landscape structure—A review on relevant process characteristics, data models and landscape metrics. *Ecol. Modell.* **2015**, *295*, 31–41. [CrossRef]

116. Hamilton, S.K.; Kellndorfer, J.; Lehner, B.; Tobler, M. Remote sensing of floodplain geomorphology as a surrogate for biodiversity in a tropical river system (Madre de Dios, Peru). *Geomorphology* **2007**, *89*, 23–38. [CrossRef]

117. Zheng, Z.; Du, S.; Du, S.; Zhang, X. A multiscale approach to delineate dune-field landscape patches. *Remote Sens. Environ.* **2020**, *237*, 111591. [CrossRef]

118. Le Provost, G.; Thiele, J.; Westphal, C.; Penone, C.; Allan, E.; Neyret, M.; van der Plas, F.; Ayasse, M.; Bardgett, R.D.; Birkhofer, K.; et al. Contrasting responses of above- and belowground diversity to multiple components of land-use intensity. *Nat. Commun.* **2021**, *12*, 3918. [CrossRef]

119. Mock, J. Auswirkungen des Hochwasserschutzes. In *Eine Einführung in die Umweltwissenschaften*; Böhm, H.R., Deneke, M., Eds.; Wissenschaftliche Buchgesellschaft: Darmstadt, Germany, 1992; pp. 176–196.

120. Terrapon-Pfaff, J.; Ersoy, S.R.; Fink, T.; Amroune, S.; Jamea, E.M.; Zgou, H.; Viebahn, P. Localizing the Water-Energy Nexus: The Relationship between Solar Thermal Power Plants and Future Developments in Local Water Demand. *Sustainability* **2020**, *13*, 108. [CrossRef]

121. Klink, C.A.; Machado, R.B. Conservation of the Brazilian Cerrado. *Conserv. Biol.* **2005**, *19*, 707–713. [CrossRef]

122. Amato, V.; Aucelli, P.P.C.; Bellucci Sessa, E.; Cesarano, M.; Incontri, P.; Pappone, G.; Valente, E.; Vilardo, G. Multidisciplinary approach for fault detection: Integration of PS-InSAR, geomorphological, stratigraphic and structural data in the Venafro intermontane basin (Central-Southern Apennines, Italy). *Geomorphology* **2017**, *283*, 80–101. [CrossRef]

123. Karkani, A.; Evelpidou, N.; Tzouxanioti, M.; Petropoulos, A.; Gogou, M.; Mloukie, E. Tsunamis in the Greek Region: An Overview of Geological and Geomorphological Evidence. *Geosciences* **2022**, *12*, 4. [CrossRef]

124. Clubb, F.J.; Mudd, S.M.; Milodowski, D.T.; Valters, D.A.; Slater, L.J.; Hurst, M.D.; Limaye, A.B. Geomorphometric delineation of floodplains and terraces from objectively defined topographic thresholds. *Earth Surf. Dyn.* **2017**, *5*, 369–385. [CrossRef]

125. Bhadra, B.K.; Rehpade, S.B.; Meena, H.; Srinivasa Rao, S. Analysis of Parabolic Dune Morphometry and Its Migration in Thar Desert Area, India, using High-Resolution Satellite Data and Temporal DEM. *J. Indian Soc. Remote Sens.* **2019**, *47*, 2097–2111. [CrossRef]

126. Huang, X.; Tang, G.; Zhu, T.; Ding, H.; Na, J. Space-for-time substitution in geomorphology. *J. Geogr. Sci.* **2019**, *29*, 1670–1680. [CrossRef]

127. Marston, R.A. Geomorphology and vegetation on hillslopes: Interactions, dependencies, and feedback loops. *Geomorphology* **2010**, *116*, 206–217. [CrossRef]

128. Radebaugh, J.; Lorenz, R.; Farr, T.; Paillou, P.; Savage, C.; Spencer, C. Linear dunes on Titan and earth: Initial remote sensing comparisons. *Geomorphology* **2010**, *121*, 122–132. [CrossRef]

129. Blumberg, D.G. Remote Sensing of Desert Dune Forms by Polarimetric Synthetic Aperture Radar (SAR). *Remote Sens. Environ.* **1998**, *65*, 204–216. [CrossRef]

130. Bradley, A.V.; Haughan, A.E.; Al-Dughairi, A.; McLaren, S.J. Spatial variability in shrub vegetation across dune forms in central Saudi Arabia. *J. Arid Environ.* **2019**, *161*, 72–84. [CrossRef]

131. Warren, A.; Allison, D. The palaeoenvironmental significance of dune size hierarchies. *Palaeogeogr. Palaeoclimatol. Palaeoecol.* **1998**, *137*, 289–303. [CrossRef]

132. Blumberg, D.G. Analysis of large aeolian (wind-blown) bedforms using the Shuttle Radar Topography Mission (SRTM) digital elevation data. *Remote Sens. Environ.* **2006**, *100*, 179–189. [CrossRef]

133. Schwarz, C.; Bouma, T.J.; Zhang, L.Q.; Temmerman, S.; Ysebaert, T.; Herman, P.M.J. Interactions between plant traits and sediment characteristics influencing species establishment and scale-dependent feedbacks in salt marsh ecosystems. *Geomorphology* **2015**, *250*, 298–307. [CrossRef]

134. Selsam, P.; Schwartze, C. Remote Sensing Image Analysis Without Expert Knowledge—A Web-Based Classification Tool On Top of Taverna Workflow Management System. *IOP Conf. Ser. Earth Environ. Sci.* **2016**, *44*, 042020. [CrossRef]

135. Zander, F.; Kralisch, S.; Busch, C.; Flügel, W.-A. Data management in multidisciplinary research projects with the River Basin information System. In *Light Up the Ideas of Environmental Informatics: Proceedings of the 26th International Conference on Informatics for Environmental Protection, EnviroInfo 2012, Dessau, Germany, 29–31 August 2012*; Shaker Verlag: Herzogenrath, Germany, 2012; pp. 143–149.

136. Kralisch, S.; Böhm, B.; Böhm, C.; Busch, C.; Fink, M.; Fischer, C.; Schwartze, C.; Selsam, P.; Zander, F.; Flügel, W.A. ILMS—A software platform for integrated environmental management. In Proceedings of the 6th International Congress on Environmental Modelling and Software, Leipzig, Germany, 1 July 2012; pp. 2864–2871.

137. Xia, W.; Chen, J.; Liu, J.; Ma, C.; Liu, W. Landslide Extraction from High-Resolution Remote Sensing Imagery Using Fully Convolutional Spectral–Topographic Fusion Network. *Remote Sens.* **2021**, *13*, 5116. [CrossRef]

138. Marceau, D.J.; Howarth, P.J.; Dubois, J.M.; Gratton, D.J. Evaluation Of The Grey-level Co-occurrence Matrix Method For Land-cover Classification Using Spot Imagery. *IEEE Trans. Geosci. Remote Sens.* **1990**, *28*, 513–519. [CrossRef]

139. Lausch, A.; Borg, E.; Bumberger, J.; Dietrich, P.; Heurich, M.; Huth, A.; Jung, A.; Klenke, R.; Knapp, S.; Mollenhauer, H.; et al. Understanding Forest Health with Remote Sensing, Part III: Requirements for a Scalable Multi-Source Forest Health Monitoring Network Based on Data Science Approaches. *Remote Sens.* **2018**, *10*, 1120. [CrossRef]

140. Berger, A.R. Assessing rapid environmental change using geoindicators. *Environ. Geol.* **1997**, *32*, 36–44. [CrossRef]

141. Amatulli, G.; McInerney, D.; Sethi, T.; Strobl, P.; Domisch, S. Geomorpho90m, empirical evaluation and accuracy assessment of global high-resolution geomorphometric layers. *Sci. Data* **2020**, *7*, 162. [CrossRef]

142. Schrodt, F.; Bailey, J.J.; Kissling, W.D.; Rijsdijk, K.F.; Seijmonsbergen, A.C.; van Ree, D.; Hjort, J.; Lawley, R.S.; Williams, C.N.; Anderson, M.G.; et al. To advance sustainable stewardship, we must document not only biodiversity but geodiversity. *Proc. Natl. Acad. Sci. USA* **2019**, *116*, 16155–16158. [CrossRef]

143. Gray, M. Geodiversity: Developing the paradigm. *Proc. Geol. Assoc.* **2008**, *119*, 287–298. [CrossRef]

144. Gray, M.; Gordon, J.E.; Brown, E.J. Geodiversity and the ecosystem approach: The contribution of geoscience in delivering integrated environmental management. *Proc. Geol. Assoc.* **2013**, *124*, 659–673. [CrossRef]

145. Troll, C. Die geographische Landschaft und ihre Erforschung. In *Studium Generale*; Springer: Berlin/Heidelberg, Germany, 1950; pp. 163–181.

146. Schmithüsen, J. Naturraumliche Gliederung und landschaftsraumliche Gliederung. *Ber. Dtsch. Landeskd.* **1967**, *39*, 125–131.

147. Neef, E. Topologische und chorologische Arbeitsweisen in der Landschaftsforschung. *PGM* **1963**, *107*, 249–259.

148. Neef, E. Elementaranalyse und Komplexanalyse in der Geographie. *Mitt. Österr. Geogr. Ges.* **1965**, *107*, 177–189.

149. Mannsfeld, K. *Die Naturräumliche Ordnung als Grundlage für die Landschaftsdiagnose im Mittleren Maßstab*; Umweltforschung: Gotha, Germany, 1984.

150. Haase, G. *Beiträge zur Landschaftsanalyse und Landschaftsdiagnose*; Abhandlung, Math.-nat. Kl., Band 59, Heft 1; Hirzel, S., Ed.; S. Hirzel Verlag GmbH: Stuttgart, Germany; Leipzig, Germany, 1999; ISBN 978-3-7776-0955-3.

151. Haase, G. Naturraumkartierung und Bewertung des Naturraumpotential. In Proceedings of the Deutscher Rat für Landes Pflege: Naturschutz und Landschaftspflege in den Neuen Bundesländ; Heft 59. Druck Center Meckenheim, Ed.; Der Schriftenreihe des Deutschen Rates für Landespflege: Meckenheim, Germany, 1991; pp. 921–943.

152. Fränzle, O.; Kappen, L.; Blume, H.-P.; Dierssen, K. (Eds.) *Ecosystem Organization of a Complex Landscape*; Springer: Berlin/Heidelberg, Germany, 2008; ISBN 978-3-540-75810-5.

153. Mosimann, T. *Landschaftsökologische Komplexanalyse*; Wissenschaftliche Paperbacks; Geographie: Wiesbaden, Germany, 1984.

154. Forman, R.T.T.; Godron, M. *Landscape Ecology*; Wiley: New York, NY, USA, 1986; ISBN 0-47187037.

155. Mannsfeld, K.; Haase, G. (Eds.) *Naturraumeinheiten, Landschaftsfunktionen und Leitbilder am Beispiel von Sachsen*; Forschungen zur Deutschen Landeskunde, Band 250; Deutsche Akademie für Landeskunde, Selbstverlag: Flensburg, Germany, 2002.

156. Mannsfeld, K.; Bastian, O.; Bieler, J.; Gerber, S.; König, A.; Lütz, M.; Schulze, S.; Syrbe, R.-U. *Geochorologische Verfahren zur Analyse, Kartierung und Bewertung von Naturräumen*; Berichte zur Geographie, Band 34; Akademie Verlag: Berlin, Germany, 2007.

157. Haase, G.; Barsch, H.; Hubrich, H.; Mannsfeld, K.; Schmidt, R. *Naturraumerkundung und Landnutzung. Geochorologische Verfah-ren zur Analyse, Kartierung und Bewertung von Naturräumen*; Beitraege; Akademie Verlag: Leipzig, Germany, 1991; ISBN 0138-4422.

158. Bastian, O.; Bieler, J.; Röder, M.; Sandner, E.; Syrbe, R.-U. *Naturraumeinheiten, Landschaftsfunktionen und Leitbilder am Beispiel von Sachsen*; Forschung zur Deutschen Landeskunde, Bd. 250; Haase, G., Mannsfeld, K., Eds.; Deutsche Akademie für Landeskunde e.V., Selbsverlag: Flensburg, Germany, 2002; ISBN 9783881430715.

159. Sandner, E. Dimensionsspezifische Einheiten des Naturraums und seiner Komponenten. *Geokontext* **2015**, *3*, 21–29.

160. Syrbe, R.-U.; Walz, U. Spatial indicators for the assessment of ecosystem services: Providing, benefiting and connecting areas and landscape metrics. *Ecol. Indic.* **2012**, *21*, 80–88. [CrossRef]

161. Zhao, Z.; Martin, P.; Grosso, P.; Los, W.; de Laat, C.; Jeffrey, K.; Hardisty, A.; Vermeulen, A.; Castelli, D.; Legre, Y.; et al. Reference Model Guided System Design and Implementation for Interoperable Environmental Research Infrastructures. In Proceedings of the 2015 IEEE 11th International Conference on e-Science, IEEE, Munich, Germany, 31 August–4 September 2015; pp. 551–556.

162. Cavender-Bares, J.; Gamon, J.A.; Townsend, P.A. (Eds.) *Remote Sensing of Plant Biodiversity*; Springer International Publishing: Cham, Switzerland, 2020; ISBN 978-3-030-33156-6.

163. Goerre, S.; Egli, C.; Gerber, S.; Defila, C.; Minder, C.; Richner, H.; Meier, B. Impact of weather and climate on the incidence of acute coronary syndromes. *Int. J. Cardiol.* **2007**, *118*, 36–40. [CrossRef]

164. Lindstrom, E.; Gunn, J.; Fischer, A.; McCurdy, A.; Glover, L.K.; Members, T.T. *A Framework for Ocean Observing*; UNESCO: Paris, France, 2012.

165. Bojinski, S.; Verstraete, M.; Peterson, T.C.; Richter, C.; Simmons, A.; Zemp, M. The concept of essential climate variables in support of climate research, applications, and policy. *Bull. Am. Meteorol. Soc.* **2014**, *95*, 1431–1443. [CrossRef]

166. Scholes, R.J.; Walters, M.; Turak, E.; Saarenmaa, H.; Heip, C.H.; Tuama, É.Ó.; Faith, D.P.; Mooney, H.A.; Ferrier, S.; Jongman, R.H.; et al. Building a global observing system for biodiversity. *Curr. Opin. Environ. Sustain.* **2012**, *4*, 139–146. [CrossRef]

167. Pereira, H.M.; Ferrier, S.; Walters, M.; Geller, G.N.; Jongman, R.H.G.; Scholes, R.J.; Bruford, M.W.; Brummitt, N.; Butchart, S.H.M.; Cardoso, A.C.; et al. Essential Biodiversity Variables. *Science* **2013**, *339*, 277–278. [CrossRef]

168. Skidmore, A.K.; Coops, N.C.; Neinavaz, E.; Ali, A.; Schaepman, M.E.; Paganini, M.; Kissling, W.D.; Vihervaara, P.; Darvishzadeh, R.; Feilhauer, H.; et al. Priority list of biodiversity metrics to observe from space. *Nat. Ecol. Evol.* **2021**, *5*, 896–906. [CrossRef]

169. Wilkinson, M.D.; Dumontier, M.; Aalversberg, I.J.; Appleton, G.; Axton, M. Comment: The FAIR Guiding Principles for scienti fi c data management and stewardship. *Nat. Commun.* **2016**, *3*, 160018.

170. Grenon, P.; Smith, B. SNAP and SPAN: Towards Dynamic Spatial Ontology. *Spat. Cogn. Comput.* **2004**, *4*, 69–104. [CrossRef]

171. Lausch, A.; Schmidt, A.; Tischendorf, L. Data mining and linked open data—New perspectives for data analysis in environmental research. *Ecol. Modell.* **2015**, *295*, 5–17. [CrossRef]

172. Díaz, S.; Kattge, J.; Cornelissen, J.H.C.; Wright, I.J.; Lavorel, S.; Dray, S.; Reu, B.; Kleyer, M.; Wirth, C.; Colin Prentice, I.; et al. The global spectrum of plant form and function. *Nature* **2016**, *529*, 167–171. [CrossRef]

173. Weiss, D.J.; Walsh, S.J. Remote Sensing of Mountain Environments. *Geogr. Compass* **2009**, *3*, 1–21. [CrossRef]

174. Meybeck, M.; Green, P.; Vörösmarty, C. A New Typology for Mountains and Other Relief Classes. *Mt. Res. Dev.* **2001**, *21*, 34–45. [CrossRef]

175. Ganci, G.; Cappello, A.; Bilotta, G.; Del Negro, C. How the variety of satellite remote sensing data over volcanoes can assist hazard monitoring efforts: The 2011 eruption of Nabro volcano. *Remote Sens. Environ.* **2020**, *236*, 111426. [CrossRef]

176. Ganci, G.; James, M.R.; Calvari, S.; Negro, C. Del Separating the thermal fingerprints of lava flows and simultaneous lava fountaining using ground-based thermal camera and SEVIRI measurements. *Geophys. Res. Lett.* **2013**, *40*, 5058–5063. [CrossRef]

177. Casagli, N.; Frodella, W.; Morelli, S.; Tofani, V.; Ciampalini, A.; Intrieri, E.; Raspini, F.; Rossi, G.; Tanteri, L.; Lu, P. Spaceborne, UAV and ground-based remote sensing techniques for landslide mapping, monitoring and early warning. *Geoenviron. Disasters* **2017**, *4*, 9. [CrossRef]

178. Van der Meer, F.; Hecker, C.; van Ruitenbeek, F.; van der Werff, H.; de Wijkerslooth, C.; Wechsler, C. Geologic remote sensing for geothermal exploration: A review. *Int. J. Appl. Earth Obs. Geoinf.* **2014**, *33*, 255–269. [CrossRef]

179. Coppola, D.; Laiolo, M.; Cigolini, C.; Massimetti, F.; Delle Donne, D.; Ripepe, M.; Arias, H.; Barsotti, S.; Parra, C.B.; Centeno, R.G.; et al. Thermal Remote Sensing for Global Volcano Monitoring: Experiences From the MIROVA System. *Front. Earth Sci.* **2020**, *7*, 1746–1763. [CrossRef]

180. Reath, K.; Pritchard, M.; Poland, M.; Delgado, F.; Carn, S.; Coppola, D.; Andrews, B.; Ebmeier, S.K.; Rumpf, E.; Henderson, S.; et al. Thermal, Deformation, and Degassing Remote Sensing Time Series (CE 2000–2017) at the 47 most Active Volcanoes in Latin America: Implications for Volcanic Systems. *J. Geophys. Res. Solid Earth* **2019**, *124*, 195–218. [CrossRef]

181. Liang, G.; Xiao, K.; Zheng, H.; Zhao, W.; Zhang, Q.; Gao, C. Rockfall monitoring based on multichannel synthetic aperture radar. *Vibroeng. Procedia* **2019**, *22*, 146–152.

182. Cabré, A.; Remy, D.; Aguilar, G.; Carretier, S.; Riquelme, R. Mapping rainstorm erosion associated with an individual storm from InSAR coherence loss validated by field evidence for the Atacama Desert. *Earth Surf. Process. Landf.* **2020**, *45*, 2091–2106. [CrossRef]

183. Caviezel, A.; Gerber, W. Brief Communication: Measuring rock decelerations and rotation changes during short-duration ground impacts. *Nat. Hazards Earth Syst. Sci.* **2018**, *18*, 3145–3151. [CrossRef]

184. Fanos, A.M.; Pradhan, B.; Alamri, A.; Lee, C.W. Machine Learning-Based and 3D Kinematic Models for Rockfall Hazard Assessment Using LiDAR Data and GIS. *Remote Sens.* **2020**, *12*, 1755. [CrossRef]

185. Lato, M.J.; Anderson, S.; Porter, M.J. Reducing Landslide Risk Using Airborne Lidar Scanning Data. *J. Geotech. Geoenviron. Eng.* **2019**, *145*, 06019004. [CrossRef]

186. Liu, H.; Wang, X.; Liao, X.; Sun, J.; Zhang, S. Rockfall Investigation and Hazard Assessment from Nang County to Jiacha County in Tibet. *Appl. Sci.* **2019**, *10*, 247. [CrossRef]

187. Caviezel, A.; Demmel, S.E.; Ringenbach, A.; Bühler, Y.; Lu, G.; Christen, M.; Dinneen, C.E.; Eberhard, L.A.; von Rickenbach, D.; Bartelt, P. Reconstruction of four-dimensional rockfall trajectories using remote sensing and rock-based accelerometers and gyroscopes. *Earth Surf. Dyn.* **2019**, *7*, 199–210. [CrossRef]

188. Hormes, A.; Adams, M.; Amabile, A.S.; Blauensteiner, F.; Demmler, C.; Fey, C.; Ostermann, M.; Rechberger, C.; Sausgruber, T.; Vecchiotti, F.; et al. Innovative methods to monitor rock and mountain slope deformation. *Geomech. Tunn.* **2020**, *13*, 88–102. [CrossRef]

189. Lambert, S.; Nicot, F. (Eds.) *Rockfall Engineering*; John Wiley & Sons, Inc.: Hoboken, NJ, USA, 2013; ISBN 9781118601532.

190. Bonneau, D.A.; Hutchinson, D.J.; DiFrancesco, P.-M.; Coombs, M.; Sala, Z. Three-dimensional rockfall shape back analysis: Methods and implications. *Nat. Hazards Earth Syst. Sci.* **2019**, *19*, 2745–2765. [CrossRef]

191. Valade, S.; Ley, A.; Massimetti, F.; D'Hondt, O.; Laiolo, M.; Coppola, D.; Loibl, D.; Hellwich, O.; Walter, T.R. Towards Global Volcano Monitoring Using Multisensor Sentinel Missions and Artificial Intelligence: The MOUNTS Monitoring System. *Remote Sens.* **2019**, *11*, 1528. [CrossRef]

192. Pattathal, V.A.; Sahoo, M.M.; Porwal, A.; Karnieli, A. Deep-learning-based latent space encoding for spectral unmixing of geological materials. *ISPRS J. Photogramm. Remote Sens.* **2022**, *183*, 307–320. [CrossRef]

193. Godone, D.; Allasia, P.; Borrelli, L.; Gullà, G. UAV and Structure from Motion Approach to Monitor the Maierato Landslide Evolution. *Remote Sens.* **2020**, *12*, 1039. [CrossRef]

194. Wu, Q.; Song, C.; Liu, K.; Ke, L. Integration of TanDEM-X and SRTM DEMs and Spectral Imagery to Improve the Large-Scale Detection of Opencast Mining Areas. *Remote Sens.* **2020**, *12*, 1451. [CrossRef]

195. Song, W.; Song, W.; Gu, H.; Li, F. Progress in the Remote Sensing Monitoring of the Ecological Environment in Mining Areas. *Int. J. Environ. Res. Public Health* **2020**, *17*, 1846. [CrossRef]

196. Nascimento, F.S.; Gastauer, M.; Souza-Filho, P.W.M.; Nascimento, W.R.; Santos, D.C.; Costa, M.F. Land cover changes in open-cast mining complexes based on high-resolution remote sensing data. *Remote Sens.* **2020**, *12*, 611. [CrossRef]

197. Schmidt, H.; Glaesser, C. Multitemporal analysis of satellite data and their use in the monitoring of the environmental impacts of open cast lignite mining areas in eastern germany. *Int. J. Remote Sens.* **1998**, *19*, 2245–2260. [CrossRef]

198. Verma, S.; Malpe, D.B. Mining Activity Monitoring Through Remote Sensing and GIS- A Case Study from Wani Area of Yavatmal District, Maharashtra. *Int. J. Adv. Remote Sens. GIS* **2017**, *6*, 2458–2465. [CrossRef]

199. Bhattacharya, R.K.; Das Chatterjee, N.; Das, K. Impact of instream sand mining on habitat destruction or transformation using coupling models of HSI and MLR. *Spat. Inf. Res.* **2020**, *28*, 67–85. [CrossRef]

200. Gläßer, C.; Birger, J.; Herrmann, B. Integrated monitoring and management system of lignite opencast mines using multiple remote sensing data and GIS. In *Operational Remote Sensing for Sustainable Development*; Nieuwenhuis, G.J.A., Vaughan, R.A., Molehaar, M., Eds.; Operational Remote Sensing for Sustainable Development: Rotterdam, The Netherlands, 1999; pp. 439–444.

201. Götze, C.; Beyer, F.; Gläßer, C. Pioneer vegetation as an indicator of the geochemical parameters in abandoned mine sites using hyperspectral airborne data. *Environ. Earth Sci.* **2016**, *75*, 613. [CrossRef]

202. Salepci, N. Multi-Sensor Synergy For Persistent Scatterer Interferometry Based Ground Subsidence Monitoring. Ph.D. Thesis, Chemical-Geoscientific Faculty, Friedrich Schiller University of Jena, Jena, Germany, 2015. Available online: https://www.db-thueringen.de/receive/dbt_mods_00026315 (accessed on 5 March 2022).

203. Platt, R.V.; Manthos, D.; Amos, J. Estimating the Creation and Removal Date of Fracking Ponds Using Trend Analysis of Landsat Imagery. *Environ. Manag.* **2018**, *61*, 310–320. [CrossRef]

204. Bai, Z.G.; Dent, D.L.; Olsson, L.; Schaepman, M.E. Proxy global assessment of land degradation. *Soil Use Manag.* **2008**, *24*, 223–234. [CrossRef]

205. Borrelli, P.; Robinson, D.A.; Fleischer, L.R.; Lugato, E.; Ballabio, C.; Alewell, C.; Meusburger, K.; Modugno, S.; Schütt, B.; Ferro, V.; et al. An assessment of the global impact of 21st century land use change on soil erosion. *Nat. Commun.* **2017**, *8*, 2013. [CrossRef]

206. Khan, N.M.; Rastoskuev, V.V.; Sato, Y.; Shiozawa, S. Assessment of hydrosaline land degradation by using a simple approach of remote sensing indicators. *Agric. Water Manag.* **2005**, *77*, 96–109. [CrossRef]

207. Symeonakis, E.; Drake, N. Monitoring desertification and land degradation over sub-Saharan Africa. *Int. J. Remote Sens.* **2004**, *25*, 573–592. [CrossRef]

208. Hunter, F.D.L.; Mitchard, E.T.A.; Tyrrell, P.; Russell, S. Inter-Seasonal Time Series Imagery Enhances Classification Accuracy of Grazing Resource and Land Degradation Maps in a Savanna Ecosystem. *Remote Sens.* **2020**, *12*, 198. [CrossRef]

209. Giuliani, G.; Mazzetti, P.; Santoro, M.; Nativi, S.; Van Bemmelen, J.; Colangeli, G.; Lehmann, A. Knowledge generation using satellite earth observations to support sustainable development goals (SDG): A use case on Land degradation. *Int. J. Appl. Earth Obs. Geoinf.* **2020**, *88*, 102068. [CrossRef]

210. Del Valle, H.F.; Blanco, P.D.; Metternicht, G.I.; Zinck, J.A. Radar Remote Sensing of Wind-Driven Land Degradation Processes in Northeastern Patagonia. *J. Environ. Qual.* **2010**, *39*, 62–75. [CrossRef] [PubMed]

211. Eagleston, H.; Marion, J.L. Application of airborne LiDAR and GIS in modeling trail erosion along the Appalachian Trail in New Hampshire, USA. *Landsc. Urban Plan.* **2020**, *198*, 103765. [CrossRef]

212. Ding, C.; Zhang, L.; Liao, M.; Feng, G.; Dong, J.; Ao, M.; Yu, Y. Quantifying the spatio-temporal patterns of dune migration near Minqin Oasis in northwestern China with time series of Landsat-8 and Sentinel-2 observations. *Remote Sens. Environ.* **2020**, *236*, 111498. [CrossRef]

213. Abdelkareem, M.; Gaber, A.; Abdalla, F.; El-Din, G.K. Use of optical and radar remote sensing satellites for identifying and monitoring active/inactive landforms in the driest desert in Saudi Arabia. *Geomorphology* **2020**, *362*, 107197. [CrossRef]

214. Davis, J.M.; Grindrod, P.M.; Boazman, S.J.; Vermeesch, P.; Baird, T. Quantified Aeolian Dune Changes on Mars Derived From Repeat Context Camera Images. *Earth Sp. Sci.* **2020**, *7*, e2019EA000874. [CrossRef]

215. Dong, P.; Chen, Q. *LiDAR Remote Sensing and Its Applications*; CRC Press: Boca Raton, FL, USA; Taylor & Francis Group: Abingdon, UK, 2018; ISBN 978-1-4822-4301-7.

216. Baughman, C.A.; Jones, B.M.; Bodony, K.L.; Mann, D.H.; Larsen, C.F.; Himelstoss, E.; Smith, J. Remotely Sensing the Morphometrics and Dynamics of a Cold Region Dune Field Using Historical Aerial Photography and Airborne LiDAR Data. *Remote Sens.* **2018**, *10*, 792. [CrossRef]

217. Sharma, P.; Heggy, E.; Farr, T.G. Exploring morphology, layering and formation history of linear terrestrial dunes from radar observations: Implications for Titan. *Remote Sens. Environ.* **2018**, *204*, 296–307. [CrossRef]

218. Ewing, R.C.; Kocurek, G.; Lake, L.W. Pattern analysis of dune-field parameters. *Earth Surf. Process. Landf.* **2006**, *31*, 1176–1191. [CrossRef]

219. Grohmann, C.H.; Sawakuchi, A.O. Influence of cell size on volume calculation using digital terrain models: A case of coastal dune fields. *Geomorphology* **2013**, *180–181*, 130–136. [CrossRef]

220. Michel, S.; Avouac, J.-P.; Ayoub, F.; Ewing, R.C.; Vriend, N.; Heggy, E. Comparing dune migration measured from remote sensing with sand flux prediction based on weather data and model, a test case in Qatar. *Earth Planet. Sci. Lett.* **2018**, *497*, 12–21. [CrossRef]

221. Shahabi, H.; Shirzadi, A.; Ghaderi, K.; Omidvar, E.; Al-Ansari, N.; Clague, J.J.; Geertsema, M.; Khosravi, K.; Amini, A.; Bahrami, S.; et al. Flood Detection and Susceptibility Mapping Using Sentinel-1 Remote Sensing Data and a Machine Learning Approach: Hybrid Intelligence of Bagging Ensemble Based on K-Nearest Neighbor Classifier. *Remote Sens.* **2020**, *12*, 266. [CrossRef]

222. Hong Quang, N.; Tuan, V.A.; Thi Thu Hang, L.; Manh Hung, N.; Thi The, D.; Thi Dieu, D.; Duc Anh, N.; Hackney, C.R. Hydrological/Hydraulic Modeling-Based Thresholding of Multi SAR Remote Sensing Data for Flood Monitoring in Regions of the Vietnamese Lower Mekong River Basin. *Water* **2019**, *12*, 71. [CrossRef]

223. Alexandre, C.; Johary, R.; Catry, T.; Mouquet, P.; Révillion, C.; Rakotondraompiana, S.; Pennober, G. A Sentinel-1 Based Processing Chain for Detection of Cyclonic Flood Impacts. *Remote Sens.* **2020**, *12*, 252. [CrossRef]

224. Zhang, M.; Chen, F.; Tian, B.; Liang, D.; Yang, A. Characterization of Kyagar Glacier and Lake Outburst Floods in 2018 Based on Time-Series Sentinel-1A Data. *Water* **2020**, *12*, 184. [CrossRef]

225. Costache, R.; Pham, Q.B.; Sharifi, E.; Linh, N.T.T.; Abba, S.I.; Vojtek, M.; Vojteková, J.; Nhi, P.T.T.; Khoi, D.N. Flash-Flood Susceptibility Assessment Using Multi-Criteria Decision Making and Machine Learning Supported by Remote Sensing and GIS Techniques. *Remote Sens.* **2019**, *12*, 106. [CrossRef]

226. San Martín, L.; Morandeira, N.S.; Grimson, R.; Rajngewerc, M.; González, E.B.; Kandus, P. The contribution of ALOS/PALSAR-1 multi-temporal data to map permanently and temporarily flooded coastal wetlands. *Int. J. Remote Sens.* **2020**, *41*, 1582–1602. [CrossRef]

227. Alsdorf, D.E.; Melack, J.M.; Dunne, T.; Mertes, L.A.K.; Hess, L.L.; Smith, L.C. Interferometric radar measurements of water level changes on the Amazon flood plain. *Nature* **2000**, *404*, 174–177. [CrossRef] [PubMed]

228. Ogashawara, I.; Curtarelli, M.P.; Ferreira, C.M. The Use of Optical Remote Sensing For Mapping Flooded Areas. *J. Eng. Res. Appl.* **2013**, *3*, 1956–1960.

229. Wang, Y.; Colby, J.D.; Mulcahy, K.A. An efficient method for mapping flood extent in a coastal floodplain using Landsat TM and DEM data. *Int. J. Remote Sens.* **2002**, *23*, 3681–3696. [CrossRef]

230. Himayoun, D.; Roshni, T. Geomorphic changes in the Jhelum River due to an extreme flood event: A case study. *Arab. J. Geosci.* **2020**, *13*, 23. [CrossRef]

231. Walker, J.J.; Soulard, C.E.; Petrakis, R.E. Integrating stream gage data and Landsat imagery to complete time-series of surface water extents in Central Valley, California. *Int. J. Appl. Earth Obs. Geoinf.* **2020**, *84*, 101973. [CrossRef]

232. Caballero, I.; Ruiz, J.; Navarro, G. Sentinel-2 Satellites Provide Near-Real Time Evaluation of Catastrophic Floods in the West Mediterranean. *Water* **2019**, *11*, 2499. [CrossRef]

233. Gläßer, C.; Reinartz, P. Multitemporal and Multispectral Remote Sensing Approach for Flood Detection in the Elbe-Mulde Region 2002. *Acta Hydrochim. Hydrobiol.* **2005**, *33*, 395–403. [CrossRef]

234. Grimaldi, S.; Xu, J.; Li, Y.; Pauwels, V.R.N.; Walker, J.P. Flood mapping under vegetation using single SAR acquisitions. *Remote Sens. Environ.* **2020**, *237*, 111582. [CrossRef]

235. Olivera-Guerra, L.; Merlin, O.; Er-Raki, S. Irrigation retrieval from Landsat optical/thermal data integrated into a crop water balance model: A case study over winter wheat fields in a semi-arid region. *Remote Sens. Environ.* **2020**, *239*, 111627. [CrossRef]

236. Jerome Morrissey, P.; McCormack, T.; Naughton, O.; Meredith Johnston, P.; William Gill, L. Modelling groundwater flooding in a lowland karst catchment. *J. Hydrol.* **2020**, *580*, 124361. [CrossRef]

237. Riedel, F. Der Einsatz Hyperspektraler Fernerkundungsdaten zur Analyse Schwermetallbedingter Boden- und Pflanzenbe-lastungen in Einem Auenökosystem unter Besonderer Berücksichtigung der Feinmorphologie. Ph.D. Thesis, Universität Halle-Wittenberg, Halle, Germany, 2018; pp. 1–226. Available online: http://digital.bibliothek.uni-halle.de/hs/content/titleinfo/2923679 (accessed on 7 November 2020).
238. Liu, Y.; Zhang, P.; He, Y.; Peng, Z. River detection based on feature fusion from synthetic aperture radar images. *J. Appl. Remote Sens.* **2020**, *14*, 1. [CrossRef]
239. Mandlburger, G.; Hauer, C.; Wieser, M.; Pfeifer, N. Topo-Bathymetric LiDAR for Monitoring River Morphodynamics and Instream Habitats—A Case Study at the Pielach River. *Remote Sens.* **2015**, *7*, 6160–6195. [CrossRef]
240. Allen, G.H.; Pavelsky, T. Global extent of rivers and streams. *Science* **2018**, *361*, 585–588. [CrossRef]
241. Bird, S.; Hogan, D.; Schwab, J. Photogrammetric monitoring of small streams under a riparian forest canopy. *Earth Surf. Process. Landf.* **2010**, *970*, 952–970. [CrossRef]
242. Bizzi, S.; Demarchi, L.; Grabowski, R.C.; Weissteiner, C.J. The use of remote sensing to characterise hydromorphological properties of European rivers. *Aquat. Sci.* **2016**, *78*, 57–70. [CrossRef]
243. Wheaton, J.M.; Fryirs, K.A.; Brierley, G.; Bangen, S.G.; Bouwes, N.; O'Brien, G. Geomorphic mapping and taxonomy of fluvial landforms. *Geomorphology* **2015**, *248*, 273–295. [CrossRef]
244. Demarchi, L.; Bizzi, S.; Piégay, H. Regional hydromorphological characterization with continuous and automated remote sensing analysis based on VHR imagery and low-resolution LiDAR data. *Earth Surf. Process. Landf.* **2017**, *42*, 531–551. [CrossRef]
245. Pinheiro, M.; Amao-Oliva, J.; Scheiber, R.; Jaeger, M.; Horn, R.; Keller, M.; Fischer, J.; Reigber, A. Dual-frequency airborne SAR for large scale mapping of tidal flats. *Remote Sens.* **2020**, *12*, 1827. [CrossRef]
246. Lorenz, R.D.; Lopes, R.M.; Paganelli, F.; Lunine, J.I.; Kirk, R.L.; Mitchell, K.L.; Soderblom, L.A.; Stofan, E.R.; Ori, G.; Myers, M.; et al. Fluvial channels on Titan: Initial Cassini RADAR observations. *Planet. Space Sci.* **2008**, *56*, 1132–1144. [CrossRef]
247. Smith, L.C.; Pavelsky, T.M. Estimation of river discharge, propagation speed, and hydraulic geometry from space: Lena River, Siberia. *Water Resour. Res.* **2008**, *44*, 1–11. [CrossRef]
248. Tarpanelli, A.; Brocca, L.; Barbetta, S.; Faruolo, M.; Lacava, T.; Moramarco, T. Coupling MODIS and Radar Altimetry Data for Discharge Estimation in Poorly Gauged River Basins. *IEEE J. Sel. Top. Appl. Earth Obs. Remote Sens.* **2015**, *8*, 141–148. [CrossRef]
249. Belletti, B.; Dufour, S.; Piégay, H. What is the Relative Effect of Space and Time to Explain the Braided River Width and Island Patterns at a Regional Scale? *River Res. Appl.* **2015**, *31*, 1–15. [CrossRef]
250. Finotello, A.; D'Alpaos, A.; Bogoni, M.; Ghinassi, M.; Lanzoni, S. Remotely-sensed planform morphologies reveal fluvial and tidal nature of meandering channels. *Sci. Rep.* **2020**, *10*, 54. [CrossRef]
251. Naito, K.; Parker, G. Can Bankfull Discharge and Bankfull Channel Characteristics of an Alluvial Meandering River be Cospecified From a Flow Duration Curve? *J. Geophys. Res. Earth Surf.* **2019**, *124*, 2381–2401. [CrossRef]
252. Lallias-Tacon, S.; Liébault, F.; Piégay, H. Step by step error assessment in braided river sediment budget using airborne LiDAR data. *Geomorphology* **2014**, *214*, 307–323. [CrossRef]
253. Houser, C.; Hamilton, S. Morphodynamics of a 1000-year flood in the Kamp River, Austria, and impacts on floodplain morphology. *Earth Surf. Process. Landf.* **2009**, *34*, 613–628. [CrossRef]
254. Yang, C.; Cai, X.; Wang, X.; Yan, R.; Zhang, T.; Zhang, Q.; Lu, X. Remotely sensed trajectory analysis of channel migration in Lower Jingjiang Reach during the period of 1983-2013. *Remote Sens.* **2015**, *7*, 16241–16256. [CrossRef]
255. Peixoto, J.M.A.; Nelson, B.W.; Wittmann, F. Spatial and temporal dynamics of river channel migration and vegetation in central Amazonian white-water floodplains by remote-sensing techniques. *Remote Sens. Environ.* **2009**, *113*, 2258–2266. [CrossRef]
256. Dépret, T.; Riquier, J.; Piégay, H. Evolution of abandoned channels: Insights on controlling factors in a multi-pressure river system. *Geomorphology* **2017**, *294*, 99–118. [CrossRef]
257. Yang, X.; Damen, M.C.J.; Van Zuidam, R.A. Satellite remote sensing and GIS for the analysis of channel migration changes in the active Yellow River Delta, China. *ITC J.* **1999**, *1*, 146–157. [CrossRef]
258. Wen, Z.; Yang, H.; Zhang, C.; Shao, G.; Wu, S. Remotely Sensed Mid-Channel Bar Dynamics in Downstream of the Three Gorges Dam, China. *Remote Sens.* **2020**, *12*, 409. [CrossRef]
259. Garofalo, D. The Influence of Wetland Vegetation on Tidal Stream Channel Migration and Morphology. *Estuaries* **1980**, *3*, 258. [CrossRef]
260. Thomas, J.; Kumar, S.; Sudheer, K.P. Channel stability assessment in the lower reaches of the Krishna River (India) using multi-temporal satellite data during 1973–2015. *Remote Sens. Appl. Soc. Environ.* **2020**, *17*, 100274. [CrossRef]
261. Biron, P.M.; Choné, G.; Buffin-Bélanger, T.; Demers, S.; Olsen, T. Improvement of streams hydro-geomorphological assessment using LiDAR DEMs. *Earth Surf. Process. Landf.* **2013**, *38*, 1808–1821. [CrossRef]
262. Zakharova, E.; Nielsen, K.; Kamenev, G.; Kouraev, A. River discharge estimation from radar altimetry: Assessment of satellite performance, river scales and methods. *J. Hydrol.* **2020**, *583*, 124561. [CrossRef]
263. Tourian, M.J.; Sneeuw, N.; Bárdossy, A. A quantile function approach to discharge estimation from satellite altimetry (ENVISAT). *Water Resour. Res.* **2013**, *49*, 4174–4186. [CrossRef]
264. Perks, M.T.; Russell, A.J.; Large, A.R.G. Technical Note: Advances in flash flood monitoring using UAVs. *Hydrol. Earth Syst. Sci. Discuss.* **2016**, *20*, 4005–4015. [CrossRef]

265. Emery, C.M.; Paris, A.; Biancamaria, S.; Boone, A.; Calmant, S.; Garambois, P.-A.; Santos da Silva, J. Large-scale hydrological model river storage and discharge correction using a satellite altimetry-based discharge product. *Hydrol. Earth Syst. Sci.* **2018**, *22*, 2135–2162. [CrossRef]

266. Ridolf, E.; Manciola, P. Water Level Measurements from Drones: A Pilot Case Study at a Dam Site. *Water* **2018**, *10*, 297. [CrossRef]

267. Hirpa, F.A.; Hopson, T.M.; De Groeve, T.; Brakenridge, G.R.; Gebremichael, M.; Restrepo, P.J. Upstream satellite remote sensing for river discharge forecasting: Application to major rivers in South Asia. *Remote Sens. Environ.* **2013**, *131*, 140–151. [CrossRef]

268. Gilvear, D.J.; Davids, C.; Tyler, A.N. The use of remotely sensed data to detect channel hydromorphology; River Tummel, Scotland. *River Res. Appl.* **2004**, *20*, 795–811. [CrossRef]

269. Wyrick, J.R.; Senter, A.E.; Pasternack, G.B. Revealing the natural complexity of fluvial morphology through 2D hydrodynamic delineation of river landforms. *Geomorphology* **2014**, *210*, 14–22. [CrossRef]

270. Brousse, G.; Arnaud-Fassetta, G.; Liébault, F.; Bertrand, M.; Melun, G.; Loire, R.; Malavoi, J.; Fantino, G.; Borgniet, L. Channel response to sediment replenishment in a large gravel-bed river: The case of the Saint-Sauveur dam in the Buëch River (Southern Alps, France). *River Res. Appl.* **2020**, *36*, 880–893. [CrossRef]

271. Heeren, D.M.; Mittelstet, A.R.; Fox, G.A.; Storm, D.E.; Al-Madhhachi, A.T.; Midgley, T.L.; Stringer, A.F.; Stunkel, K.B.; Tejral, R.D. Using Rapid Geomorphic Assessments to Assess Streambank Stability in Oklahoma Ozark Streams. *Trans. ASABE* **2012**, *55*, 957–968. [CrossRef]

272. Hamshaw, S.D.; Bryce, T.; Rizzo, D.M.; O'Neil-Dunne, J.; Frolik, J.; Dewoolkar, M.M. Quantifying streambank movement and topography using unmanned aircraft system photogrammetry with comparison to terrestrial laser scanning. *River Res. Appl.* **2017**, *33*, 1354–1367. [CrossRef]

273. Johansen, K.; Grove, J.; Denham, R.; Phinn, S. Assessing stream bank condition using airborne LiDAR and high spatial resolution image data in temperate semirural areas in Victoria, Australia. *J. Appl. Remote Sens.* **2013**, *7*, 073492. [CrossRef]

274. Resop, J.P.; Lehmann, L.; Hession, W.C. Drone Laser Scanning for Modeling Riverscape Topography and Vegetation: Comparison with Traditional Aerial Lidar. *Drones* **2019**, *3*, 35. [CrossRef]

275. Meinen, B.U.; Robinson, D.T. Streambank topography: An accuracy assessment of UAV-based and traditional 3D reconstructions. *Int. J. Remote Sens.* **2020**, *41*, 1–18. [CrossRef]

276. Micheli, E.R.; Kirchner, J.W. Effects of wet meadow riparian vegetation on streambank erosion. 1. Remote sensing measurements of streambank migration and erodibility. *Earth Surf. Process. Landf.* **2002**, *27*, 627–639. [CrossRef]

277. Vázquez-Tarrío, D.; Borgniet, L.; Liébault, F.; Recking, A. Using UAS optical imagery and SfM photogrammetry to characterize the surface grain size of gravel bars in a braided river (Vénéon River, French Alps). *Geomorphology* **2017**, *285*, 94–105. [CrossRef]

278. Carbonneau, P.E.; Bizzi, S.; Marchetti, G. Robotic photosieving from low-cost multirotor sUAS: A proof-of-concept. *Earth Surf. Process. Landf.* **2018**, *43*, 1160–1166. [CrossRef]

279. Carbonneau, P.E.; Dugdale, S.J.; Breckon, T.P.; Dietrich, J.D.; Fonstad, M.A.; Miyamoto, H.; Woodget, A.S. Generalised classification of hyperspatial resolution airborne imagery of fluvial scenes with deep convolutional neural networks. *Geophys. Res. Abstr.* **2019**, *21*, 1.

280. Carbonneau, P.E.; Lane, S.N.; Bergeron, N.E. Catchment-scale mapping of surface grain size in gravel bed rivers using airborne digital imagery. *Water Resour. Res.* **2004**, *40*, W07202. [CrossRef]

281. Rainey, M.; Tyler, A.; Gilvear, D.; Bryant, R.; McDonald, P. Mapping intertidal estuarine sediment grain size distributions through airborne remote sensing. *Remote Sens. Environ.* **2003**, *86*, 480–490. [CrossRef]

282. Piégay, H.; Arnaud, F.; Belletti, B.; Bertrand, M.; Bizzi, S.; Carbonneau, P.; Dufour, S.; Liébault, F.; Ruiz-Villanueva, V.; Slater, L. Remotely sensed rivers in the Anthropocene: State of the art and prospects. *Earth Surf. Process. Landf.* **2020**, *45*, 157–188. [CrossRef]

283. Cassel, M.; Piégay, H.; Fantino, G.; Lejot, J.; Bultingaire, L.; Michel, K.; Perret, F. Comparison of ground-based and UAV a-UHF artificial tracer mobility monitoring methods on a braided river. *Earth Surf. Process. Landf.* **2020**, *45*, 1123–1140. [CrossRef]

284. Dietrich, J.T. Bathymetric Structure-from-Motion: Extracting shallow stream bathymetry from multi-view stereo photogrammetry. *Earth Surf. Process. Landf.* **2017**, *42*, 355–364. [CrossRef]

285. Legleiter, C.J. Remote measurement of river morphology via fusion of LiDAR topography and spectrally based bathymetry. *Earth Surf. Process. Landf.* **2012**, *37*, 499–518. [CrossRef]

286. Legleiter, C.J.; Overstreet, B.T.; Glennie, C.L.; Pan, Z.; Fernandez-Diaz, J.C.; Singhania, A. Evaluating the capabilities of the CASI hyperspectral imaging system and Aquarius bathymetric LiDAR for measuring channel morphology in two distinct river environments. *Earth Surf. Process. Landf.* **2016**, *41*, 344–363. [CrossRef]

287. Dürr, H.H.; Laruelle, G.G.; van Kempen, C.M.; Slomp, C.P.; Meybeck, M.; Middelkoop, H. Worldwide Typology of Nearshore Coastal Systems: Defining the Estuarine Filter of River Inputs to the Oceans. *Estuaries Coasts* **2011**, *34*, 441–458. [CrossRef]

288. Barale, V. Environmental Remote Sensing of the Mediterranean Sea. *J. Environ. Sci. Health Part A* **2003**, *38*, 1681–1688. [CrossRef]

289. Boak, E.H.; Turner, I.L. Shoreline Definition and Detection: A Review. *J. Coast. Res.* **2005**, *214*, 688–703. [CrossRef]

290. Moore, L.J.; Griggs, G.B. Long-term cliff retreat and erosion hotspots along the central shores of the Monterey Bay National Marine Sanctuary. *Mar. Geol.* **2002**, *181*, 265–283. [CrossRef]

291. Valderrama-Landeros, L.; Blanco y Correa, M.; Flores-Verdugo, F.; Álvarez-Sánchez, L.F.; Flores-de-Santiago, F. Spatiotemporal shoreline dynamics of Marismas Nacionales, Pacific coast of Mexico, based on a remote sensing and GIS mapping approach. *Environ. Monit. Assess.* **2020**, *192*, 123. [CrossRef]

292. Kanwal, S.; Ding, X.; Sajjad, M.; Abbas, S. Three Decades of Coastal Changes in Sindh, Pakistan (1989–2018): A Geospatial Assessment. *Remote Sens.* **2019**, *12*, 8. [CrossRef]

293. Ford, M.R.; Dickson, M.E. Detecting ebb-tidal delta migration using Landsat imagery. *Mar. Geol.* **2018**, *405*, 38–46. [CrossRef]

294. Marghany, M.; Sabu, Z.; Hashim, M. Mapping coastal geomorphology changes using synthetic aperture radar data. *Int. J. Phys. Sci.* **2010**, *5*, 1890–1896.

295. Shu, Y.; Li, J.; Gomes, G. Shoreline Extraction from RADARSAT-2 Intensity Imagery Using a Narrow Band Level Set Segmentation Approach. *Mar. Geod.* **2010**, *33*, 187–203. [CrossRef]

296. Elnabwy, M.T.; Elbeltagi, E.; El Banna, M.M.; Elshikh, M.M.Y.; Motawa, I.; Kaloop, M.R. An approach based on landsat images for shoreline monitoring to support integrated coastal management—A case study, ezbet elborg, nile delta, Egypt. *ISPRS Int. J. Geo.-Inf.* **2020**, *9*, 199. [CrossRef]

297. Toure, S.; Diop, O.; Kpalma, K.; Maiga, A. Shoreline Detection using Optical Remote Sensing: A Review. *ISPRS Int. J. Geo.-Inf.* **2019**, *8*, 75. [CrossRef]

298. Vousdoukas, M.I.; Ranasinghe, R.; Mentaschi, L.; Plomaritis, T.A.; Athanasiou, P.; Luijendijk, A.; Feyen, L. Sandy coastlines under threat of erosion. *Nat. Clim. Change* **2020**, *10*, 260–263. [CrossRef]